UNIVERSIDADE ESTADUAL PAULISTA "JÚLIO DE MESQUITA FILHO"
FACULDADE DE MEDICINA DE BOTUCATU

ESTUDO DOSE-RESPOSTA E PERFIL DE EXPRESSÃO GÊNICA DO HERBICIDA DIURON [3-(3,4-DICLOFENIL)-1,1-DIMETILURÉIA] EM BEXIGA URINÁRIA DE RATOS WISTAR MACHOS

SHADIA MUHAMMAD IHLASEH

Tese apresentada ao Programa de Pós-Graduação em Patologia da Faculdade de Medicina de Botucatu, Universidade Estadual Paulista – UNESP para obtenção do título de Doutora em Patologia.

BOTUCATU – SP

2011

UNIVERSIDADE ESTADUAL PAULISTA "JÚLIO DE MESQUITA FILHO"
FACULDADE DE MEDICINA DE BOTUCATU

ESTUDO DOSE-RESPOSTA E PERFIL DE EXPRESSÃO GÊNICA DO HERBICIDA DIURON [3-(3,4-DICLOFENIL)-1,1-DIMETILURÉIA] EM BEXIGA URINÁRIA DE RATOS WISTAR MACHOS

Doutoranda: Shadia Muhammad Ihlaseh

Orientador: Prof. Titular João Lauro Viana de Camargo

Tese apresentada ao Programa de Pós-Graduação em Patologia da Faculdade de Medicina de Botucatu, Universidade Estadual Paulista – UNESP para obtenção do título de Doutora em Patologia.

BOTUCATU – SP

2011

SAO PAULO STATE UNIVERSITY "JÚLIO DE MESQUITA FILHO"
BOTUCATU MEDICAL SCHOOL

DOSE-RESPONSE AND GENE EXPRESSION PROFILE OF THE HERBICIDE DIURON [3-(3,4-DICHLOROPHENYL)-1,1-DIMETHYLUREA] IN URINARY BLADDER OF MALE WISTAR RATS

Candidate: Shadia Muhammad Ihlaseh

Supervisor: João Lauro Viana de Camargo, M.D., Ph.D.

Thesis submitted to the Graduate Program in Paathology, Botucatu Medical School, Sao Paulo State University – UNESP for the title of Philosophical Doctor in Pathology.

BOTUCATU – SP

2011

Dedicatória

Dedication

A Deus que sempre se faz presente em minha vida e a quem eu devo tudo.

Aos meus pais, Muhammad e Zilda (*in memorian*), pelo amor incondicional que sempre me dedicaram e pela alegria que ambos devam estar sentindo com a realização deste trabalho.

Ao meu amado Caio, que se tornou esposo no decorrer deste trabalho, por participar da minha vida, sempre me incentivando, e por compartilhar a sua comigo.

"Ainda que eu falasse a lingua dos homens, e falasse a lingua dos anjos, sem amor, eu nada seria"

Agradecimentos especiais

Special Acknowledgments

Ao meu orientador, Prof. Dr. João Lauro V. Camargo, pelo exemplo de pesquisador, educador e pessoa. Minha sincera admiração e gratidão!

Ao Prof. Dr. Doug Wolf, que me recebeu em sua instituição, pela oportunidade, pelos ensinamentos e pela amizade.

To Doug Wolf, who welcomed me in his Institution, for the opportunity, for teaching me the meaning of the "Philosophical"word that precedes the Doctor (Ph.D.), and for your friendship.

I've learned that the easiest way for me to grow as a person is to surround myself with people smarter than I am"

(William Shakespeare)

Agradecimentos

Acknowledgments

À minha família pelo carinho, incentivo, orações e compreensão.

Aos meus amigos: Ivana, Diego, Cibele, Rebeca, Juliana, Renato, Mariana, por tornarem o caminho mais alegre.

Aos amigos do laboratório Toxicam: Viviane, Carla, Merielen, Mitscheli,Marize, Meire, Alexandre, Tony, João, Bianca, Gabrielli, Rafaela e Lígia pela ajuda e pela amizade.

A Ana Paula, pela amizade e pela ajuda, essencial desde o início deste trabalho

À secretária Cristina, que sempre ajudou com dedicação e carinho contribuindo para a realização desde trabalho

Aos técnicos Paulo, Mara, PC e Ivana, que possibilitaram a realização deste trabalho.

À Dra. Maria Luiza Cotrim Sartor de Oliveira pela colaboração no desenvolvimento deste estudo

Aos amigos do Departamento de Patologia, professores e funcionários, pela ajuda e por colaborarem com meu amadurecimento como pós-graduanda

Aos meus novos amigos de trabalho da BASF S.A, pelas boas-vindas com que me recepcionaram e pelo voto de confiança

Aos pesquisadores e funcionários da U.S. Environmental Protection Agency (USEPA), em especial Susan, Katie, Hongzu, Carlton, Bill, Chis, Mitch, pela paciência e pelo crescimento profissional que me proporcionaram

À Fundação de Amparo a Pesquisa do Estado de São Paulo – FAPESP, pelo suporte financeiro.

Ao Núcleo de Avaliação do Impacto Ambiental Sobre a Saúde Humana, TOXICAM, pelo suporte na realização deste trabalho.

A todas as pessoas que contribuíram para que este trabalho fosse concluído, meu muito obrigada!

CONTENTS

INTRODUCTION **13**

Diuron 13

Urinary Bladder Carcinogenesis 16

Toxicogenomics and Microarray 19

REFERENCES **21**

GENERAL OBJECTIVE **26**

MANUSCRIPT 1 ..... **27**

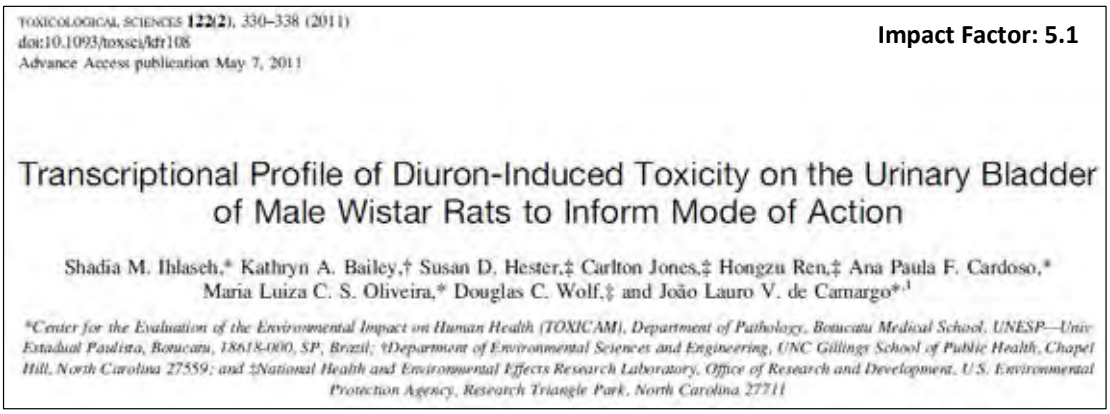

TOXICOLOGICAL SCIENCES **122(2)**, 330–338 (2011)
doi:10.1093/toxsci/kfr108
Advance Access publication May 7, 2011

Impact Factor: 5.1

Transcriptional Profile of Diuron-Induced Toxicity on the Urinary Bladder of Male Wistar Rats to Inform Mode of Action

Shadia M. Ihlaseh,* Kathryn A. Bailey,† Susan D. Hester,‡ Carlton Jones,‡ Hongzu Ren,‡ Ana Paula F. Cardoso,* Maria Luiza C. S. Oliveira,* Douglas C. Wolf,‡ and João Lauro V. de Camargo*,[1]

*Center for the Evaluation of the Environmental Impact on Human Health (TOXICAM), Department of Pathology, Botucatu Medical School, UNESP—Univ Estadual Paulista, Botucatu, 18618-000, SP, Brazil; †Department of Environmental Sciences and Engineering, UNC Gillings School of Public Health, Chapel Hill, North Carolina 27559; and ‡National Health and Environmental Effects Research Laboratory, Office of Research and Development, U.S. Environmental Protection Agency, Research Triangle Park, North Carolina 27711

Supplementary tables **37**

MANUSCRIPT 2 ..... **46**

1 Abstract **48**

2 Introduction **49**

3 Materials And Methods **51**

3.1 Chemicals 51

3.2 Animal treatment and sample collection 51

3.3 Scanning-Electron Microscopy (SEM) 52

3.4 Statistical analyses 53

3.5 RNA extraction 53
3.6 Affymetrix microarray hybridization 53
3.7 Microarray data analysis 54
4 Results 55
4.1 Body weight, water and diet consumption 55
4.2 Urothelial morphology by histological and SEM analyses 56
4.3 Microarray analysis 56
4.4 Gene expression profile and urothelial morphology after 7 days of exposure to diuron 58
4.5 Time relationship – comparison of gene expression profiles of 7-day and 20-week studies 58
5 Discussion 60
6 Suplementary Data 62
7 Funding 62
8 Acknowledgements 63
9 References 63
10 Tables 67
11 Figure Legends 68
12 Supplementary tables 74
CONCLUSION 107
ATTACHMENTS 108

INTRODUCTION

Diuron

Diuron [3-(3,4-dichlorophenyl)-1,1-dimethylurea] (CAS number: 330-54-1) is an herbicide in the urea chemical family (Figure 1) used on a variety of both crop and non-crop areas. Diuron has been registered in the United States since 1967, and the average annual domestic use is approximately nine to ten million pounds of active ingredient, two thirds of which is used on agricultural crops (USEPA, 2003). Crops with the highest percent of use are citrus, berries, asparagus and pineapple. In Brazil, it is widely used on soy bean, cotton, and sugar cane fields. The use of diuron on sugar cane has broad impact in Brazil as sugar cane is not only a food crop but also a source of biofuel. In addition to its use on commodity crops, diuron is also used as a moldicide in paints and stains, and as an algaecide in commercial fish production.

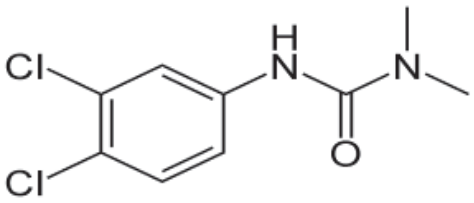

Figure 1: Diuron chemical structure

The mechanism of herbicidal action of diuron is inhibition of photosynthesis by preventing oxygen production (Wessels and Van der Veen, 1956). The formation of reactive oxygen species (ROS) by diuron results in peroxidative destruction of pigments, proteins, and nucleic acid as well as disintegration of cellular membrane systems by lipid peroxidation (Geoffroy et al., 2002).

Regarding diuron physical and chemical properties, it is a colourless crystalline non-ionic compound in its pure form, with moderate water solubility. The rate of its hydrolysis is negligible at neutral pH but increases as the conditions become strongly acidic or alkaline, leading to its principal derivative, 3,4-dichloroaniline (3,4-DCA) (Salvestrini, 2002), considered the major breakdown product of diuron in the environment and an important environmental pollutant (Giacomazzi & Cochet, 2004). Diuron is highly persistence, with half-life from one month to one year, allowing finding it in many environment compartments such as soil, water and groundwater (Field et al., 2003).

Diuron has low acute toxicity, by oral, dermal or inhalation routes of exposure, with oral LD_{50} for rats of aproximately 4000 mg/Kg body weigh (b.w.) (USEPA, 2003; EFSA, 2005). Diuron is rapidly absorbed by gastrointestinal and respiratory systems; the primary diuron target sites are blood, kidneys, and urinary bladder. It is metabolized within 24 to 48 hours post orally administration by gavage in Sprague-Dawley rats. In both sexes of the exposed rats, urine is the major route of excretion, with 3,4(dichlorophenyl)urea (DCPU) the predominant metabolite, followed by smaller amounts of 3,4(dichlorophenyl)methylurea (DCPMU), DCA, and 3,4-dichlorophenol (DCP) (Hodge et al., 1967). In humans, it is metabolized within hours by hydroxylation and N-dealkylation, then excreted via urine (Hayes, 1982).

Diuron did not affect the fertility rate in reproductive toxicity studies (Iyer, 2002). The developmental (fetal) NOAEL was determined to be 80 mg/kg/day, based on increases in delayed ossification of vertebrae and sternebrae as well as decreased fetal weights at the LOAEL of 400 mg/kg/day (U.S. EPA, 2001).

It has been shown that diuron induces methaemoglobinemia, splenomegaly, hemolytic anemia and compensatory hematopoiesis in rats (USEPA, 2003). High doses of diuron

exposure caused severe depletion of splenic white pulp compartment associated to a decreased number of CD4+ T lymphocytes, increased extramedullary hematopoiesis and deposition of hemosiderinin in the red pulp after a 28-day study (Domingues et al., 2011).

Diuron has been considered a nongenotoxic agent. Although some of studies suggested that it is genotoxic (Agrawal et al., 1996; Agrawal and Mehrota, 1997; Bouilly et al., 2007; Canna-Michaelidou and Nicolaou, 1996), others report that diuron is a nongenotoxic compound (APVMA, 2005; Gee, 1997; Iyer, 2002; USEPA, 2003). Two previous studies from our laboratory showed absence of genotoxicity in the standard alkaline version of the single-cell gel (comet) assay conducted with urinary bladder cells and peripheral blood leukocytes of male Wistar rats exposed through diet for 20 weeks to different concentrations of diuron (Nascimento et al., 2006) and in the specialized *in vitro* comet assay protocol designed to detect cross-linking in CHO cells (Rocha et al., 2010).

Diuron has been characterized as a "known/likely" human carcinogen by the U.S Environmental Protection Agency (EPA) based on a two-year bioassay that demonstrated urinary bladder carcinomas in both sexes of the Wistar rat, renal pelvis carcinomas in the Wistar male rat and mammary gland carcinomas in the female NMRI mouse after exposure to 2500 ppm diuron in the diet (Iyer, 2002; USEPA, 2003, 2004). A previous study from our laboratory observed increased incidence of urothelial necrosis and increased urothelial cell proliferation in male Wistar rats exposed to the carcinogenic dose of diuron for 20 weeks, suggesting that cell death and consequent regenerative hyperplasia, but not direct mitogenesis, was the carcinogenic MOA of this herbicide (Nascimento et al., 2006). Recently, effects such as changes in urinary solids and pH have been shown not to be key events in diuron-induced carcinogenicity and it is was proposed that direct action of diuron and/or its urinary metabolites caused sustained urothelial cytotoxicity and necrosis followed

by regenerative hyperplasia, which eventually leads to urothelial neoplastic development (Rocha et al., 2010). The specific MOA and molecular events trigged by diuron, however, have not been previously assessed.

Urinary Bladder Carcinogenesis

Bladder cancer is one of most common urologic malignancies worldwide, with approximately 330,000 new cases occurring each year (Sanderson et al., 2007). The most common type of bladder cancer is urothelial carcinoma, also called transitional-cell carcionama (TCC) (Eble et al., 2004). The TCC can be classified as papillary, which is usually low grade and rarely invasive, and as nonpapillary type, that trends to be high grade and invasive (Dinney et al., 2004; Crawford, 2008). In animal models, the TCC can be similar to the disease in humans, but tend to occur separatedely: in the rat it is nearly always the papillary type, with morphologic stages of simple hyperplasia, papillary and nodular hyperplasia, papilloma, noninvasive and invasive carcinoma; in the mouse it can follow a sequence from dysplasia, with or without hyperplasia, to carcinoma in situ and to high grade invasive carcinomas (Cohen, 1998).

Since Rehn in 1895, a practicing surgeon in Germany, reported the occupational bladder cancer in men in the aniline dye industry, several environmental factors have been involved in urinary bladder carcinogenesis (Cohen & Johansson, 1992; Hirao et al., 2009). Posterior studies reveled that the aromatic amines, such as 2-naphthylamine and benzidine, were responsible for bladder cancer in workers from dyestuff, rubber and textile industries (Murta-Nascimento, et al., 2007). Cigarette smoking is the major etiologic factor for urinary bladder cancer, in part due to the production of aromatic amines (Sanderson et al., 2007). Other possible and largely variable risk factors are chronic exposure to environmental

contaminants in drinking water, as triahalomethanes and arsenic, radiation, chronic urinary tract infection caused by *Schistosoma haematobium*, diets high in fat, changes in urinary pH, and hereditary polymorphisms of xenobiotic-metabolizing enzymes such as N-acetyltransferases (NATs) and glutathione S-transferases (GSTs) (Scelo and Brennan, 2007; Sanderson et al., 2007).

Coumponds known to be carcinogen to humans have primarily been identified by epidemiological studies. However, epidemiological data are usually not suitable to stablish risk from exposure to different levels of human carcinogens and are available only after exposed humans develop cancers (Scelo and Brennan, 2007). The two-year rodent bioassay was then developed to provide a standardized screening procedure for evaluating chemicals with the assumption that these were predictive of human carcinogenic risk (Cohen, 2004). However, due to the elevated cost, extended time to conduct that study and limited data based only on morphological endpoint without knowledge of how the agent trigged that specific endpoint (study "black-box" type), several alternatives to the two-year bioassay have been proposed, based in mechanistic approaches to animal bioassays. Therefore, defining the mode of action (MOA) by wich chemicals induce tumors in experimental models has become a key to judgments about the relevance of such tumor data for human risk assessment (Cohen et al., 2004).

Carcinogens to the urinary tract epithelium (urothelium) have been shown to operate mechanistically in animal models via DNA reactive, when genotoxic or via sustained stimulation of cell proliferation, a nongenotoxic MOA (Cohen et al., 1998). Genotoxic coumpound binds covalently to DNA, forming adducts that can interfere with normal DNA metabolism, causing DNA mutations that without repair can lead to carcinogenicity (Fukushima et al., 2010). Nongenotoxic coumpounds produce errors in DNA indirectly, by

decreasing cell death or increasing cell proliferation; increased cell division can occur either by direct mitogenesis, associated with growth factor stimuli and receptors, or by toxicity and regenerative proliferation (Cohen, 2004). No bladder carcinogenic agents have been shown to act by inhibiting cell death (Cohen et al., 2007a).

There are essentially two MOAs that induce cytotoxicity and regenerative proliferation in the urinary bladder. The best understood process is related to the urinary solids formation, such as precipitates, microcrystlas and calculi, usually with alterations in urinary pH or composition. Solids present in urine can cause abrasion of the mucosal surface, resulting in necrosis followed by regenerative proliferation that lead to urothelial hyperplasia and, eventually to cancer (Cohen and Lawson, 1995). This MOA of bladder cancer based on calculi formation has been demonstrated to present low relevance to humans, probably due to the difference of rodent horizontal urinary bladder versus human vertical urinary bladder, which affects the carcinogenic hazard from calculi (Cohen and Lawson, 1995). For example, melamine produces calculi and bladder tumors in rats but not in humans (Cohen, 2004).

Other possible MOA for toxicity and regeneration is direct activity of the chemical and/or its metabolites excreted in urine. O-phenylphenol, an agricultural fungicide and hospital desinfectant, induces hyperplasia of the rat urinary bladder and ultimately leads to bladder tumors, without urinary solids formation but with cytotoxicity and regeneration of the superficial layer of the urothelium (Appel, 2000; Cohen et al., 1998). Also, organic arsenics have been shown to be carcinogenic to rat urinary bladder, through a nongenotoxic MOA that involves toxic metabolites formation in urine that cause cell death followed by regenerative cell proliferation (Cohen et al., 2007a; Sams II et al., 2007).

Scanning-electron microscopy (SEM) is a powerfull technical procedure for morphological analysis that allows the visualization of subtle signs of citotoxicity and

necrosis of the superficial cell layer, that are not seen by light microscopy. Therefore, SEM is currently a more reliable and convenient means of evaluating the large luminal surface area of urothelium than light microscopy (Cohen et al., 2007b).

Toxicogenomics and Microarray

Toxicogenomics is defined as the application of molecular technologies (genome sequence analysis, gene expression profiling, proteomics, metabolomics) to study the adverse effects of environmental and pharmaceutical chemicals on human health and the environment (NRC, 2007). The combination of toxicogenomics with conventional toxicology allows investigating the interaction between genes and environmental stress in disease causation, what can provide response of biological pathways and networks to chemical perturbation (NRC, 2007; Waters and Fostel, 2004).

Toxicogenomic technologies present new opportunities to improve risk assessment by potentially increasing the understanding of dose-response relationships, crossspecies extrapolations, exposure quantification, the underlying mechanisms of toxicity, and the basis of individual susceptibilities to particular compounds. Also, toxicogenomics can provide additional molecular level information and tests that add to the "weight of the evidence" for refining judgments about the risks posed by environmental toxicants and drugs (NRC, 2007).

Microarrays enabled the rise of toxicogenomics in the late 1990s (Schmidt, 2002). Microarrays are silicon or glass chips coated with thousands of discrete spots of nucleic acids called probes. Each probe corresponds to a specific DNA sequence. To use the technology, RNA from a biological sample is "reverse transcribed", or used to produce an identical copy of the gene that would normally be produced in a living cell. This complementary DNA (cDNA) is labeled with a fluorescent tag and bound to the chip. Ideally, each molecule in the

labeled cDNA hybridizes to its complementary probe on the array. Using quantitative imaging techniques that read the fluorescence is possible to identify the genes expressed in the original biological sample and their relative levels of expression (Schmidt, 2002).

Several studies are using the microarray technology in an integrative manner with the traditional toxicology to explore dose-response relationships for greater understanding of mode of action (MOA) (Sen et al., 2005; Nesnow et al., 2009; Ludwig et al., 2011). This approach may lead to the recognition of pathways signatures of toxic injury indicative of the MOA, observed prior to its morphological and or clinical manifestation. However, this relatively recent tool bears important challenges such as to extract biological meaning from the high-throughput microarray data, since the current understanding of the global molecular-landscape encompasses only a lower level of complexity (Waters & Fostel, 2004).

Toxicogenomic studies are improving our knowledge of the underlying biology and the regulatory networks that integrate the signaling cascades involved in toxicity. Thus, toxicogenomic data may advance the introduction of mechanistic insight into risk assessment and fulfill the promise of more accurate and expedited elucidation of class-related biologic effects or predictive toxicity.

REFERENCES

1. Agrawal, R.C., Kumar, S., and Mehrotra, N.K. (1996). Micronucleus induction by diuron in mouse bone marrow. *Toxicol Lett.* **89,** 1-4.
2. Agrawal, R.C., and Mehrotra, N.K. (1997). Effect of diuron on germ cells of mice. *Indian J Exp Biol.* **35,** 1256-7.
3. Appel, K.E. (2000). The carcinogenicity of the biocide ortho-phenylphenol. *Arch Toxicol.* **74**, 61-71.
4. Australian Pesticides and Veterinary Medicine Authority (APVMA). (2005). The reconsideration of approvals of the active constituent diuron, registrations of products containing diuron and their associated labels. *Tech. Assess. Rep*. **2,** 13–14.
5. Bouilly, K., Bonnard, M., Gagnaire, B., Renault, T., and Lape`gue, S. (2007). Impact of diuron on aneuploidy and hemocyte parameters in Pacific oysters, Crassostrea gigas. *Arc. Environ Contam Toxicol*. **52**, 58–63.
6. Canna-Michaelidou, S., and Nicolaou, A.S. (1996). Evaluation of the genotoxicity potential (by Mutatox^{TM} test) of ten pesticides found as water pollutants in Cyprus. *Sci Total Environ.* **193,** 27-35.
7. Cohen, S. M. (1998). Urinary bladder carcinogenesis. *Toxicol. Pathol*. **26**, 121–127.
8. Cohen, S.M., Johansson, S.L. (1992). Epidemiology and etiology of bladder cancer. *Urol Clin North Am*. **19,** 421-428.
9. Cohen, S.M., Lawson, T.A. (1995). Rodent bladder tumors do not always predict for humans. *Cancer Lett.* **93,** 9-16.
10. Cohen, S.M. (2004). Human carcinogenic risk evaluation: an alternative approach to the two-year rodent bioassay. *Toxicol Sci*. **80,** 225-229.

11. Cohen, S.M., Klaunig, J., Meek, M.E., Hill, R.N., Pastoor, T., Lehman-McKeeman, L., Bucher, J., Longfellow, D.G., Seed, J., Dellarco, V., Fenner-Crisp, P., Patton, D. (2004). Evaluationg the human relevance of chemically induced animal tumors. *Toxicol Sci.* **78,** 181-186.

12. Cohen, S.M., Ohnishi, T., Arnold, L., Le, X.C. (2007a). Arsenic-induced bladder cancer in animal model. *Toxicol Appl Pharmacol*. **222**, 258-263.

13. Cohen, S.M., Ohnishi, T., Clark, N.M., He, J., Arnold, L.L. (2007b). Investigations of rodent urinary bladder carcinogens: collection, processing, and evaluation of urine and bladders. *Toxicol Pathol* **35**, 337-47.

14. Crawford J.M. (2008). The origins of bladder cancer. *Lab Invest.* **88**, 686-693.

15. Dinney, C.P.N., McConkey, D.J., Milikan, R.E., Wu, X., Bar-Eli, M., Adam, L., Kamat, A.M., Siefker-Radtke, A.O., Tuziak, T., Sabichi, A.L., Grossman, B., Benedict, W.F., Czerniak, B. (2004). Focus oon bladder cancer. *Cancer Cell.* **6,** 111-116.

16. Domingues, A., Barbisan, L.F., Martins, P.R., Spinardi-Barbisan, A.L.T. (2011). Diuron exposure induces systemic and organ-specific toxicity following acute and sub-chronic exposure in male Wistar rats. *Environ Toxicol Pharmacol*. **31**, 387-96.

17. Eble JN et al. (Eds; 2004) World Health Organization classification of tumours-pathology and genetics of tumours of the urinary system and male genital organs. Lyon: International Agency for Research on Cancer.

18. European Food Safety Authority (EFSA). (2005). Draft assessment report (DAR) – Diuron – Toxicology and metabolism. Volume 3, Annex B6, pp. 367.

19. Field, J.A., Reed, R.L., Sawyer, T.E., Griffith, S.M., Wigington, P.J. (2003). Diuron occurrence and distribution in soil and surface and ground water associated with grass seed production. *J Environ Qual*. **32**, 171–179.

20. Fukushima, S., Wei, M., Kakehashi,A., Wanibuchi, H. (2010). Threshols for genotixoc carcinogens: evidence from mechanism-based carcinogenicity studies. In Cancer risk assessment (C. H. Hsu and T. Stedeford, Eds.), 1st ed., pp. 207-221. John Wiley & Sons Inc. Publication, Hoboken, New Jersey.

21. Gee J. (1997). Summary on toxicologic data. Diuron. Medical Toxicology Branch. Department of Pesticide Regulation. California Environmental Protection Agency. 7p. Accessed on cdpr.ca.gov/docs/risk/toxsums/pdfs/231.pdf.

22. Geoffroy, L., Teisseire, H., Couderchet, M., and Vernet, G. (2002). Effect of oxyfluorfen and diuron alone and in mixture on antioxidative enzymes of Scenedesmus obliquus. *Pestic. Biochem. Physiol*. **72**, 178-185.

23. Giacomazzi, S., Cochet, N. (2004). Environmental impact of diuron transformation: a review. *Chemosphere* **56**, 1021–1032.

24. Hayes, W.J.Jr. (1982). Pesticides studied in man. Williams and Wilkins, Baltimore, MD, p. 672.

25. Hirao, Y., Kim, W.J., Fujimoto, K. (2009). Environmental pfactors promoting bladder cancer. *Curr Opin Urol.* **19,** 494-499.

26. Hodge, H.C., Downs, W.L., Panner, B., Smith, D., Maynard, E., Clayton, J.Jr., Rhodes, R. (1967). Oral toxicity and metabolism of Diuron in rats and dogs. *Food Cosmet Toxicol* **5**, 513.

27. Iyer, P. (2002). Evidence on the Development and Reproductive Toxicity of Diuron Draft. Reproductive and Cancer Hazard Assessment Section. The Office of Environmental Health Hazard Assessment, California Environmental Protection Agency, Sacramento, CA. p. 43.

28. Ludwig S., Tinwell, H., Schorsch, F., Cavaille´, C., Pallardy, M., Rouquie´, D., Bars, R. (2011). A Molecular and Phenotypic Integrative Approach to Identify a No-Effect Dose Level for Antiandrogen-Induced Testicular Toxicity. Tox Sci. **122**, 52-63.

29. Murta-Nascimento, C., Schmitz-Dräger, B. J., Zeegers, M. P., Steineck, G., Kogevinas, M., Real, F. X., and Malats, N. (2007). Epidemiology of urinary bladder cancer: from tumor development to patient's death. *World J. Urol.* **25**, 285-295.

30. Nascimento, M. G., de Oliveira, M. L. C. S., Lima, A. S., and de Camargo, J. L. V. (2006). Effects of diuron [3-(3,4-dichlorophenyl)-1,1-dimethylurea] on the urinary bladder mucosa of male Wistar rats. *Toxicology.* **224**, 66-73.

31. National Research Council (NRC). (2007). Applications of Toxicogenomic Technologies to Predictive Toxicology and Risk Assessment. National Academies of Science, Wasington, pp.301.

32. Nesnow, S., Ward, W., Moore, T., Ren, H., and Hester, S. D. (2009). Discrimination of tumorigenic triazole conazoles from phenobasbital by transcriptional analyses of mouse liver gene expression. *Toxicol. Sci.* **110**, 68-83.

33. Rocha, M. S., Nascimento, M. G., Cardoso A. P. F., Lima, P. L. A., Zelandi, E. A., Camargo, J. L. V., de Oliveira, M. L. C. S. (2010). Cytotoxicity and regenerative proliferation as the mode of action for diuron-induced urothelial carcinogenesis in the rat. *Toxicol. Sci.* **113**, 37-44.

34. Salvestrini, S., Di Cerbo, P., Capasso, S. (2002). Kinetics of the chemical degradation of diuron. *Chemosphere* **48**, 69-73.

35. Sams II, R., Wolf, D. C., Ramasamy, S., Ohanian, Ed., Chen, J., and Lowit, A. (2007). Workshop overview: arsenic research and risk assessment. *Toxicol App. Pharmacol.* **222**, 245-251.

36. Sanderson, S., Salanti, G., Higgins, J. (2007). Joint effects of the N-acetiltransferase 1 and 2 (NAT1 and NAT2) genes and smoking on bladder carcinogenesis: a literature-based systematic HuGE review and evidence synthesis. *Am J Epidemiol* **166**, 741-751.

37. Scélo, G., and Brennan, P. (2007). The epidemiology of bladder and kidney cancer. *Nat Clin Pract* **4**, 205-17.

38. Schimidt, C.W. (2002). Focus Toxicogenimics: an emerging discipline. *Env Health Prospec.* **110,** 750-755.

39. Sen, B., Wang, A., Hester, S., Robertson, J. L., Wolf, D. C. (2005). Gene expression profiling of response to dimethylarsenic acid in female F344 rat urothelium. *Toxicology*. **215**, 214-226.

40. USEPA (2002). Evidence on the developmental and reproductive toxicity of diuron. Reproductive and cancer hazard assessment section. Office of Environmental Health Hazard Assessment. California Environmental Protection Agency – Draft. 43p.

41. U.S. Environmental Protection Agency (USEPA). (2003). Registration Eligibility Decision for Diuron List A. Case 0046. Office of Prevention, Pesticides and Toxic Substances, USEPA, Washington, DC, p. 22.

42. U. S. Environmental Protection Agency (USEPA). (2004). Chemicals evaluated for carcinogenic potential. Office of Pesticide Programs, Health Effects Division. Science Information Management Branch, Washington, D.C., 106.

43. Waters, M. D., Fostel, J. M. Toxicogenomics and systems toxicology: aims and prospects. (2004). *Nat Rev Genet.* **5**, 937-948.

44. Wessels, J.S., Van, D.E.R., Veen, R. (1956). The action of some derivatives of phenylurethan and of 3-phenyl-1, 1-dimethylurea on the Hill reaction. *Biochem Biophys Acta.* **19**, 548-9.

GENERAL OBJECTIVE

The present studies were conducted to inform the mode of action of diuron on the urinary bladder urothelium of male Wistar rats focusing particularly on dose- and time-response of molecular and morphological alterations registered after 7-day and 20-week long periods of exposure to the herbicide.

Approach:

- To determine the genome-wide gene expression profiles in urothelial cells using cDNA microarray
- To compare the gene expression profiles observed after 7-day and 20-week periods of exposure in order to verify the functional pathways involved in diuron toxicity at an early time point.
- To describe morphologicaly urothelial lesions induced by diuron by histology and scanning-electron microscopy (SEM) in short- and medium-term periods do exposure
- To compare the gene expression profile with the morphological lesions to relate the gene expression changes directly to observed toxic effects in the target tissue and determine if it is possible to distinguish toxic from non-toxic doses by gene expression studies.

Manuscript 1

TOXICOLOGICAL SCIENCES **122(2)**, 330–338 (2011)
doi:10.1093/toxsci/kfr108
Advance Access publication May 7, 2011

Transcriptional Profile of Diuron-Induced Toxicity on the Urinary Bladder of Male Wistar Rats to Inform Mode of Action

Shadia M. Ihlaseh,* Kathryn A. Bailey,† Susan D. Hester,‡ Carlton Jones,‡ Hongzu Ren,‡ Ana Paula F. Cardoso,* Maria Luiza C. S. Oliveira,* Douglas C. Wolf,‡ and João Lauro V. de Camargo*,[1]

**Center for the Evaluation of the Environmental Impact on Human Health (TOXICAM), Department of Pathology, Botucatu Medical School, UNESP—Univ Estadual Paulista, Botucatu, 18618-000, SP, Brazil; †Department of Environmental Sciences and Engineering, UNC Gillings School of Public Health, Chapel Hill, North Carolina 27559; and ‡National Health and Environmental Effects Research Laboratory, Office of Research and Development, U.S. Environmental Protection Agency, Research Triangle Park, North Carolina 27711*

[1]To whom correspondence should be addressed. Fax: +55-014-3815-2348. E-mail: decam@fmb.unesp.br.

Received February 9, 2011; accepted April 27, 2011

Diuron (3-(3,4-dichlorophenyl)-1,1-dimethylurea) is a substituted urea herbicide that induces rat urinary bladder urothelial tumors at high dietary levels (2500 ppm). The specific mode of action and molecular alterations triggered by diuron, however, have not been clarified. The present study evaluated the dose-dependent effects of mucosal alterations and transcriptional changes in the urinary bladder of rats exposed to diuron. Six-week-old male Wistar rats were treated with 0, 60, 125, 1250, and 2500 ppm of diuron in the diet for 20 weeks. Histologic examination showed urothelial hyperplasia present in rats treated with either 1250 or 2500 ppm of diuron but not 60 or 125 ppm. Comprehensive gene expression analyses of urothelial cell RNA were conducted using Affymetrix microarrays. The numbers of differentially expressed transcripts between each treatment group and control increased with diuron dose. Based on similar histology and gene expression responses, the treatment groups were regrouped into a high-dose (1250 and 2500 ppm) and low-dose group (60 and 125 ppm). These data suggest that persistent exposure to high dietary concentrations of diuron induces oxidative stress, increases cellular metabolism, and enhances cell death that is associated with sustained urothelial hyperplasia.

Key Words: **diuron; urinary bladder; carcinogenesis; gene expression profiling; microarray analysis.**

Diuron (3-(3,4-dichlorophenyl)-1,1-dimethylurea) is a substituted urea herbicide used on a variety of both crop and noncrop areas. The main crops treated with diuron in the United States are citrus, berries, asparagus, pineapple, and cotton (USEPA, 2004). In Brazil, it is widely used on soybean, cotton, and sugar cane fields. The use of diuron on sugar cane has broad impact in Brazil as sugar cane is not only a food crop but also a source of biofuel. In addition to its use on commodity crops, diuron is also used as a moldicide in paints and stains and as an algaecide in commercial fish production. Therefore, there is great potential for widespread human exposure.

The mechanism of herbicidal action of diuron is inhibition of photosynthesis (Geoffroy *et al.*, 2002). A previous study indicated that diuron generates reactive oxygen species (ROS) in plants, leading to peroxidative destruction of pigments, proteins, nucleic acids, and lipids (Geoffroy *et al.*, 2002). Diuron does accumulate in the environment. It can be found in the soil, water and in fewer amounts in groundwater, because of its slow breakdown (a month to a year) (Cox, 2003; Giacomazzi and Cochet, 2004). The U.S. Department of Agriculture reported a half-life of 90 days for diuron in the soil (*apud* Cox, 2003). In rats and dogs fed diuron, the predominant metabolite in urine is 3,4-(dichorophenil) urea and only small amounts of DCA and others are found (Hodge *et al.*, 1967). DCA was pointed as the most important pollutant resulting from the breakdown of diuron in the environment; however, there is no evidence to state that the DCA is the main compound in soil (Giacomazzi and Cochet, 2004). Because of the lack of epidemiological data, we are not aware of parental diuron or diuron metabolites in the urine of humans.

Diuron has been characterized as a "known/likely" human carcinogen by the U.S. Environmental Protection Agency (USEPA) based on a 2-year bioassay that demonstrated urinary bladder carcinomas in both sexes of the Wistar rat, renal pelvis carcinomas in the Wistar male rat, and mammary gland carcinomas in the female NMRI mouse after exposure to 2500 ppm diuron in the diet (Iyer, 2002; USEPA, 2003, 2004). A previous study from our laboratory observed an increased incidence of urothelial necrosis and hyperplasia associated with increased urothelial cell proliferation in male Wistar rats exposed to the carcinogenic dose of diuron for 20 weeks (Nascimento *et al.*, 2006). As genotoxicity evaluations of diuron have generally been negative, the urothelial carcinogenicity of diuron is believed to occur through a nongenotoxic mode of action (MOA) (Gee, 1997; Iyer, 2002; Nascimento *et al.*, 2006; Rocha *et al.*, 2010; USEPA, 2003). Indirect effects

such as changes in urinary solids and pH have been shown not to be key events in diuron-induced carcinogenicity (Rocha *et al*., 2010). It is proposed that direct action of diuron and/or one of its urinary metabolites causes sustained cytotoxicity and necrosis followed by regenerative hyperplasia, which eventually leads to urothelial neoplastic development (Nascimento *et al*., 2006; Rocha *et al*., 2010).

The specific MOA and molecular alterations triggered by diuron, however, have not been defined. The present study aimed to evaluate diuron-induced alterations and to assess the dose-response of diuron on urinary bladder urothelium in male Wistar rats. As the first genomic screening to determine the major altered pathways involved in diuron-induced urothelial toxicity in rats, genome-wide gene expression profiling of RNA combined with light microscopy was used to evaluate the urothelium. It was anticipated that data from the transcript profiling would inform the MOA. The microarray data were compared with the histological observations to relate the gene expression changes directly to observed toxic effects in the target tissue and determine if it is possible to distinguish toxic from nontoxic doses by gene expression studies.

MATERIALS AND METHODS

Chemicals. Diuron (3-(3,4-dichlorophenyl)-1,1-dimethyl-urea) was obtained from Sigma Chemical Co. (CAS no. 30-54-1, 97% purity, St Louis, MO). It was mixed with Nuvilab powdered commercial diet from Nuvital (Colombo, PR, Brazil) at final diuron concentrations of 60, 125, 1250, and 2500 ppm.

Animal treatment and sample collection. This study was approved by the Committee for Ethics in Animal Experimentation of the UNESP Medical School (SP, Brazil). Six-week-old male Wistar rats were obtained from the Multidisciplinary Center for Biological Investigation—UNICAMP (Campinas, SP, Brazil). Following 2 weeks of acclimation, the rats were randomized into 5 groups of 15 animals each and received diuron in the pelleted feed at final concentrations of 0 (control), 60, 125, 1250, and 2500 ppm. Water and feed were provided *ad libitum*. Animals were monitored daily and cages, and bedding were changed three times per week. Water, feed consumption, and body weight were determined for each animal every other week of the experiment.

After 20 weeks, the rats were anesthetized with 3% sodium pentobarbital i.p. (30 mg/kg). Urinary bladders were removed from 10 rats in each group and processed by routine methods for histological analysis. Briefly, the urinary bladders were injected with Bouin's fixative, removed, and immersed in the same fixative for 4 h. They were then sectioned mid-sagitally, washed in 70% alcohol, embedded in paraffin, and stained with hematoxylin and eosin. Immediately after removal of the bladder, the animals were euthanized by opening the abdominal cavity and sectioning the inferior vena cava.

Five animals per group were used for RNA isolation from the urothelium and subsequent gene expression analysis. The rats were anesthetized and the urinary bladder exteriorized, tied off adjacent to the trigone, and removed. Urine was withdrawn from the bladders which were then injected with 1 ml of cold RNase-free PBS (Applied Biosystems, Foster City, CA) to remove exfoliated cells. All steps were carried out rapidly to minimize autolysis. The bladder was everted on a glass rod to expose the epithelium. The cells were gently shaved and transferred to 1 ml of TRIzol solution (Invitrogen Corporation, Carlsbad, CA). The urinary bladders were also inserted into the TRIzol solution followed by brief vortexing and kept for 10 min at room temperature, was then removed, and the TRIzol was transferred to liquid nitrogen followed by storage at −70°C until RNA extraction. The remaining urinary bladder was fixed in formalin and processed for histological examination as described above to evaluate the efficiency of removal of the urothelium. The efficiency of removal was graded according to the percentage (%) of epithelial cells remaining per bladder strip, being: < 5%—grade 0; 5 to 10%—grade 1; 11 to 50%—grade 2, and > 50%—grade 3. Only samples with grades 0 and 1 and with intact basal membrane were used in subsequent RNA isolation steps. The best three samples per group to proceed with the microarray experiments were chosen.

Urinary pH determination. The urine collection procedures were performed according to Cohen *et al*. (2007b). Briefly, for each rat, freshly voided urine was collected directly into a 1.5-ml microtube in the morning between 7:00 and 9:00 AM during the 6th and 14th weeks of the experiment. The urinary pH was measured immediately after collection of urine using a microelectrode (Analyser Comercio e Industria Ltda., Sao Paulo, SP).

Statistical analyses. Body weight, water and diet consumption, and urinary pH results were compared among the experimental groups using a one-way ANOVA ($p < 0.05$). Data demonstrating significant differences were then further evaluated with a Tukey's test to determine significant differences among groups ($p < 0.05$). A chi-square test was applied to evaluate the incidence of urinary histological lesions. The significance level of 5% was adopted for all analyses and were performed using Prism 3 (San Diego, CA).

RNA extraction. Total RNA was isolated using TRIzol Reagent in accordance with the manufacturer's protocol (Invitrogen). The total RNA pellet was resuspended in 100 μl of water and purified using the RNeasy Mini kit (Qiagen, Valencia, CA). Purified total RNA was eluted in dH_2O and its concentration was measured using a NanoDrop ND-1000 spectrometer (NanoDrop, Wilmington, DE). The quality of RNA was assessed using an Agilent Bioanalyzer (Agilent Technologies, Santa Clara, CA) and only samples having an RNA integrity number > 7.0 were used for microarray analyses. In the present study, one chip was used per animal and three chips were used per exposure group.

Affymetrix microarray hybridization. Gene expression analyses were conducted using Affymetrix GeneChip Rat Genome 230_2.0 Arrays (Affymetrix, Santa Clara, CA) which contain > 31,000 probe sets representing ~28,700 known rat genes. Total RNA (1 μg) for each sample was amplified and labeled by the BioArray RNA Amplification and Biotin labeling System (Enzo Life Science, Farmingdale, NY). For each array, 12 μg of amplified biotin-cRNA was fragmented and hybridized to the array for 16 h at 45°C in a rotating hybridization oven using the Affymetrix Eukaryotic Target Hybridization controls and protocol. The arrays were washed using the EukGE-WS2v5 protocol of the Affymetrix Fluidics Station FS450 and scanned using the Affymetrix Scanner 3000.

Microarray data analysis. Data from each microarray scan (.cel file) was imported into Rosetta Resolver version 7.1 (Rosetta Inpharmatics, Kirkland, WA) for data normalization (Weng *et al*., 2006) and for determination of transcripts that were differentially expressed between control and treated groups. To survey the data for within-group outliers and trends in data quality, unsupervised principal component analysis (PCA) was performed (Rosetta).

Transcripts that were differentially expressed among all treatment groups were identified using a one-way ANOVA with a false discovery rate (Benjamini-Hochberg test) of $p \leq 0.05$. A Tukey-Kramer *post hoc* test ($p \leq 0.05$) was then used to identify significant changes in expression between each group. Expression values for each differentially expressed transcript (DET) were reported in terms of their relative abundance in each treatment versus control group. Venn diagrams using DETs were employed to identify unique and common sequences between treatment groups. Pathway analysis was performed using Ingenuity Pathways Analysis (IPA) (Ingenuity Systems, http://www.ingenuity.com). The most significant biological functions and altered canonical pathways associated with the DETs in each of the treatment groups were determined using IPA.

TABLE 1
Body Weight Gain, Consumption of Water, Food, and Estimated Diuron Intake

Groups[a]	Final body weight (g)	Water consumption (ml/rat/day)	Food consumption (g/rat/day)	Diuron consumption (mg/rat/day)
Control	503.7 ± 45.7	33.3 ± 2.7	24.8 ± 1.5	—
60 ppm	477.2 ± 35.1	32.4 ± 2.0	22.4 ± 1.6	1.3 ± 0.1
125 ppm	487.5 ±50.7	34.2 ± 2.9	23.5 ± 1.6	2.9 ± 0.2
1250 ppm	448.5 ± 54.9[1]	32.8 ± 2.1	22.3 ± 1.8	22.9 ± 2.2
2500 ppm	390.5 ± 38.4[1,2]	28.0 ± 2.2[1,2]	19.0 ± 1.8[1]	47.8 ± 4.5

Note. 1, Significantly different from the control; 2, significantly different from 60-, 125-, and 1250-ppm groups.

[a]The groups represent the amount of diuron added to the food.

$p < 0.05$.

Cell cycle gene database. To evaluate genes related to cell proliferation, a series of genes have been identified that have cell cycle–dependent expression changes as observed in the HeLa cervical cancer cell line (Whitfield *et al*., 2002). The complete list of 1134 human genes was downloaded from http://genome-www.stanford.edu/Human-CellCycle/HeLa/data.shtml. The lists of DETs at 60, 125, 1250, and 2500 ppm were mapped to the 1134 human genes list to find the significant genes altered in a cell cycle phase-specific pattern (Fig. 5) (Nesnow *et al*., 2009).

RESULTS

Body Weight, Water and Diet Consumption, Urinary pH, and Histological Analyses

Table 1 summarizes the final body weigh and water and diet consumption. In general, all animals gained weight during the experiment. Mean body weight of the 2500-ppm group was less than control beginning from the third week of the experiment onward ($p < 0.05$). The 1250-ppm group also had significantly lower mean body weight gain compared with the control group. There was a reduction of food consumption by the 1250- and 2500-ppm groups ($p < 0.05$), and water consumption was significantly decreased in the 2500-ppm group (Table 1). The reduction in food consumption did not affect the relative diuron intake levels across the groups (Table 1).

Urinary pH values of each treatment group did not differ from the control (data not shown). Light microscopic examination of the urinary bladders identified an increased incidence of simple hyperplasia (SH) in rats treated with 1250- and 2500-ppm diuron (Table 2; Fig. 1).

Gene Expression Analysis

PCA was applied to the statistically significant DETs from all exposure groups (0, 60, 125, 1250, and 2500 ppm). PCA provides a 3D view of gene expression data, reducing its dimensionality and capturing the variability of the data set. Each chip is represented by a single point and points that cluster close together in 3D space have similar expression profiles. PCA therefore allows for the rapid and clear identification of outliers within treatment groups and similarities in expression trends among groups. Two clusters of separation were observed among the groups: the control, 60-ppm, and 125-ppm groups clustered together, whereas the 1250- and 2500-ppm groups clustered together separate from the control/low-dose cluster (Fig. 2).

TABLE 2
Incidence of Urinary Bladder Urothelial Lesions in Different Groups of Wistar Male Rats Fed for 20 Weeks with Diuron

Groups	*N*	Normal	Simple hyperplasia
Control	10	10	0
60 ppm	10	9	1
125 ppm	10	10	0
1250 ppm	10	2	8[a]
2500 ppm	10	3	7[a]

[a]Chi-square test, $p < 0.05$.

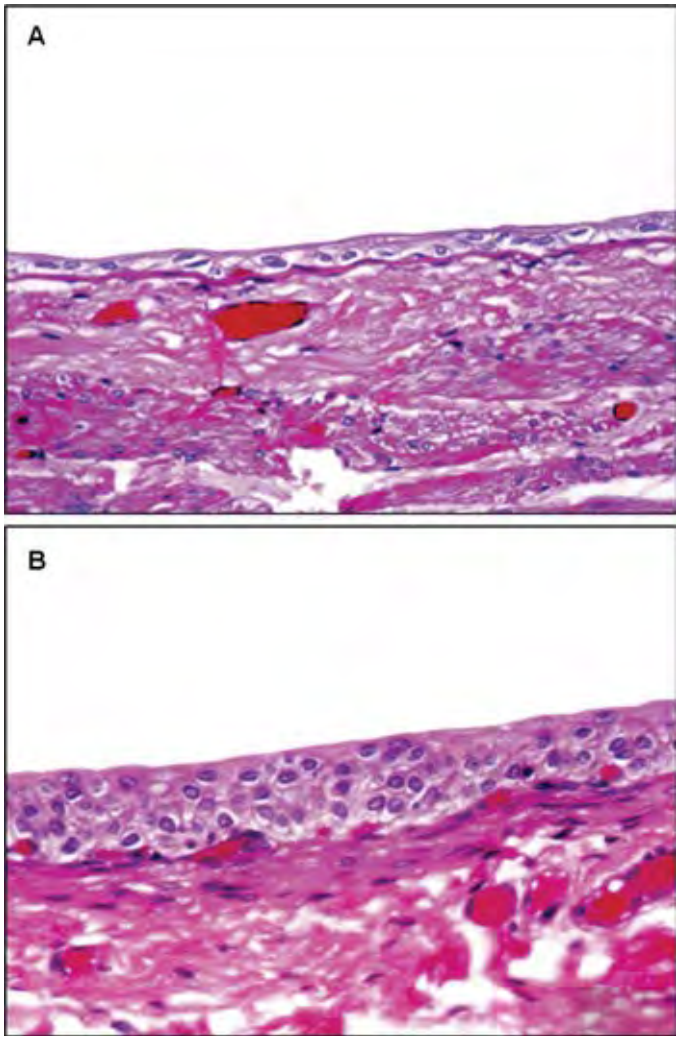

FIG. 1. Urinary bladder histology showing (A) normal epithelium in control and (B) simple hyperplasia in 2500 ppm diuron (hematoxylin and eosin ×40).

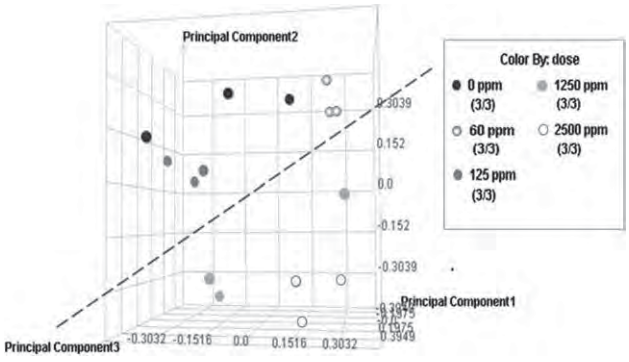

FIG. 2. PCA showing a separation of the high doses (1250 and 2500 ppm) from the low doses (60 and 125 ppm) and controls. Each chip is represented as a single data point.

TABLE 3
Number of DETs in the Wistar Rat Urothelium Modulated by 20 Weeks of Diuron Dietary Exposure Compared with Control

Groups	DET[a]	Increased expression	Decreased expression
60 ppm	257	90 (35%)	167 (65%)
125 ppm	291	231 (79%)	60 (21%)
1250 ppm	532	263 (49%)	269 (51%)
2500 ppm	997	450 (45%)	547 (55%)

[a]Determined using a one-way ANOVA by dose + Benjamini-Hochberg false discovery rate (FDR) ($p \leq 0.05$) followed by Tukey-Kramer *post hoc* test ($p \leq 0.05$) (Rosetta Resolver).

The number of DETs modulated by diuron treatment increased with the dietary concentrations of the herbicide. There were 257, 291, 532, and 997 DETs in cells from the 60-, 125-, 1250-, and 2500-ppm diuron-exposed groups, respectively (Table 3). The complete gene list is attached as a spreadsheet (.excel) as Supplementary data. More than 50% of DETs had reduced expression in the 60-, 1250-, and 2500-ppm groups, whereas ~21% of DETs had reduced expression in the 125-ppm group (Table 3).

Common and unique DETs across all groups were determined using Rosetta Resolver and are illustrated in Figure 3. This analysis identified that (1) the number of unique genes was 130, 219, 101, and 518 for 60-, 125-, 1250-, and 2500-ppm groups, respectively; (2) 78% (417) of the DETs in the 1250-ppm treatment group were also present in the 2500-ppm treatment group and 73% (308) of those sequences were exclusively shared between 1250- and 2500-ppm treatment groups; and (3) there were only 6 DETs in common among all treatment groups (*AK3*, *PIK3R1*, *ATP1B1*, *HTATIP2*, *MSLN*, *PROM1*), all of which had reduced transcript levels compared with controls.

Pathway Analysis

The lists of DETs were submitted for canonical pathway level analysis (IPA); only pathways statistically significant ($p < 0.05$) and containing at least three genes were retained for further evaluation (Hester *et al.*, 2006). The most significant diseases and biological function pathways altered in high-dose animals included cancer, amino acid metabolism, small molecule biochemistry, and cell death (Supplementary table S1). The most significant pathways associated with the low-dose group were involved in drug metabolism, lipid metabolism, and small molecule biochemistry (data not shown).

Dose-Responsive Pathways

Transcripts that are associated with the higher level function of cell death were significantly altered for all doses with a dose-response relationship (Supplementary table S2). Several canonical pathways were also modulated in a dose-responsive manner, including those that participate in glutathione metabolism, xenobiotic metabolism, NRF2-mediated oxidative stress response, and tryptophan metabolism (Fig. 4). The number of significantly altered canonical pathways also had a dose-response; 60-, 125-, 1250-, and 2500-ppm diuron groups had 9, 33, 34, and 46 altered pathways, respectively. In general, the 1250- and 2500-ppm exposure groups had similar altered pathways, which were associated with oxidative stress, such as xenobiotic metabolism and antioxidant defense mediated by glutathione, with the magnitude of expression change of transcripts in these pathways increasing with dose.

Division of Treatment Doses into Two Major Groups

Patterns in the data of this study indicate that the four treatment groups could be combined into two larger groups, a low-dose group (60 and 125 ppm) and a high-dose group (1250 and 2500 ppm). This separation is supported by intragroup similarities and intergroup differences in several aspects of the data: PCA results (Fig. 2), Venn diagrams demonstrating common and unique genes (Fig. 3), pathway-level analyses (Fig. 4), and the pattern of increased SH (Table 2). Therefore, the samples were rearranged into three groups: control, low dose (LD; 60 and 125 ppm), and high dose (HD; 1250 and 2500 ppm). This analysis showed that compared with the control, the numbers of DETs were 93 and 832 for LD and HD, respectively. In the LD group, there were seven significantly altered pathways with three to four genes mapped to each significant pathway and a low ratio (number of altered genes/total of genes into the pathway) of the significantly altered pathways. The results showed predominantly *CYP1A*, *CYP1B1*, and *UGT1A6* genes changed, reflecting metabolic effects. The HD group had 38 significantly altered pathways with an elevated ratio and high number of genes per pathway (3–24 genes/pathway). Because of redundancy of genes participating in more than one pathway, the pathways were grouped in major categories according to function. The categories included the genes that regulated amino acid metabolism, energy metabolism, lipid metabolism, oxidative stress response, signaling, immune system,

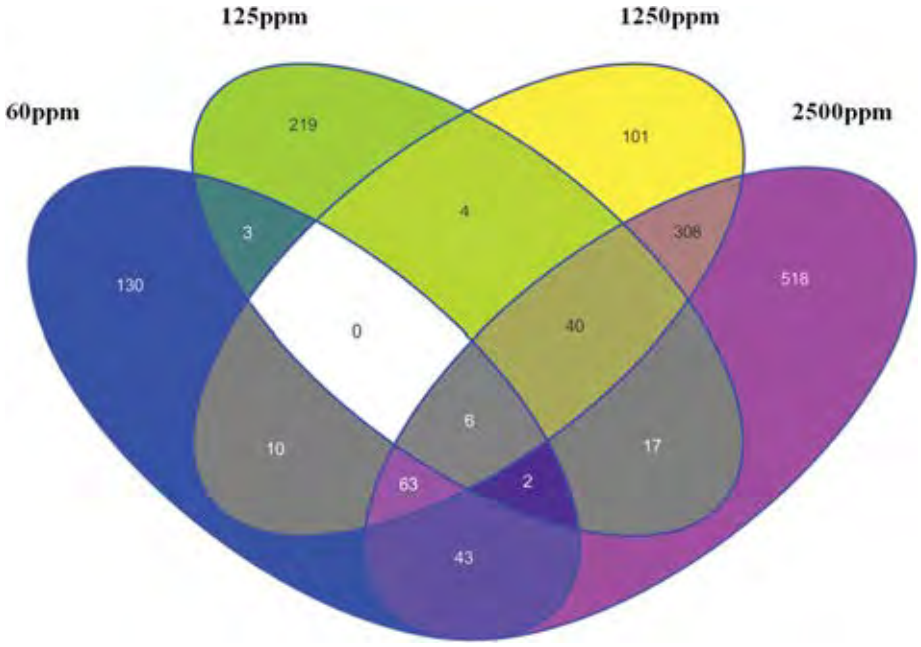

FIG. 3. Venn diagram of significantly altered transcripts for different doses after a 20-week diuron exposure.

adhesion, and cofactor/vitamin metabolism (Supplementary table S1).

Mapping DETs to Cell Cycle Database

To evaluate the relationship between changes in genes related to cell proliferation and the histological observation of simple hyperplasia, the DETs were mapped to cell cycle genes derived from Whitfield *et al.* (2002) and were organized by phases of the cell cycle (Fig. 5). There were only 6, 3, 5, and 13 genes changed at 60, 125, 1250, and 2500 ppm, respectively. Many of these genes function in G_2/M phase of the cell cycle.

DISCUSSION

The most significant finding from the present study was a dose-response characterization of urothelial toxicity after 20 weeks of treatment with diuron. The urothelial gene expression profile exhibited a dose-response effect in terms of the number of significantly modulated genes increased with diuron at progressively higher concentrations. The microarray analysis showed a clear difference in gene expression at the higher doses (1250 and 2500 ppm) in comparison with the lower doses (60 and 125 ppm). Further, these findings were consistent with the phenotypic histological response. In

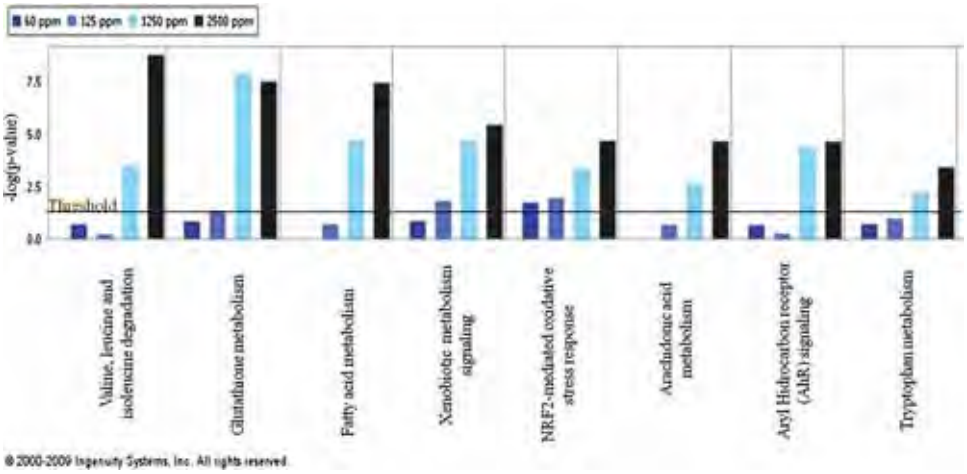

FIG. 4. Comparative analysis of significantly altered pathways presenting dose-response relationship using IPA. The y-axis depicts the probability that the genes within a data set are involved in a particular high-level biological function. The bars above the threshold line are statistically significant ($p < 0.05$).

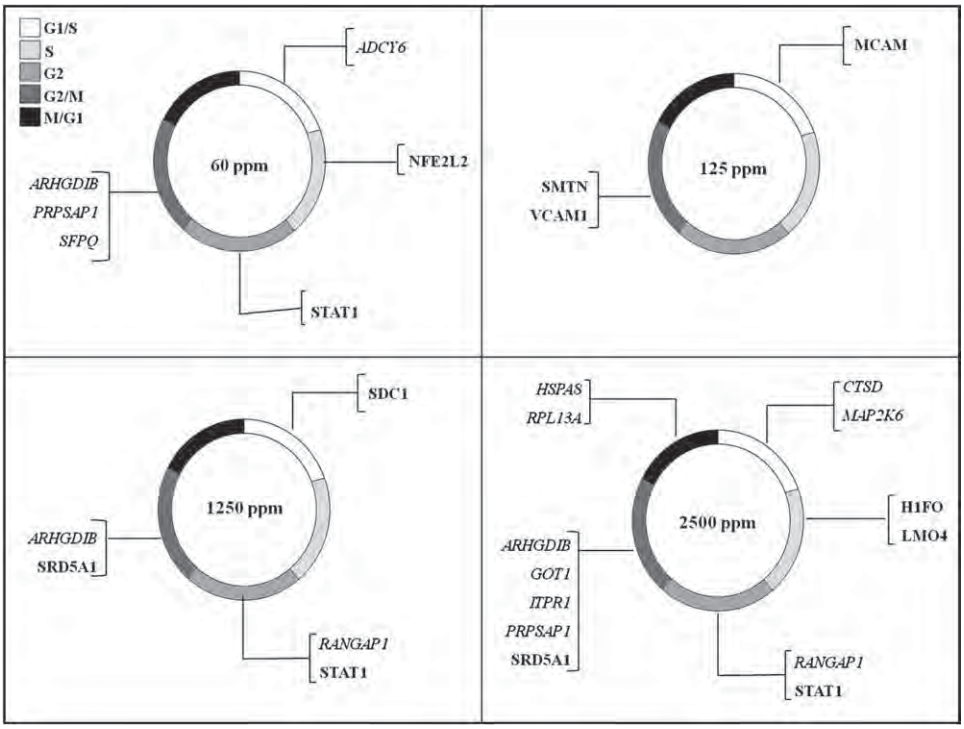

FIG. 5. Alterations of cell cycle genes within the phases of the cell cycle by the different diuron treatments after 20 weeks of exposure. Genes in bold have increased expression, whereas genes in italic have decreased expression compared with controls.

addition, the results of this study suggest that 1250-ppm diuron induces the same gene expression changes and morphological response after 20 weeks as does the tumorigenic dose of 2500 ppm. The 1250-ppm dose has not been tested in a 2-year bioassay to evaluate whether it is carcinogenic.

Previously we reported that diuron increased urothelial necrosis identified by scanning electron microscopy after treatment with 2500-ppm diuron (Nascimento *et al.*, 2006). Consistent with this finding, analyses using IPA showed a dose-dependent increase in the number of genes involved in cell death (Supplementary table S2). The specific biological pathways leading to diuron-induced necrosis is not known; however, the present study suggests several signaling pathways that could be involved, including stress-related genes such as those that control NRF2-mediated oxidative stress response, glutathione metabolism, and AHR signaling as well as those that control metabolism including amino acid, lipid, and nitrogen metabolism (Supplementary table S2). It has been proposed that diuron may act via ROS production (Geoffroy *et al.*, 2002). Although the presence of ROS has not been determined directly in this study, oxidative stress can induce several of the stress pathways described above. ROS can play an important role in cancer development, not only by causing direct macromolecule (i.e., lipid, protein, nucleic acids) damage but by induction of signaling pathways that promote carcinogenesis (Klaunig *et al.*, 2010). Therefore, sustained ROS production may contribute to necrosis and subsequent regenerative proliferation in animals exposed to high doses of diuron.

Diuron-induced urinary bladder alterations in the rat are similar to those produced by dimethylarsinic acid (DMA^V), the major urinary metabolite of inorganic arsenic in humans and rats, and a nongenotoxic rat bladder carcinogen (Sams *et al.*, 2007). Like diuron, DMA^V is believed to exert its carcinogenic effect via direct exposure to urothelial cells rather than by causing indirect changes in urine composition as in the case of sodium saccharin (Chappel, 1992; Sams *et al.*, 2007). Like most nongenotoxic urinary bladder carcinogens, DMA^V also causes necrosis followed by regenerative proliferation (Cohen *et al.*, 2007a). The precise molecular mechanisms of DMA^V carcinogenesis are unknown. It is likely they are related to the production of one or more reactive metabolites that induce oxidative stress (Chung *et al.*, 2008; Kitchin and Conolly, 2010; Wei *et al.*, 2005). In contrast, antioxidants presented minimal inhibitory activity of various arsenicals induced urothelial toxicity *in vitro* or *in vivo* showing that it is possible that other pathways also can contribute to arsenic cytotoxicity (Cohen *et al.*, 2007a; USEPA, 2005). It is unknown if DMA^V and diuron act similarly on a molecular level. In the present study, altered molecular pathways included some that were also altered by DMA^V exposure in the urothelium *in vivo*. This included lipid metabolism, protein degradation, cell death, and oxidative stress response (Supplementary table S1) (Sen *et al.*, 2005, 2007).

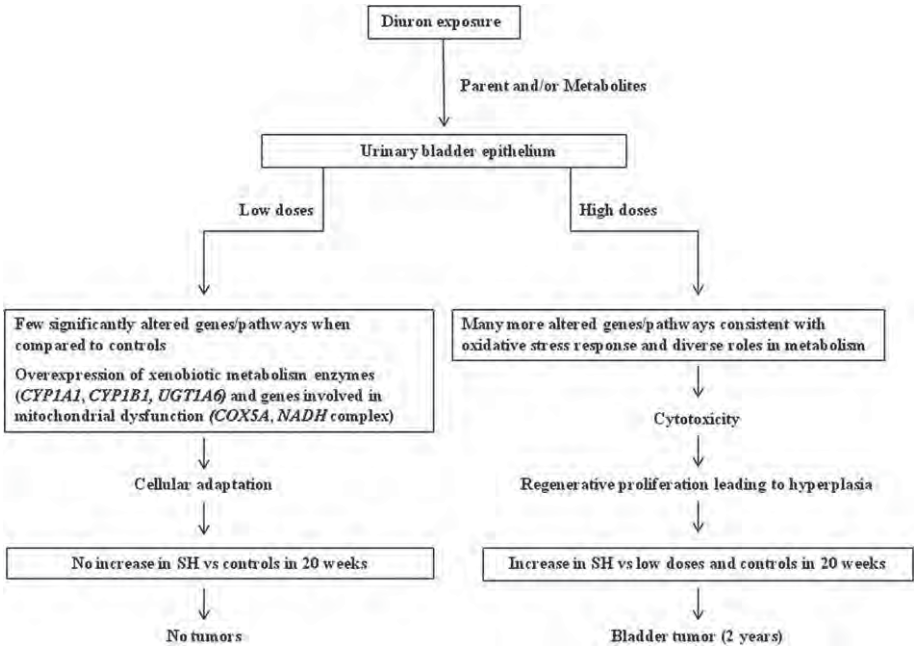

FIG. 6. Summary of the proposed key events for the MOA of diuron-induced urinary bladder tumorigenesis.

Both 1250- and 2500-ppm diuron treatment increased incidence of simple urothelial hyperplasia after 20 weeks of exposure in the present study. A previous study reported increased proliferating cell nuclear antigen (PCNA) labeling in the urothelial cells of animals exposed to 2500-ppm diuron for 20 weeks (Nascimento *et al.*, 2006). Analysis of diuron-responsive genes demonstrated individual differentially expressed genes that are associated with control of the cell cycle (Fig. 5) and could result in increased cell proliferation. As an example and based on IPA evaluations, *ARHGDIB* and *MAP2K6* genes had decreased expression and have been associated with cell adhesion and cell cycle arrest, respectively, whereas, *H1FO* and *LMO4* had increased expression and are associated with increased DNA synthesis. In this study, there was no clear modulation of cell cycle genes that promote proliferation after 20 weeks of exposure.

Some genes that have been reported to be involved in human bladder cancer, such as *GSTM1* (La Vecchia & Airoldi, 1999; Murta-Nascimento *et al.*, 2007), Cytokeratin K20 and *NINJ1* (Sanches-Carbayo *et al.*, 2003), *CAV1*, *ZYX,* and *MSN* (Sanches-Carbayo and Cordon-Cardo, 2003), had increased expression after diuron treatment in the present study, and *ARHGDIB* (Sanches-Carbayo and Cordon-Cardo, 2003) had decreased expression after diuron exposure. Alterations of lipid and protein metabolism pathways have been associated with progression in human bladder cancer (Sanches-Carbayo *et al.*, 2003) and were also found to be altered in the present study. These data suggest concordance of some pathway-level alterations between human bladder cancer and rodent urothelial toxicity that lead to a tumor response.

Taking all the data together, we have summarized a proposed set of key events that describe a hypothesized MOA for diuron-induced tumorigenesis (Fig. 6). Diuron and/or its metabolites present in the urine directly cause urothelial cytotoxicity and consequent regenerative cell proliferation. Herein we demonstrated that these processes follow a dose-response pattern. At low doses, signs of cell toxicity as demonstrated by increased expression of transcripts related to metabolism of xenobiotics, such as *CYP1A1*, *CYP1B1*, and *UGT1A,* and dysfunction of genes that regulate mitochondrial function were observed. Mitochondrial dysfunction can occur when ROS are increased in relation to antioxidant systems (Tennant *et al.*, 2009). However, the low number of transcripts, altered and involved in each molecular pathway, plus the absence of morphological lesions in the low-dose animals suggests that molecular alterations at these dose levels are involved in maintaining cellular homeostasis. Toxic doses of diuron (1250 and 2500 ppm) induced simple hyperplasia and were associated with alterations in gene expression which included effects on amino acid, lipid, phase I and phase II metabolism, and an enhanced stress response (Supplementary table S1). These data suggest that persistent exposure to high dietary concentrations of diuron induces oxidative stress, increases cellular metabolism, and enhances cell death that is associated with sustained urothelial hyperplasia. These persistent alterations have been shown to be associated with urinary bladder tumor development (Cohen, 1998).

In summary, we demonstrated that transcriptional profile analysis identified a dose-response after 20 weeks of exposure with clear differences in gene expressions at the higher doses

(1250 and 2500 ppm) in comparison with the lower doses (60 and 125 ppm). The gene expression profile in the present study was supported by the histological response. The present study suggests that 125 ppm of diuron in the feed is a no effect level for histologic alterations, and transcriptional changes are related to the preservation of urothelial homeostasis. The present data also suggest that after 20 weeks of exposure to 1250 ppm, the response of the rat urothelium is the same as when treated with 2500 ppm. The cellular and molecular pathways involved in chronic toxicity from diuron treatment may also be associated with a tumor response.

SUPPLEMENTARY DATA

Supplementary data are available online at http://toxsci.oxfordjournals.org/.

FUNDING

Sao Paulo Research Foundation (FAPESP 06/60506-1; 08/55644-1; 09/02754-7); Center for the Evaluation of the Environmental Impact on Human Health (TOXICAM); USEPA.

ACKNOWLEDGMENTS

The authors would like to thank Dr Merielen Nascimento and Mitscheli Sanches da Rocha for their expert technical assistance; Dr Mitchell Rosen for assistance in the molecular research; Dr William Ward for bioinformatics assistance; and Dr Chris Corton and Dr Jim Allen for reviewing the manuscript. This article was approved for publication by the National Health and Environmental Effects Research Laboratory of the Environmental Protection Agency (USEPA) but does not necessarily represent the opinions or policy of the USEPA.

REFERENCES

Chapell, C. I. (1992). A review and biological risk assessment of sodium saccharin. *Regul. Toxicol. Pharmacol.* **15,** 253–270.

Chung, C.-J., Huang, C. J., Pu, Y.-S., Su, C.-T., Huang, Y.-K., Chen, Y.-T., and Hsueh, Y.-M. (2008). Urinary 8-hydroxydeoguanosine and urithelial carcinoma risk in low arsenic exposure area. *Toxicol. Appl. Pharmacol.* **226,** 14–21.

Cohen, S. M. (1998). Urinary bladder carcinogenesis. *Toxicol. Pathol.* **26,** 121–127.

Cohen, S. M., and Lawson, T. A. (1995). Rodent bladder tumors do not always predict for humans. *Cancer Lett.* **93,** 9–16.

Cohen, S. M., Ohnishi, T., Arnold, L. L., and Le, X. C. (2007a). Arsenic-induced bladder cancer in an animal model. *Toxicol. Appl. Pharmacol.* **222,** 258–263.

Cohen, S. M., Ohnishi, T., Clark, N. M., He, J., and Arnold, L. L. (2007b). Investigations of rodent urinary bladder carcinogens: Collection, processing and evaluation of urine and bladders. *Toxicol. Pathol.* **35,** 337–347.

Cox, C. (2003). Herbicide factsheet—Diuron. *J. Pestic. Reform.* **23,** 12–20.

Gee, J. (1997). *Summary on Toxicologic Data. Diuron.* Medical Toxicology Branch. Department of Pesticide Regulation. California Environmental Protection Agency, p.7. Available at: cdpr.ca.gov/docs/risk/toxsums/pdfs/231.pdf Accessed December 10, 2010.

Geoffroy, L., Teisseire, H., Couderchet, M., and Vernet, G. (2002). Effect of oxyfluorfen and diuron alone and in mixture on antioxidative enzymes of Scenedesmus obliquus. *Pestic. Biochem. Physiol.* **72,** 178–185.

Giacomazzi, S., and Cochet, N. (2004). Environmental impact of diuron transformation: A review. *Chemosphere* **56,** 1021–1032.

Hester, S. D., Wolf, D. C., Nesnow, S., and Thai, S.-F. (2006). Transcriptional profiles in liver from rats treated with tumorigenic and non-tumorigenic triazole conazole fungicides: Propiconazole, triadimefon, and myclobutanil. *Toxicol. Pathol* **34,** 879–894.

Hodge, H. C., Downs, W. L., Panner, B. S., Smith, D. W., and Maynard, E. A. (1967). Oral toxicity and metabolism of diuron (N-(3,4-dichlorophenyl)-N#,N#-dimethylurea) in rats and dogs. *Food Cosmet. Toxicol.* **5,** 513–531.

Iyer, P. (2002). *Evidence on the Development and Reproductive Toxicity of Diuron Draft*. Reproductive and Cancer Hazard Assessment Section. The Office of Environmental Health Hazard Assessment. California Environmental Protection Agency, Sacramento, CA, p. 43.

Kitchin, K. T., and Conolly, R. (2010). Arsenic-induced carcinogenesis—Oxidative stress as a possible mode of action and future research needs for more biologically based risk assessment. *Chem. Res. Toxicol.* **23,** 327–335.

Klaunig, J. E., Kamendulis, L. M., and Hocevar, B. A. (2010). Oxidative stress and oxidative damage in carcinogenesis. *Toxicol. Pathol.* **38,** 96–109.

La Vecchia, C., and Airoldi, L. (1999). Human bladder cancer: Epidemiological, pathological and mechanistic aspects. *IARC Sci. Publ.* **147,** 139–157.

Murta-Nascimento, C., Schmitz-Dräger, B. J., Zeegers, M. P., Steineck, G., Kogevinas, M., Real, F. X., and Malats, N. (2007). Epidemiology of urinary bladder cancer: From tumor development to patient's death. *World J. Urol.* **25,** 285–295.

Nascimento, M. G., de Oliveira, M. L. C. S., Lima, A. S., and de Camargo, J. L. V. (2006). Effects of diuron [3-(3,4-dichlorophenyl) -1,1-dimethylurea] on the urinary bladder mucosa of male Wistar rats. *Toxicology* **224,** 66–73.

Nesnow, S., Ward, W., Moore, T., Ren, H., and Hester, S. D. (2009). Discrimination of tumorigenic triazole conazoles from phenobarbital by transcriptional analyses of mouse liver gene expression. *Toxicol. Sci.* **110,** 68–83.

Rocha, M. S., Nascimento, M. G., Cardoso, A. P. F., Lima, P. L. A., Zelandi, E. A., Camargo, J. L. V., and de Oliveira, M. L. C. S. (2010). Cytotoxicity and regenerative proliferation as the mode of action for diuron-induced urothelial carcinogenesis in the rat. *Toxicol. Sci.* **113,** 37–44.

Sams, R., II., Wolf, D. C., Ramasamy, S., Ohanian, E., Chen, J., and Lowit, A. (2007). Workshop overview: Arsenic research and risk assessment. *Toxicol. Appl. Pharmacol.* **222,** 245–251.

Sanches-Carbayo, M., and Cordon-Cardo, C. (2003). Applications of array technology: Identification of molecular targets in bladder cancer. *Br. J. Cancer.* **89,** 2172–2177.

Sanches-Carbayo, M., Socci, N. D., Lozano, J. J., Li, W., Charytonowicz, E., Belbin, T. J., Prystowsky, M. B., Ortiz, A. R., Childs, G., and Cordon-Cardo, C. (2003). Gene discovery in bladder cancer progression using cDNA microarrays. *Am. J. Pathol* **163,** 505–516.

Sen, B., Wang, A., Hester, S., Robertson, J. L., and Wolf, D. C. (2005). Gene expression profiling of response to dimethylarsenic acid in female F344 rat urothelium. *Toxicology* **215,** 214–226.

Sen, B., Wolf, D. C., Turpaz, Y., Bugrim, A., Retief, J., and Hester, S. D. (2007). Identification of interspecies concordance of mechanisms of arsenic-induced bladder cancer. *Toxicol. In Vitro* **21,** 1513–1529.

Tennant, D. A., Duràn, R. V., Boulahbel, H., and Gottlieb, E. (2009). Metabolic transformation in cancer. *Carcinogenesis* **30,** 1269–1280.

U.S. Environmental Protection Agency (USEPA). (2003). *Registration Eligibility Decision for Diuron List A. Case 0046*. Office of Prevention, Pesticides and Toxic Substances, USEPA, Washington, DC, p. 22.

U.S. Environmental Protection Agency (USEPA). (2004). *Chemicals Evaluated for Carcinogenic Potential*. Office of Pesticide Programs, Health Effects Division. Science Information Management Branch, Washington, DC, p. 106.

U.S. Environmental Protection Agency (USEPA). (2005). *Science Issue Paper: Mode of Carcinogenic Action for Cacodylic Acid (Dimethylarsinic Acid, DMAV) and Recommendations for Dose Response Extrapolation*. Health Effects Division, Office of Pesticide Programs, Washington, DC, p. 201.

Wei, M., Arnold, L. L., Cano, M., and Cohen, S. M. (2005). Effects of co-administration of antioxidants and arsenicals on the rat urinary bladder epithelium. *Toxicol. Sci.* **83,** 237–245.

Weng, L., Dai, H., Zhan, Y., He, Y., Stepaniants, S. B., and Bassett, D. E. (2006). Rosetta error model for gene expression analysis. *Bioinformatics* **22,** 1111–1121.

Whitfield, M. L., Sherlock, G., Saldanha, A. J., Murray, J. I., Ball, C. A., Alexander, K. E., Matese, J. C., Perou, C. M., Hurt, M. M., Brown, P. O., *et al*. (2002). Identification of genes periodically expressed in the human cell cycle and their expression in tumors. *Mol. Biol. Cell.* **13,** 1977–2000.

Supplementary tables

Table S1: Major functional categories of significantly ($p<0.05$) altered pathways of combined high doses (1250 and 2500 ppm) of diuron relative to control after 20 weeks of exposure.

Major categories	***Canonical Pathways***	***Molecules***
Amino acid metabolism	Valine, Leucine and Isoleucine Degradation	*HSD17B10, ACAT2, ACAA1, ACAD9, HMGCS2, ELOVL6, ACAD11, ALDH2, ALDH1A1, BCAT2, HIBADH, AUH, IVD, HSD17B4, ALDH6A1, MCCC2*
	Valine, Leucine and Isoleucine Biosynthesis	*BCAT2, IARS2, PDHA1 (includes EG:29554)*
	Glutathione Metabolism	*GSTA3, GSTM5, GSTA1, GSTA2, G6PD, GCLC, GLRX, GSTO1, GSTA4, ACSS2, GPX4, MGST3, GSTK1*
	Arginine and Proline Metabolism	*FAAH, ALDH2, ALDH1A1, VNN1, SAT1, GLUD1, GOT1, GOT2, ODC1*
	Tryptophan Metabolism	*HSD17B10, FAAH, CYP1A1, ACAT2, ACAA1, METTL7B, CYP1B1, ALDH2, ALDH1A1, AUH, CAT, HSD17B4,*

		CYP51A1
	β-alanine Metabolism	*ACAD11, ALDH2, ALDH1A1, AUH, ACAD9, IVD, ALDH6A1*
	Alanine and Aspartate Metabolism	*GPT, GOT1, AARS, GOT2, PDHA1 (includes EG:29554)*
	Phenylalanine Metabolism	*FAAH, ALDH2, PRDX1, GOT1, GOT2, ELOVL6*
	Lysine Degradation	*HSD17B10, ALDH2, WHSC1L1, CNDP2, ALDH1A1, ACAT2, ACAA1, AUH, HSD17B4, SHMT2, ELOVL6*
	Phenylalanine, Tyrosine and Tryptophan Biosynthesis	*ENO1, GOT1, GOT2, PCBD1*
	Cyanoamino Acid Metabolism	*FAAH, ACSS2, SHMT2*
	Tyrosine Metabolism	*ALDH2, COMT, GOT1, METTL7B, GOT2, ELOVL6*
Energy metabolism	Nitrogen Metabolism	*VNN1, GLS, CA5B, CA12, CCDC92 (includes EG:80212),*

	GLUD1, CA8
Carbohidrate metabolism	
- Butanoate Metabolism	*HSD17B10, ALDH2, ALDH1A1, ACAT2, ACAA1, AUH, HMGCS2, HSD17B4, PDHA1 (includes EG:29554), ELOVL6*
- Propanoate Metabolism	*ACAD11, ALDH2, ALDH1A1, ACAT2, ACAA1, AUH, ACSS2, ACSS1, ACAD9, IVD, ALDH6A1*
- Pyruvate Metabolism	*GRHPR, PKM2, AKR1B15, ALDH2, ALDH1A1, ACAT2, ACAA1, ACSS2, ACSS1, PDHA1 (includes EG:29554)*
- Glycolysis/Gluconeogenesis	*PKM2, ALDH2, ALDH1A1, ENO1, ACSS2, LRRC16A, ACSS1, PDHA1 (includes EG:29554)*
- Inositol Metabolism	*RECQL4, LSR, ERO1L, RDH12, CBR3, ALDH6A1, ADI1*
Methane Metabolism	*PRDX1, CAT, SHMT2*

Lipid Metabolism	Arachidonic Acid Metabolism	*CYP1A1, ALOX12, PTGDS, CBR3, CYP1B1, PTGES, RNF111, ACSS2, GPX4, CBR1, CYP51A1, MGST3, DHRS4, GSTK1*
	Fatty Acid Elongation in Mitochondria	*HSD17B10, ACAA1, AUH, HSD17B4*
	Fatty Acid Metabolism	*HSD17B10, CYP1A1, ACAT2, ACAA1, ACOX1, ACAD9, CYP1B1, ACAD11, ALDH2, ALDH1A1, AUH, CPT2, ACSL4, CPT1C, IVD, HSD17B4, CYP51A1*
	Biosynthesis of Steroids	*FDPS, NQO1, PDSS2, SC5DL*
	Androgen and Estrogen Metabolism	*HSD17B10, UGT1A6, SRD5A1, METTL7B, HSD17B4, HSD17B2*
	Bile Acid Biosynthesis	*ALDH2, ALDH1A1, ACAA1, CYP27A1, SRD5A1*
	Synthesis and Degradation of Ketone Bodies	*ACAT2, ACAA1, HMGCS2*

Oxidative stress response	Xenobiotic Metabolism Signaling	*MAP2K6, GSTA3, CYP1A1, UGT1A6, GSTM5, GSTA1, GSTA2, NQO1, GCLC, FMO5, CYP1B1, GSTO1, ESD, AHRR, ALDH1A1, CAMK2D, GSTA4, PPP2R2B, CAT, HSP90AA1, ALDH6A1, CITED2, MGST3, GSTK1*
	Metabolism of Xenobiotics by Cytochrome P450	*GSTA3, CYP1A1, GSTM5, UGT1A6, GSTA1, GSTA2, GSTO1, CYP1B1, ALDH2, GSTA4, MGST3, CYP51A1, EPHX1, GSTK1*
	Aryl Hydrocarbon Receptor Signaling	*GSTA3, CYP1A1, GSTM5, GSTA1, GSTA2, NQO1, CYP1B1, GSTO1, AHRR, ALDH1A1, GSTA4, HSP90AA1, NFIB, ALDH6A1, MGST3, GSTK1*
	NRF2-mediated Oxidative Stress Response	*GSTA3, MAP2K6, GSTM5, PRDX1, GSTA1, GSTA2, NQO1, HSPB8, GCLC, DNAJB2 (includes EG:3300), GSTO1, GSTA4, CAT, CBR1, MGST3, EPHX1, GSTK1*

	Glutathione Metabolism	*GSTA3, GSTM5, GSTA1, GSTA2, G6PD, GCLC, GLRX, GSTO1, GSTA4, ACSS2, GPX4, MGST3, GSTK1*
	Glutamate Metabolism	*GLS, CCDC92 (includes EG:80212), GPT, GCLC, GLUD1, GOT1, GOT2*
	LPS/IL-1 Mediated Inhibition of RXR Function	*GSTA3, APOE, GSTM5, GSTA1, ACOX1, GSTA2, FMO5, HMGCS2, GSTO1, ALDH1A1, GSTA4, CAT, CPT2, ACSL4, FABP5L2, CPT1C, ALDH6A1, MGST3, GSTK1*
Signaling	Xenobiotic Metabolism Signaling	*MAP2K6, GSTA3, CYP1A1, UGT1A6, GSTM5, GSTA1, GSTA2, NQO1, GCLC, FMO5, CYP1B1, GSTO1, ESD, AHRR, ALDH1A1, CAMK2D, GSTA4, PPP2R2B, CAT, HSP90AA1, ALDH6A1, CITED2, MGST3, GSTK1*
	Aryl Hydrocarbon Receptor Signaling	*GSTA3, CYP1A1, GSTM5, GSTA1, GSTA2, NQO1, CYP1B1, GSTO1, AHRR, ALDH1A1, GSTA4, HSP90AA1,*

		NFIB, ALDH6A1, MGST3, GSTK1
	NRF2-mediated Oxidative Stress Response	*GSTA3, MAP2K6, GSTM5, PRDX1, GSTA1, GSTA2, NQO1, HSPB8, GCLC, DNAJB2 (includes EG:3300), GSTO1, GSTA4, CAT, CBR1, MGST3, EPHX1, GSTK1*
	CTLA4 Signaling in Cytotoxic T Lymphocytes	*AP2M1, PTPN11, CLTA, PPP2R2B, CD86, AP1B1, AP2A2*
	Autoimmune Thyroid Disease Signaling	*TSHR, CD86, FAS, HLA-C*
Immuno System	Complement System	*CD59, CD55, CFI, CFH*
	CTLA4 Signaling in Cytotoxic T Lymphocytes	*AP2M1, PTPN11, CLTA, PPP2R2B, CD86, AP1B1, AP2A2*
	Autoimmune Thyroid Disease Signaling	*TSHR, CD86, FAS, HLA-C*

Adhesion	Caveolar-mediated Endocytosis	*ITGA11, CD55, ITGA6, RAB5B, ITGA7, HLA-C*
Cofactor/vitamin metabolism	Retinol Metabolism	*ALDH1A1, UGT1A6, RDH12, DHRS4*
Other	Virus Entry via Endocytic Pathways	*AP2M1, CLTA, CD55, ITGA6, AP1B1, AP2A2, HLA-C*

Table S2: Cell death related differentially expressed transcripts from IPA[1] biological functions in different diuron groups after 20 weeks of exposure.

Diuron groups	Number of *DETs*[2]	P-value
60 ppm	44	5,76E-05 – 2,03E-02
125 ppm	59	7,20E-05 – 1,58E-02
1250 ppm	86	1,73E-06 – 2,83E-02
2500 ppm	154	3,62E-06 – 2,70E-02

[1]IPA: Ingenuity Pathway Analysis; [2]DETs: differentially expressed transcripts.

Manuscript 2

Gene expression profiling of urinary bladder of rats treated with diuron in a short-term study

Shadia M. Ihlaseh*: shadia@fmb.unesp.br

Kathryn A. Bailey†: bailey.kathryn@unc.edu

Ana Paula F. Cardoso*: anaferragut@fmb.unesp.br

Hongzu Ren‡: ren.hongzu@epa.gov

Rebecca C. Fry†: rfry@unc.edu

João Lauro V. de Camargo*: decam@fmb.unesp.br

Douglas C. Wolf‡: wolf.doug@epa.gov

* Botucatu Medical School, UNESP – Univ. Estadual Paulista, Department of Pathology, Center for the Evaluation of the Environmental Impact on Human Health (TOXICAM), Botucatu, 18618-000, SP, Brazil.

†Department of Environmental Sciences and Engineering, UNC Gillings School of Public Health, Chapel Hill, NC 27559, USA.

‡National Health and Environmental Effects Research Laboratory, Office of Research and Development, U.S. Environmental Protection Agency, Research Triangle Park, NC 27711, USA.

Corresponding author:

João Lauro V. de Camargo, M.D., Ph.D.

Department of Pathology, Botucatu Medical School, Sao Paulo State University, Botucatu, 18.618-000, SP, Brazil. Tel. /fax: +55 014 3882-8255 /3815-2348.

E-mail address: decam@fmb.unesp.br

1 ABSTRACT

Diuron (3-(3,4-dichlorophenyl)-1,1-dimethylurea) is a substituted urea herbicide that at high dietary levels (2500 ppm) induces rat urinary bladder urothelial hyperplasia in 20 weeks and neoplasia in 2 years. The effects on the urothelium in a short period of exposure, however, have not been described. The present 7-day study evaluated the dose-dependent effects of urothelial alterations in the urinary bladder using histology, scanning-electron microscopy (SEM) and transcriptional profiling with Affymetrix microarrays. Six-week old male Wistar rats were treated with 0, 125, 500, 2500 ppm of diuron in the diet for 7 days. The numbers of differentially expressed genes (DEGs) in the exposed groups increased with dose. Diuron affected several functions involved with cell-to-cell interaction and tissue disorganization at transcriptional level, however, 7 days of exposure seemed to be insufficient to cause morphological lesions. Comparison of the gene expression observed at 7-day and 20-week time points indicates more differences than similarities. The present data suggests an initial adaptive response to protect the urothelium to the continuous exposure to diuron. By the 20^{th} week, the protective response is suppressed and the mucosa develops simple hyperplasia, a morphologic consequence of cytotoxicity and necrosis followed by a continuous replacement of the epithelium. This process can explain the development of urothelial bladder tumors at the end of a 2-year exposure to diuron.

Keywords: diuron, urinary bladder, carcinogenesis, gene expression profiling, microarray analysis, cell adhesion

2 INTRODUCTION

Diuron [3-(3,4-dichlorophenyl)-1,1-dimethylurea] is a substituted urea herbicide largely used on a variety of both crop and non-crop plant. This chemical is classified by the U.S Environmental Protection Agency (USEPA) as a high production volume (HPV) chemical with production exceeding 1 million pounds annually in the U.S. In Brazil, diuron is mostly used on soybeans, cotton, and sugar cane. This herbicide has been characterized as a "known/likely" human carcinogen by the USEPA based on a two-year bioassay that demonstrated urinary bladder carcinomas in both sexes of the Wistar rat, renal pelvis carcinomas in the Wistar male rat and mammary gland carcinomas in the female NMRI mouse after exposure to 2500 ppm diuron in the diet (Iyer, 2002; USEPA, 2003, 2004). Therefore, diuron has economic, environmental and human exposure relevance.

Previous studies from our laboratory reported an increased incidence of urothelial necrosis and hyperplasia associated with increased urothelial cell proliferation in male Wistar rats exposed to the carcinogenic dose of diuron for 20 weeks (Nascimento et al., 2006). As genotoxicity evaluations of diuron have generally been negative, the urothelial carcinogenicity of diuron is believed to occur through a non-genotoxic mode of action (MOA) (Gee, 1997; Iyer, 2002; USEPA, 2003; Nascimento et al., 2006; Rocha et al., 2010). Indirect effects such as changes in urinary solids and pH have been shown not to be key events in diuron-induced carcinogenicity (Rocha et al., 2010; Ihlaseh et al., 2011). It is proposed that direct action of diuron and/or one of its urinary metabolites causes sustained cytotoxicity and necrosis followed by regenerative hyperplasia, which eventually leads to urothelial neoplastic development (Nascimento et al., 2006; Rocha et al., 2010).

Microarray-based genomic profiling is used to evaluate the expression of thousands of genes and the identification of molecular pathways altered by chemical exposure. Previously,

a comprehensive gene expression analysis of urothelial cells from rats fed different dietary concentrations of diuron for 20 weeks was conducted using Affymetrix microarrays (Ihlaseh et al., 2011). There was a clear difference in gene expression at the higher dietary concentrations (1250 and 2500 ppm) in comparison with the lower ones (60 and 125 ppm), consistent with the phenotypic histological response. Toxic dietary levels of diuron (1250 and 2500ppm) induced simple urothelial hyperplasia and were associated with alteration of the molecular pathways of oxidative stress, cellular metabolism, and cell death.

There is no information about the effects of short-term exposure to diuron on the urothelium. The present study was designed to compare early molecular and morphological alterations after 7-days of treatment to those already identified after 20 weeks of exposure to diuron (Ihlaseh et al., 2011). The comparison is based on gene expression profiling, light microscopy and scanning-electron microscopy (SEM) and the study was designed to determine if a dose-response pattern is present for these endpoints.

3 MATERIALS AND METHODS

3.1 Chemicals

Diuron (3-(3,4-dichlorophenyl)-1,1-dimethyl-urea) was obtained from Sigma Chemical Co. (CAS no. 30-54-1, 97% purity, St. Louis, MO, USA). It was mixed with Nuvilab powdered commercial diet from Nuvital (Colombo, PR, Brazil) at final diuron concentrations of 125, 500 and 2500 ppm.

3.2 Animal treatment and sample collection

This study was approved by the Committee for Ethics in Animal Experimentation of the UNESP Medical School, SP, Brazil. Six-week-old male Wistar rats were obtained from the Multidisciplinary Center for Biological Investigation - UNICAMP (Campinas, SP, Brazil). Following two weeks of acclimation, the rats were randomized into four groups of 10 animals each and received diuron in the pelleted feed at final concentrations of 0 (control), 125, 500 and 2500 ppm. Water and feed were provided *ad libitum*. Animals were monitored daily and cages and bedding were changed three times during the week. Water, feed consumption and body weight were determined for each animal in the days zero (initial) and seven (final) of the experiment.

After seven days, the rats were anesthetized with 3% sodium pentobarbital i.p (30 mg/kg) and the lower abdominal wall was opened. Urinary bladders were removed from each animal. The urinary bladders from five animals in each group were used for urothelial RNA isolation as previously described (Ihlaseh et al., 2011). Briefly, the urinary bladder was removed and everted on a glass rod to expose the epithelium. The cells were gently shaved and transferred to 1 mL of TRIzol solution (Invitrogen Corporation, Carlsbad, CA) and transferred to liquid nitrogen followed by storage at -70ºC until RNA extraction. All steps were carried out rapidly to minimize autolysis. The remaining urinary bladder was fixed in

formalin and processed for histological examination to evaluate the efficiency of the urothelium removal. The efficiency of removal was graded according to the percentage (%) of epithelial cells remaining per bladder strip, being: <5% - grade 0; 5 to 10% - grade 1; 11 to 50 % - grade 2 and > 50% - grade 3. Only samples with grades 0 and 1 and with intact basal membrane were used in subsequent RNA isolation steps (Figure 1).

For histological and scanning-electron microscopy (SEM) analyses, urinary bladders were taken from the other five rats from each group. The urinary bladders were injected with Bouin's fixative while the animals were under anesthesia, removed, immersed in the same fixative for 4 h followed by washing in 70% ethyl alcohol . To be sure that we examined the dome and the ventral portion of the bladder, the bladder was sliced longitudinally, one half processed for SEM, and the other half sectioned into four slices longitudinally for embedding in paraffin and staining with hematoxylin and eosin (HE). The histological analysis of proliferative lesions considered simple hyperplasia (SH) and papillary and nodular hyperplasia (PNH). Immediately after removal of the urinary bladder, the animals were euthanized by sectioning the inferior vena cava.

3.3 Scanning-Electron Microscopy (SEM)

The hemi-bladder of five animals from each group was used for SEM analysis to identify early urothelial lesions. A Philips 515 Scanning Electron Microscope (Philips, Inc., Eindhoven, The Netherlands) was used to conduct the SEM at the Institute of Biosciences, UNESP, Botucatu, São Paulo. Urothelial alterations were classified according to five categories indicative of the severity of alterations: class 1 - flat urothelium made of polygonal superficial cells, few necrotic or exfoliated cells due to normal cell death; class 2 - occasional small foci of superficial urothelial necrosis and exfoliated cells; class 3 - pleomorphic polygonal superficial cells with numerous small foci of superficial urothelial necrosis and

exfoliated cells; classe 4 - extensive superficial urothelial necrosis; class 5 - extensive necrosis and exfoliation with piling up of small rounded cells (urothelial hyperplasia). Usually, classes 1 to 3 represent normal urothelium and classes 4 and 5 represent altered mucosa (Cohen et al., 2007).

3.4 Statistical analyses

Body weight, water and diet consumption were compared among the experimental groups using a one-way ANOVA. Data demonstrating significant differences were then further evaluated with a Tukey's test to determine significant differences among groups ($p < 0.05$). A Fisher exact test was applied to evaluate the incidence of urinary lesions by histology and SEM. The significance level of 5% was adopted for all analyses and were performed using GraphPad Instat (v.3.02, La Jolla, CA).

3.5 RNA extraction

Total RNA was isolated using TRIzol Reagent in accordance with the manufacturer's protocol (Invitrogen, Carlsbad, CA). The total RNA pellet was resuspended in 100 µl of water and purified using the RNeasy Mini kit (Qiagen, Valencia, CA, USA). Purified total RNA was eluted in dH_20 and its concentration was measured using a NanoDrop ND-1000 spectrometer (NanoDrop, Wilmington, DE). The quality of RNA was assessed using an Agilent Bioanalyzer (Agilent Technologies, Santa Clara, CA) and only samples having an RNA integrity number (RIN) >7.0 were used for microarray analyses. In the present study, one chip was used per animal and four chips were used per exposure group.

3.6 Affymetrix microarray hybridization

Gene expression analyses were conducted using Affymetrix GeneChip Rat Genome 230_2.0 Arrays (Affymetrix, Santa Clara, CA) which contain >31,000 probe sets representing

~28,700 known rat genes. Total RNA (300 ng) for each sample was amplified and labeled by the 3' IVT Express Kit (Affymetrix, Santa Clara, CA). For each array, 12 µg of amplified biotin-cRNA was fragmented and hybridized to the array for 16 h at 45ºC in a rotating hybridization oven. The arrays were washed on the Affymetrix Fluidics Station FS450 and scanned using the Affymetrix Scanner 3000 according to the manufacturer's protocols. The resulting .CEL files were analyzed with Affymetrix Expression Console software for quality control purpose.

3.7 Microarray data analysis

Data from each microarray scan (.cel file) was imported into Rosetta Resolver version 7.1 (Rosetta Inpharmatics, Kirkland, WA) for normalization (Weng et al., 2006) and determination of transcripts that were differentially expressed relative to the control group. To survey the data for within-group outliers and trends in data quality, unsupervised principal component analysis (PCA) was performed (Rosetta).

Differentially expressed genes (DEGs) among all treatment groups were identified using a 1-way ANOVA with a false discovery rate (Benjamini-Hochberg test; $p \leq 0.05$). A Tukey-Kramer post-hoc test ($p \leq 0.05$) was then used to identify significant changes in expression between groups. Expression values of DEGs in each treatment group were reported in terms of their change in abundance compared to controls. Transcripts were included among the DEGs in each treatment group only if they had a relative change in expression at least 1.5-fold compared to controls [i.e., only DEGs with a relative fold change (FC) of ≤ -1.5 and ≥ 1.5]. Unique and common transcripts between treatment groups were identified using Venn diagrams. IPA software (version 8.8, Ingenuity® Systems, www.ingenuity.com) was used to analyze enriched biological functions and molecular interactions associated with DEGs in diuron-exposed groups. The Ingenuity Knowledge Base

within IPA is a literature-based database of known molecular interactions and functional annotations based on known relationships between cells, cellular components, drugs and diseases. For network generation, DEGs from each group were mapped to their corresponding object within the Ingenuity Knowledge Base. These objects were then overlaid on the global network of known molecular interactions, and smaller networks of interacting molecules ($\leq$25 molecules) within the global network were algorithmically generated based on their connectivity. Statistically significant associations of DEGs with biological functions and diseases ($p<0.005$) and canonical pathways ($p<0.05$) were also determined using IPA. All p values were calculated in IPA using a right-tailed Fisher's exact test, which calculates the probability that associated functions, pathways and network interactions were generated due to chance alone.

The gene expression profiles associated to diuron exposure obtained in this 7-day long study and the one registered in a previous 20-week long study (Ihlaseh et al., 2011) were compared. Both studies were conducted at our laboratory under the same processing procedures and analyses (1-way ANOVA with Benjamini-Hochberg-FDR test + Tukey-Kramer + FC; $p \leq 0.05$) to generate comparable DEGs lists.

4 RESULTS

4.1 Body weight, water and diet consumption

There was no treatment-related significant differences in final body weights in treated compared to control animals although the high dose animals had a lower mean final body weight (Table 1). However, there was a significant ($p<0.05$) reduction of food consumption by rats fed 2500 ppm what was associated with a significantly lower gain of body weight compared to the control (data not shown) and consistent with the lower mean final body

weight. That reduction did not affect the relative diuron intake levels across the groups (Table 1).

4.2 Urothelial morphology by histological and SEM analyses

There were no histological or SEM lesions in the urinary bladders of any group. Two samples (2/5) from 500 ppm and one sample from 2500 ppm (1/5) showed SEM class 4, with necrosis and hyperplastic cells. One single sample from the 125 ppm group was classified as SEM class 5; histologically, it also had severe papillary urothelial hyperplasia which was assumed not to be treatment-related as similar lesions have not been reported associated with diuron after longer exposures (Nascimento et al., 2006; Rocha et al., 2010; Ihlaseh et al., 2011). Therefore, that urinary bladder sample was excluded from further evaluation and analysis.

4.3 Microarray analysis

Principal Component Analysis (PCA) was applied to the statistically significant DEGs from all exposed groups (0, 125, 500 and 2500 ppm). PCA reduces the dimensionality and captures the variability of a data set. Each chip is represented by a single point, and points that cluster close together suggest similar expression profiles. PCA allows for rapid identification of outliers within a treatment group and similarities in expression across groups. Samples within each group clustered together (Figure 2). In addition, the 2500 ppm dose was separated from the control, 125 ppm and 500 ppm groups (Figure 2). One sample from control and one sample from the 125 ppm group were outliers across multiple dimensions and were excluded from the supervised statistical analysis (data not shown).

The number of DEGs modulated by diuron exposure increased with dietary level. There were 406, 850 and 1306 DEGs from the 125, 500 and 2500 ppm diuron-exposed

groups, respectively. After filtering all DEGs by fold change, 210, 520 and 713 sequences remained, respectively from the 125, 500 and 2500 ppm groups; more than 75% of the DEGs showed reduced expression in each group (Table 2). DEGs had a significant degree of overlap among the exposure levels, as demonstrated by the Venn diagram (Figure 4A). Besides, the number of unique genes was 42, 144 and 281 for 125, 500 and 2500 ppm groups respectively. One hundred and thirteen DEGs were common to all treatment groups, being down-regulated to all exposed groups.

Functional analysis was performed uploading the lists of DEGs into the software IPA (Ingenuity System) to evaluate the biological relevance of the transcripts displaying a diuron dose-dependent pattern of expression. Several functions/disorders were modulated in a dose-responsive manner, including cellular movement, cancer, connective tissue disorder, cellular growth and proliferation, inflammatory disease and nucleic acid metabolism (Figure 5A). The transcripts within each significant pathway are in Suplementary Data (Table S1, Supplemental data). The different lists of unique DEGs and of DEGs common to all exposure levels were affecting similar functions, which were associated with cell function and maintenance, cellular development, cellular growth and proliferation, lipid metabolism, and connective tissue disorder. A similar observation was noted after network level analysis. The top network (determined by the IPA tool) in the high concentration group (2500 ppm) was "connective tissue disorder and genetic disorder" (Figure 6). This network includes collagenic genes (Col1a2, Col3a1, Col5a1, Col5a2, Col5a3, Col6a1, Col6a2 and Col7a1) and the transforming growth factors-beta gene (Tgfβ) at its center. Specifically, the Tgfb3 gene was down-regulated in the 500 and 2500 ppm groups.

4.4 Gene expression profile and urothelial morphology after 7 days of exposure to diuron

The ultrastructural SEM analysis detected foci of decreased cell adhesion and necrosis after 500 and 2500 ppm but the incidences of these lesions were not significant (Figure 1E-F). Several deregulated molecular pathways were related to cell-to-cell interactions and tissue organization (Figure 5A). For example, genes from collagen (Col), matrix metallopeptidase (Mmp) and tissue inhibitor of metalloproteinase (Timp) families such as Col7A, Mmps 3 and 13, were up-regulated, and nine collagen genes (Col1A1, Col1A2, Col3A1, Col5A1, Col5A2, Col5A3, Col6A1, Col6A2, Col14A1) and the Mmps 2 and 14 e Timp 1, 2 and 3 were among the down-regulated transcripts.

4.5 Time relationship – comparison of gene expression profiles of 7-day and 20-week studies

The urothelial cells gene expression profiling of rats exposed to diuron presented a dose-response pattern at the end of both 7-day and 20-week periods of exposure. However, microarray analysis conducted at the end of these periods showed more differences than similarities in the gene expression profile. After 20 weeks, the top five pathways were involved with amino acid and lipid metabolism, xenobiotic metabolism, oxidative stress and cellular toxicity (Ihlaseh et al., 2011). After 7 days, the main significant pathways were involved with loss of cell adhesion and genetic disorder (Figures 5 and 6). Interestingly, there were no DEGs present in all dose groups across both studies (i.e., 7 days: 125, 500, 2500 ppm and 20 weeks: 60, 125, 1250, 2500 ppm). Considering only the known carcinogenic dose (2500 ppm), there were 61 DEGs in common at 7 days and 20 weeks (Figure 4B). The functional analysis of these 61 DEGs showed that cancer, organic development, lipid metabolism, and cellular movement are the top involved pathways at both time periods (P-value range: 2E-06 – 2E-02) and that the genes of cytochrome P450, Cyp1a1, Cyp1b1,

glutathione S-transferase alpha-2 (Gsta2) and aryl-hydrocarbon receptor repressor (Ahrr) were within several of the significant functions and presented all down-regulated at 7 days and up-regulated at 20 weeks. Regarding the unique genes for each period of exposure, while amino acid metabolism, gluthatione metabolism and xenobiotic metabolism were highly significant at 20 weeks; cellular movement, tissue development and connective tissue disorder were highly significant only at the 7^{th} day (Figure 5B).

5 DISCUSSION

In this study, male Wistar rats were exposed to different concentrations of diuron in the diet for 7 days. Urinary bladders were analyzed for changes in gene expression. This study represents the earliest time urothelial genomic analysis has been performed after diuron exposure. Microarray data was compared with histological and scanning-electron microscopy (SEM) analyses and also with gene expression alterations after 20 weeks of exposure (Ihlaseh et al., 2011). Diuron influenced in a dose-response manner several functions at transcriptional level after 7 days of exposure; however, no morphological lesions were identified at this time point.

After 7 days of diuron feeding, the gene expression profile of urothelial cells had altered pathways related to cell-to-cell interactions in a dose-response manner, with the genes for collagen, Mmps, and Timps mostly down-regulated. At this time point, the gene expression profile suggests that the early influence of diuron and/or its metabolites on the urothelium of rats may results in loss of cell-to-cell adhesion and local tissue disorganization. On the contrary, gene expression profile registered in the 20-week long study, when the differences between low and high diuron exposures were more evident (Ihlaseh et al., 2011), indicated that cellular toxicity, increased metabolism and general stress played a major role, suggesting that as exposure to the chemical is extended in time various adaptive functions become expressed. In addition, initial tissue injury, a process integral to many nongenotoxic carcinogens, is accompanied by changes in gene expression and increase in the number of deregulated genes reflects the dose-response relationship for tissue injury caused by chemicals (Foster et al., 2007).

Several studies have used the microarray technology integrated with a traditional toxicology approach to explore dose-response relationships and to increase the understanding

of the test chemical mode of action (MOA) through the recognition of pathway signatures of toxic injury (Sen et al., 2005; Nesnow et al., 2009; Ludwig et al., 2011). For many of these studies transcriptional changes were observed prior to a morphological and clinical manifestation. The application of transcriptomics enables a more rapid extraction of biological meaning even though the investigation be focused at a very low level of biological organization (Waters & Fostel, 2004). Since there were few gene expression changes common to the 7-day and 20-week studies, it was difficult to directly predict that the diuron-induced alterations at 7 days are associated with the necrosis and hyperplasia present at the end of the 20th week. A subset of genes, including Ahrr, Cyp1a1, Cyp1b1, Gsta2, that were down-regulated at 7 days and up-regulated at 20 weeks, are within the functions/pathways altered for both periods. Some of them have been associated with increased human bladder cancer risk (Figueroa et al., 2008). A genomic study of arsenate-induced toxicity in the mouse urinary bladder also demonstrated a reversal in gene expression direction, with down-regulation after 1 week and up-regulation after 12 weeks of exposure (Clewell et al., 2011). In addition, the main pathways associated with arsenate exposure in the urothelium were cellular morphogenesis, inflammation and proliferation (Clewell et al., 2011). The similarities between diuron and arsenate in differential gene expression, and the already known key-events of cytotoxicity and regenerative proliferation leading to hyperplasia and urinary bladder tumors in rodents, suggest a MOA in common for both chemicals.

The top molecular network depicting biological interactions amongst genes affected by diuron in the urinary bladder cells was related to connective tissue and genetic disorders. In addition to the decreased expression of several collagen genes, the Tgfb gene was a major node in this network. In normal epithelial cells, Tgfb acts as an anti-proliferative factor, regulating several biological activities as cellular growth and differentiation, production of

extracellular matrix and chemotaxis (Lee& Nowak, 2000; Hill et al., 2009). Specifically, Tgfb3 was down-regulated in groups exposed to diuron 500 and 2500 ppm. Low levels of Tgfb3 mRNA have already been associated with human urinary bladder tumors, suggesting a possible relationship between the lack of the tumor suppressor activity of Tgfb and urothelial neoplasia (Eder et al., 1997).

In conclusion, our study on genomic responses of the rat urinary bladder urothelium after short-term exposure to diuron through diet demonstrated a dose-response relationship in the number of differentially expressed genes. Diuron affected several functions involved with cell-to-cell interaction and tissue disorganization at transcriptional level. However, 7 days of exposure to the herbicide was insufficient to cause histological lesions. Comparison of gene expressions observed at 7-day and 20-week time points indicates more differences than similarities. The present data suggest an initial adaptive response to protect the urothelium to the constant exposure to diuron. By the 20^{th} week, the protective response is suppressed and the mucosa develops simple hyperplasia, a morphologic consequence of cytotoxicity and necrosis followed by a continuous replacement of the epithelium. This process can explain the development of urothelial bladder tumors at the end of a 2-year exposure to diuron.

6 SUPLEMENTARY DATA

Supplemental Table 1: Significant deregulated biological functions in urinary bladder epithelial cells of rats treated with diuron for 7 days.

7 FUNDING

This work was supported by the Fundação de Amparo à Pesquisa do Estado de São Paulo (FAPESP 06/60506-1; 08/55644-1; 09/02754-7); Center for the Evaluation of the Environmental Impact on Human Health (TOXICAM); U.S. Environmental Protection

Agency (U.S. EPA), and the National Institute of Environmental Health Sciences (T32 ES7018).

8 ACKNOWLEDGEMENTS

The authors would like to thank Dr. Maria Luisa C. S. de Oliveira and Dr. Merielen Nascimento e Pontes for their expert technical assistance. This manuscript was approved for publication by the National Health and Environmental Effects Research Laboratory of the Environmental Protection Agency (U.S. EPA) but does not necessarily represent the opinions or policy of the U.S. EPA.

9 REFERENCES

1. Clewell, H.J., Thomas, R.S., Kenyon, E.M., Hughes, M.F., Adair, B.M., Gentry, P.R., Yager, J.W. (2011). Concentration- and time-dependent genomic changes in the mouse urinary bladder following exposure to arsenate in drinking water for up to 12 weeks. *Toxicol Sci*. **123**, 421-432.
2. Cohen, S.M., Ohnishi, T., Clark, N.M., He, J., Arnold, L.L. (2007). Investigations of Rodent Urinary Bladder Carcinogens: Collection, Processing, and Evaluation of Urine and Bladders. *Toxicol Pathol***. 35**, 337-347.
3. Eder IE, Stenzl A, Hobisch A, Cronauer MV, Bartsch G and Klocker H. (1997). Expression of transforming growth factors beta-I,beta 2 and beta 3 in human bladder carcinomas. *Br J Cancer*. **75**, 1753-1760.
4. Figueroa, J.D., Malats, N., Garcia-Closas, M., Real, F.X., Silverman, D., Kogevinas, M., Chanock, S., Welch, R., Dosemeci, M., Lan, Q., Tardon, A., Serra, C., Carrato, A., Garcia-Closas, R., Castan˜o-Vinyals, G., Rothman, N. (2008). Bladder cancer risk and

genetic variation in AKR1C3 and other metabolizing genes. *Carcinogenesis*. **29**, 1955-1962.

5. Le, X.C. (2002). Possible role of dimethylarsinous acid in dimethylarsinic acid-induced urothelial toxity and regeneration in the rat. *Chem Res Toxicol* **15**, 1150-57.
6. Filmus J. (2001). Mini review: Glypicans in growth control and cancer. Glycobiology. **11**, 19-23.
7. Foster, W.R., Chen, S.J., He, A., Truong, A., Bhaskaran, V., Nelson, D.M., Dambach, D.M., Lehman-Mckeeman, L.D., Car, B.D. (2007). A Retrospective Analysis of Toxicogenomics in the Safety Assessment of Drug Candidates. *Toxicol Pathol*. **35**, 621-635.
8. Gee J. (1997). Summary on toxicologic data. Diuron. Medical Toxicology Branch. Department of Pesticide Regulation. California Environmental Protection Agency. 7p. Accessed on cdpr.ca.gov/docs/risk/toxsums/pdfs/231.pdf.
9. Hill JJ, Tremblay T-L, Cantin C, O'Connor-McCourt M, Kelly JF, Lenferink AEG. (2009). Glycoproteomic analysis of two mouse mammary cell lines during transforming growth factor (TGF)-β induced epithelial to mesenchymal transition. *Proteome Sci.* **7**, 1-17.
10. Ihlaseh, S. M., Bailey, K. A., Hester, S. D., Jones, C., Ren, H., Cardoso, A. P. F., Oliveira, M. L. C. S., Wolf, D. C., Camargo, J. L. V. (2011). Transcriptional profile of diuron-induced toxicity on the urinary bladder of male Wistar rats to inform mode of action. *Tox Sci.* **122**, 330-338.
11. Iyer, P. (2002). Evidence on the Development and Reproductive Toxicity of Diuron Draft. Reproductive and Cancer Hazard Assessment Section. The Office of Environmental Health Hazard Assessment, California Environmental Protection Agency, Sacramento, CA. p. 43.

12. Kim H., Xu, G. L., Borczuk, A. C., Busch, S., Filmus, J., Capurro, M., Brody, J. S., Lange, J., D'Armiento, J. M., Rothman, P. B., Powell, C. A. (2003). The heparan sulfate proteoglycan GPC3 is a potential lung tumor suppressor. Am J Respir Cell Mol Biol. 29, 694-701.

13. Lee, B. S. & Nowak, R. A. Lee B-S, Nowak RA. (2001). Human leiomyoma smooth muscle cells show increased expression of transforming growth factor-b3 (TGFb3) and altered responses to the antiproliferative effects of TGFB. *J Clin Endocrinol Metab*. **86**, 913-920.

14. Ludwig S., Tinwell, H., Schorsch, F., Cavaille´, C., Pallardy, M., Rouquie´, D., Bars, R. (2011). A Molecular and Phenotypic Integrative Approach to Identify a No-Effect Dose Level for Antiandrogen-Induced Testicular Toxicity. Tox Sci. **122**, 52-63.

15. Nascimento, M. G., de Oliveira, M. L. C. S., Lima, A. S., and de Camargo, J. L. V. (2006). Effects of diuron [3-(3,4-dichlorophenyl)-1,1-dimethylurea] on the urinary bladder mucosa of male Wistar rats. *Toxicology.* **224**, 66-73.

16. Nesnow, S., Ward, W., Moore, T., Ren, H., and Hester, S. D. (2009). Discrimination of tumorigenic triazole conazoles from phenobasbital by transcriptional analyses of mouse liver gene expression. *Toxicol. Sci.* **110**, 68-83.

17. Rocha, M. S., Nascimento, M. G., Cardoso A. P. F., Lima, P. L. A., Zelandi, E. A., Camargo, J. L. V., de Oliveira, M. L. C. S. (2010). Cytotoxicity and regenerative proliferation as the mode of action for diuron-induced urothelial carcinogenesis in the rat. *Toxicol. Sci.* **113**, 37-44.

18. Sen, B., Wang, A., Hester, S., Robertson, J. L., Wolf, D. C. (2005). Gene expression profiling of response to dimethylarsenic acid in female F344 rat urothelium. *Toxicology*. **215**, 214-226.

19. Waters, M. D., Fostel, J. M. Toxicogenomics and systems toxicology: aims and prospects. (2004). *Nat Rev Genet.* **5**, 937-948.

20. Waters, M.D., Olden, K., Tennant, R.W. (2003). Toxicogenomic approach for assessing toxicant-related disease. *Mutat Res.* **544**, 415-424.

21. Weng, L., Dai, H., Zhan, Y., He, Y., Stepaniants, S. B., and Bassett, D. E. (2006). Rosetta error model for gene expression analysis. *Bioinformatics*. **22**, 1111-1121.

22. U. S. Environmental Protection Agency (USEPA). (2003). Registration eligibility decision for diuron list A. Case 0046. Office of Prevention, Pesticides and Toxic Substances. USEPA, Washington, DC, 22.

23. U. S. Environmental Protection Agency (USEPA). (2004). Chemicals evaluated for carcinogenic potential. Office of Pesticide Programs, Health Effects Division. Science Information Management Branch, Washington, D.C., 106.

10 TABLES

Table 1: Body weight gain, consumption of water, food and estimated diuron intake after 7 days of exposure.

Groups[1]	Final body weight (g)	Water consumption (mL/rat/day)	Food consumption (g/rat/day)	Diuron consumption (mg/rat/day)
Control	247.1±31.3	34,13±4,78	24,04±1,91	-
125 ppm	254.6±21.6	37,24±3,01	24,18±0,65	**3,02±0,08[a]**
500 ppm	252.1±19.7	35,25±2,48	23,78±0,99	**11,89±0,49[b]**
2500 ppm	232.8±20.5	33,08±3,43	**19,02±2,42[a]**	**47,55±6,06[c]**

Data are represented as Average ±SD. [1]The groups represent the amount of diuron added to the food. [2]Food consumption: [a]2500 ppm<Controle = 60 = 125 = 500 = 1250 ($p<0,05$). [3]Diuron intake: a<b<c ($p<0,05$); One-Way ANOVA followed by Tukey-Kramer.

Table 2: Number of differentially expressed transcripts (DET) in the Wistar rat urothelium modulated by 7 days of diuron dietary exposure compared to control.

Groups	DEGs[1]	Decreased Expression	Increased Expression
125 ppm	210	163 (78%)	47 (22%)
500 ppm	520	465 (89%)	55 (11%)
2500 ppm	713	602 (84%)	111 (16%)

[1]Determined using a one-way ANOVA by dose + Benjamini-Hochberg FDR ($p \leq 0.05$) followed by Tukey–Kramer post hoc test ($p \leq 0.05$) (Rosetta Resolver) + fold change (FC) cut off of +/- 1.5 ($FC \leq -1.5$ and $FC \geq 1.5$).

11 FIGURE LEGENDS

Figure 1. Histology (HE) of urinary bladder after Thizol processing to confirm epithelial cells removal: A- urinary bladder reverted in a glass stick to expose the urothelium (4x); B- presence of epithelial cells; the arrow indicates the limit between the epithelium and the lamina propria; C) absence of epithelial cells, indicating that the removal of cells was successful for this sample. (40x).

Figure 2. Scanning-electron microscopy (SEM) of urinary bladder of rats treated with diuron for 7 days. A- Class 1, normal cells, Control, 1600x; B- Class 2, exfoliation foci, 125 ppm, 600x; C- Class 3, necrotic area, 500 ppm, 300x; D- Class 4, necrosis and hyperplastic cells (arrowhead), 2500 ppm, 600x. Showing the initial loss of cell adhesion E- 500 ppm, 300x and F- 125 ppm, 1200x.

Figure 3. Principal component analysis (PCA) showing a good separation in two groups between the high dose versus control, 125 ppm and 500 ppm. Each chip is represented as a single data point.

Figure 4. Venn diagrams of significantly altered genes (DEGs) for A) different doses after a 7-day diuron exposure and B) the diuron 2500 ppm after 7 days and 20 weeks of exposure.

Figure 5. Comparative analyses of significantly altered biological functions A) DEGs from 125, 500 and 2500 ppm presenting dose-response relationship after 7 days; B) DEGs at 2500 ppm unique for 7 days versus DEGs unique for 20 weeks. The Y axis depicts the probability that the genes within a dataset are involved in a particular high level biological function. The bars above the threshold line are statistically significant ($p<0.05$), using IPA. * = functions related to cell interaction and adhesion.

Figure 6. First network for 2500 ppm group called “Connective tissue disorder and genetic disorder”. The genes in green are down-regulated, red are up-regulated and white are not changed compared to the control. Interaction amongst the genes generated by IPA analysis tool.

Figure 1

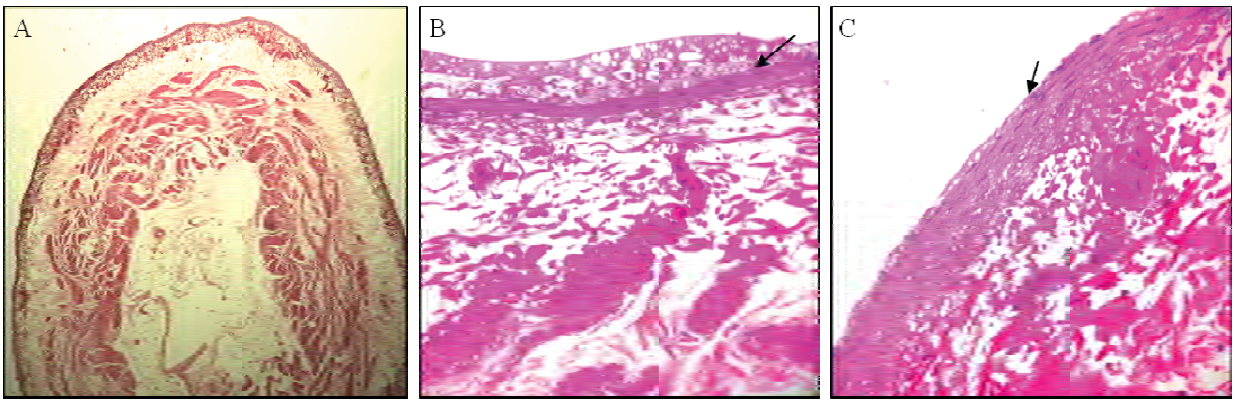

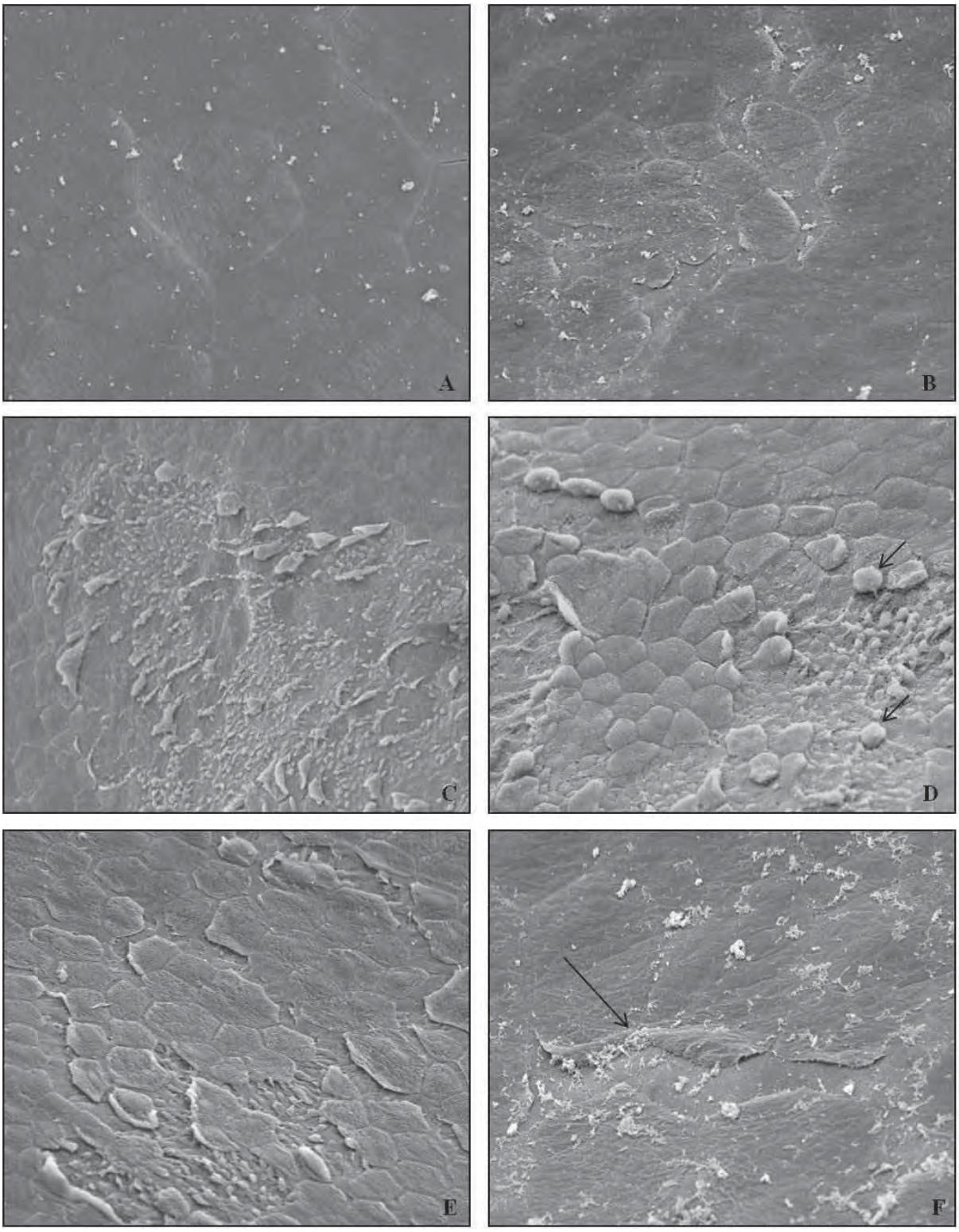

Figure 2

Figure 3

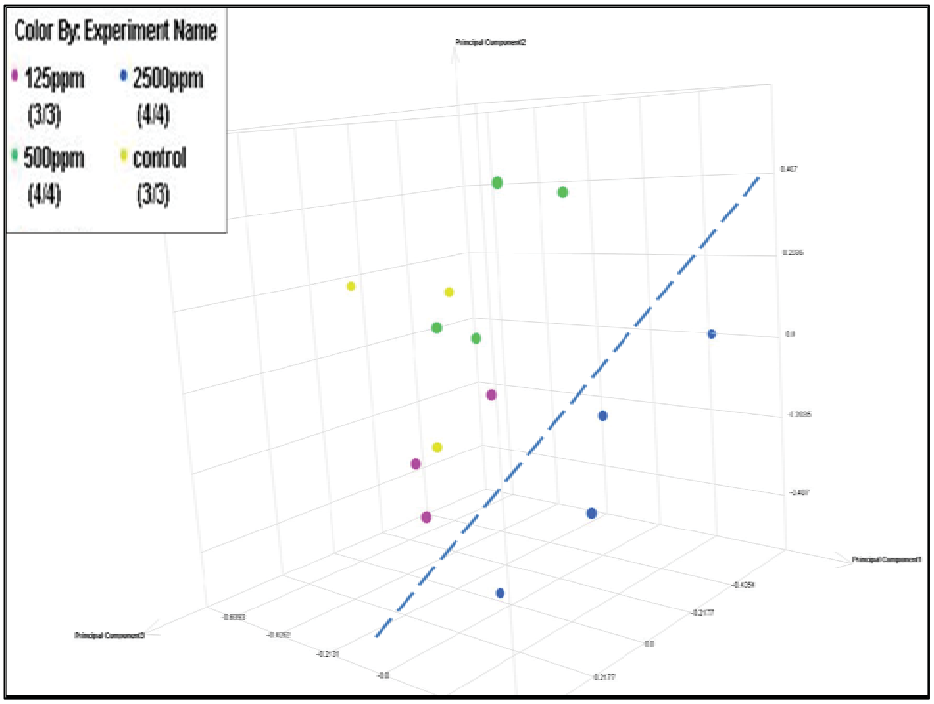
Color By: Experiment Name
125ppm (3/3)
2500ppm (4/4)
500ppm (4/4)
control (3/3)

A

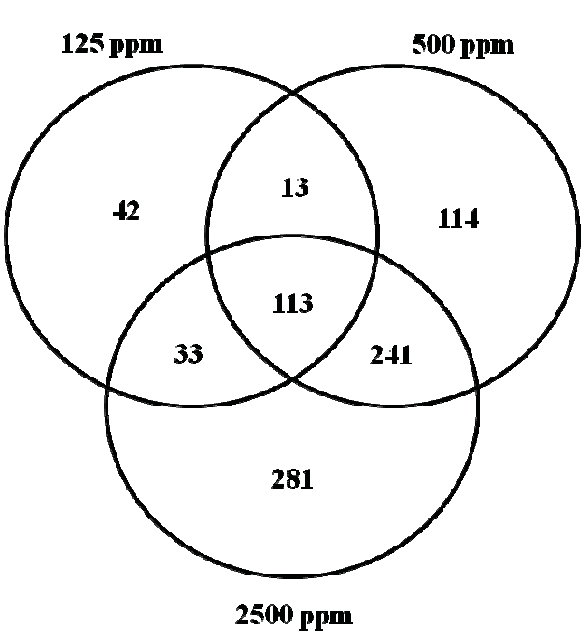
7 days
125 ppm
500 ppm
42
13
114
113
33
241
281
2500 ppm

B

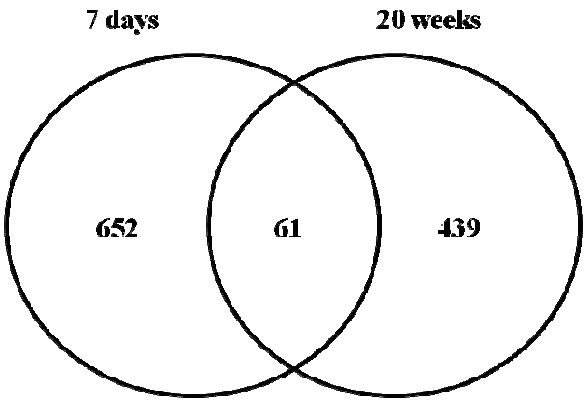
2500 ppm
7 days
20 weeks
652
61
439

Figure 4

Figure 5

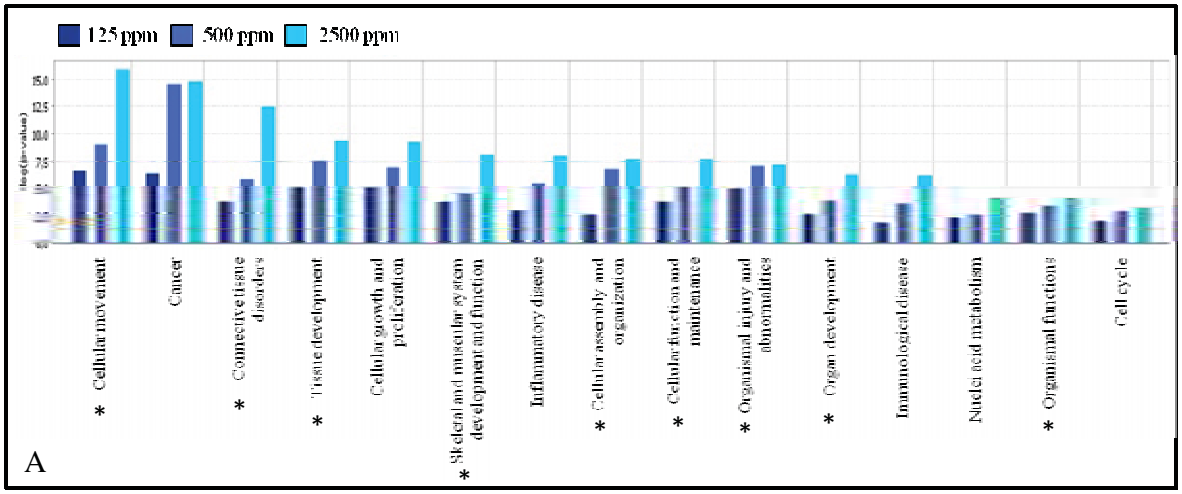

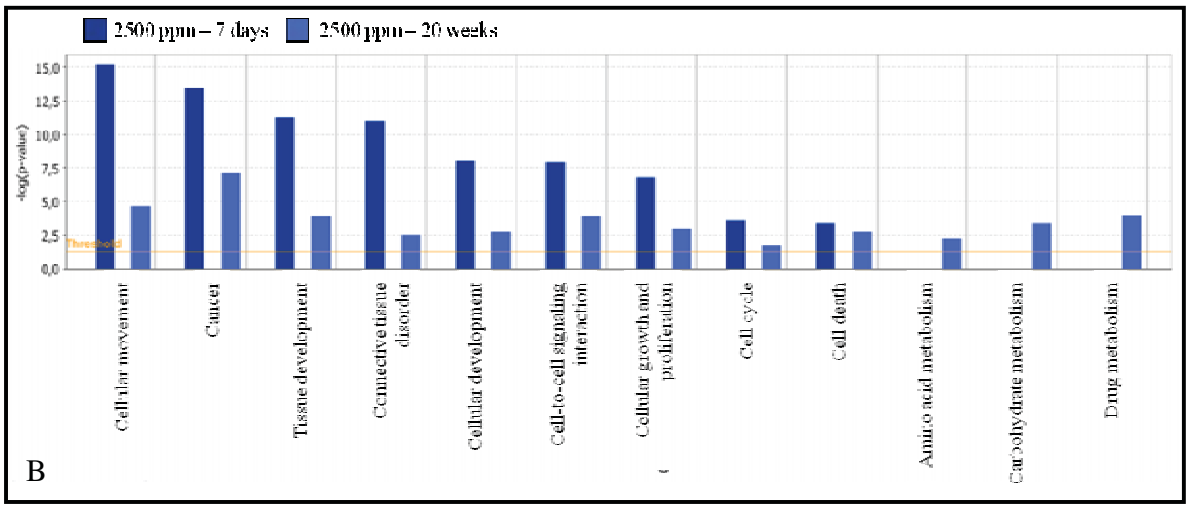

Figure 6

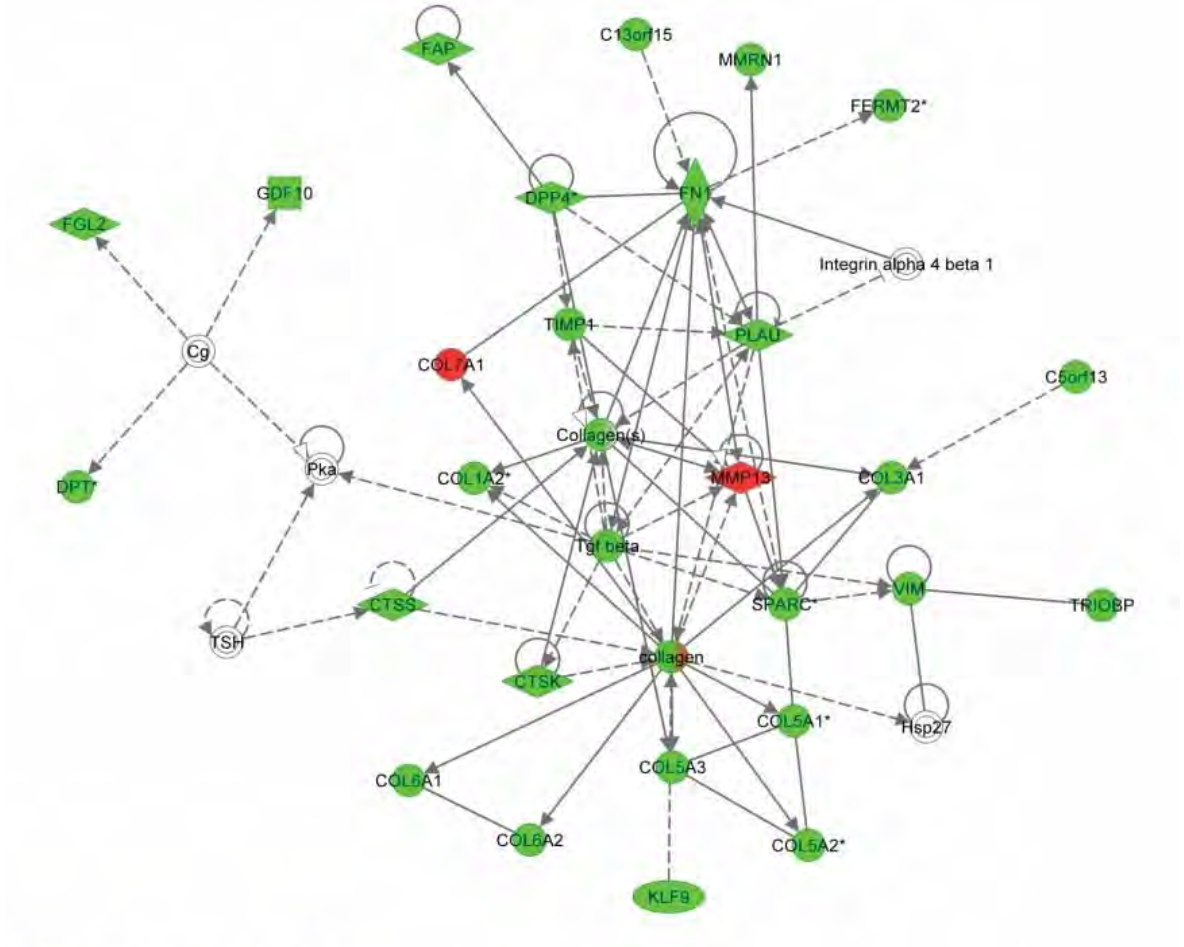
FAP
C13orf15
MMRN1
FERMT2*
GDF10
DPP4*
FN1
FGL2
Integrin alpha 4 beta 1
TIMP1
PLAU
Cg
COL7A1
C5orf13
Collagen(s)
Pka
DPT*
COL1A2*
MMP13
COL3A1
Tgf beta
VIM
CTSS
SPARC*
TRIOBP
TSH
collagen
CTSK
COL5A1*
Hsp27
COL5A3
COL6A1
COL6A2
COL5A2*
KLF9

12 Supplementary tables

Table S1: Significant deregulated biological functions in urinary bladder epithelial cells of rats treated with diuron for 7 days

Biological Functions*	Doses	Molecules
Cellular Movement	125ppm	NAB2, SLIT3, AOC3, TPM1, NFIX, MMP14, PTPN14, Dclk1, SERPINA3, ANPEP, SOD3, VCAN, LAMC1, FSTL1, DDR2, CTSS, SDC2, PPAP2B, CAV1, FIGF, TNFRSF11B, AGT, TIMP3, SFRP4, NBL1, GUCY1A3, CXCR4, FGFR1, PCSK6, LAMA2, SERPINF1, VIM, IGFBP5, THBD, ANGPTL1, PMP22, NTRK2, NOV, CXCL12, LSP1, PLTP, PLAU, TFPI, TMEM176B, AGTR1
	500ppm	SLIT3, DBN1, GAS6, XDH, Dclk1, SERPINA3, MYLK, SRPX2, CTSS, CAV1, MGP, FIGF, AIF1, TIMP2, SFRP4, GUCY1A3, DCN, THBD, NDN, PLTP, SFRP1, FYN, APOE, SERPING1, FHL1, FN1, PTPN14, GDF15, ADIPOQ, ANPEP, SOD3, VCAN, FSTL1, CA3, AR, IGF1, PTPRJ, PPAP2B, PDGFRA, FAP, CTSK, FCGR2A, SERPINF1, VIM, AXL, F3, NOV, TNFSF13, LSP1, PLAU, RARRES2, FGL2, MMP16, MAP1B, ENTPD5, POSTN, CAST, FXYD5, TNFRSF11B, IGFBP6, FST, CXCL9, PCSK6, LAMA2, GSN, ANGPTL1, IL33, S100B, TGFB3, PNOC, TMEM176B, TNS1, C2, AGTR1, AOC3, LOX, TPM1, NFIX, RECK, ADAM33, CLIC4, SDC2, DDR2, ANXA1, CFB, CCRL1, ENPP2, AGT, TIMP3, DPP4, VCAM1, NBL1, CD48, CD36, EGFL7, PMP22, NTRK2, NT5E, CXCL12, C4B (includes others), SPARC, C5orf13
	2500ppm	SLIT3, DPYSL2, DBN1, GAS6, XDH, Dclk1, SERPINA3, SPAG9, SPDEF, LAMC1, PTPRO, CTSS, ABCC1, CAV1, MGP, FIGF, ANGPT4, AIF1, WNT5B, TIMP2, SFRP4, PRKCQ, GUCY1A3, MED1, DCN, FERMT2, MMP2, IGFBP5, THBD, NDN, SPON2, NR1D1, WASF2, PLTP, FYN, SERPING1, FN1, HNRNPA2B1, LRP6, ADIPOQ, BMPR2, ANPEP, CDH11, SOD3, VCAN, FSTL1, CA3, YY1, IGF1, PPAP2B, MXD1, PDGFRA, FAP, CTSK, FCGR2A, SERPINF1, VIM, CYP1B1, KITLG, GNAI3, TRIO, NOV, TNFSF13, LSP1, FCER1G, S1PR1, PLAU, RNF20, PSEN1, RARRES2, MMP3, FGL2, NR2F2, MMP13, POSTN, CAST, KLF2, TEK, TNFRSF11B, IGFBP6, FST, CXCL9, FGFR1, LAMA2, PCSK6, IFNGR1, GSN, ANGPTL1, IL33, CBL, CXCR7, S100B, TGFB3, IGFBP3, MAP2, TMEM176B,

		TNS1, SRRM1, AGTR1, C2, COL7A1, AOC3, LOX, NFIX, RECK, MMP14, TPR, NRG1, ADAM33, CLIC4, ANGPTL4, DDR2, TIMP1, SDC2, MCAM, CFB, ENPP2, MARCKS, AGT, DPP4, TIMP3, VCAM1, S1PR2, NBL1, CD36, SERPINE2, COL1A1, PMP22, EBF1, NRTN, NTRK2, NT5E, CXCL12, C4B (includes others), SPARC, C5orf13
Cancer	125ppm	SLIT3, MSX1, SERPINA3, GPX3, CRIP1, IKZF2, CTSS, TNNT3, SDPR, CAV1, FIGF, TNFRSF11B, SFRP4, TTR, DDIT4, GUCY1A3, LRRC17, FGFR1, PCSK6, IGFBP5, THBD, ANGPTL1, BST2, CD3G, PRSS23, FBN1, CD248, TFPI, TMEM176B, AGTR1, APOD, AOC3, TPM1, KLK1, ITGBL1, MMP14, MSLN, ANPEP, IFITM3, VCAN, C1R, KLF9, AEBP1, SDC2, DPT, PPAP2B, HLA-DRA, GDF10, CYGB, LTBP4, C9orf150, AGT, PLA2G16, TIMP3, CXCR4, MYLPF, SERPINF1, VIM, PMP22, NTRK2, NOV, CXCL12, LSP1, CAPN9, PLAU
	500ppm	SLIT3, DBN1, XDH, MSX1, SERPINA3, CP, TNXB, FGG, PCOLCE, DOCK11, SLC26A3, KRT13, CTSS, MGP, CAV1, FIGF, AIF1, LYVE1, TIMP2, PTGIS, WT1, SFRP4, DDIT4, GUCY1A3, MFAP5, GSTM3, DCN, SPOCK2, THBD, FMOD, GPM6A, SFRP1, PCBD1, STEAP3, APOD, COL3A1, APOE, FYN, SERPING1, FN1, ITGBL1, HTR4, GDF15, ADIPOQ, MSLN, CES1, ANPEP, VCAN, SELENBP1, C1R, KLF9, CA3, AR, PTPRJ, IGF1, FGF18, DPT, PRRX1, PPAP2B, GDF10, PDGFRA, TBX2, C9orf150, PLA2G16, CTSK, APOBEC1, EMP3, FCGR2A, TUBB2C, MYLPF, OLFML3, SERPINF1, FAM3B, VIM, AXL, F3, STXBP6, LTBP1, NOV, SULT1A1, BNC1, ATP1A2, LSP1, IHH, PLAU, SYNGR1, MAOA, RTN1, GPC3, NNMT, GPX3, CRIP1, ENTPD5, SDPR, TNNT3, NUPR1, POSTN, CAST, TSPAN4, TNFRSF11B, NMBR, IGFBP6, FST, CXCL9, LRRC17, C1S, PCSK6, MAGED2, GSN, ANGPTL1, BST2, IL33, PRSS23, LOXL1, C2orf40, TGFB3, FBN1, CD248, AKR1B1, TNS1, TMEM176B, AGTR1, RBP4, AOC3, TPM1, LOX, SRPX, IFI27, SCARA5, RECK, IFITM3, LOXL2, AEBP1, COL6A1, GNG11, SDC2, ANXA1, CFB, C7, CYGB, LTBP4, ENPP2, GBP2, AGT, DPP4, TIMP3, VCAM1, RNASE3, CKM, CD36, CD48, EGFL7, PMP22, GHR, NTRK2, ACOT2, CLDN1, NT5E, SLC16A1, CXCL12, C4B (includes others), SPARC, NFIB, EFEMP1, GAP43, CLEC10A

	2500ppm	SLIT3, DPYSL2, DBN1, XDH, CHRNB1, CP, SERPINA3, SPDEF, ADAM8, CAV1, MGP, AIF1, ALDH3A1, HSD17B3, PRKCQ, EZH1, DDIT4, MFAP5, FERMT2, IGFBP5, ZEB1, FMOD, PRELP, CFLAR, STEAP3, APOD, SERPING1, HTR4, ADIPOQ, ANPEP, C1R, DUSP5, DPT, LY6E, CYP1A1, APOBEC1, ENTPD1, TUBB2C, FCGR2A, EMP3, SERPINF1, OLFML3, VIM, NOV, SULT1A1, ATP1A2, QPCT, PSEN1, CFD, MMP3, SCAMP2, RTN1, C13orf15, MMP13, CD163, GPC3, NNMT, GPX3, STAB1, CAST, TEK, TNFRSF11B, PCSK6, ZC3H13, TBL1X, ANGPTL1, IGFBP3, CD248, PRRC2C, TMEM176B, TNS1, AGTR1, RBP4, KIAA1370, LOX, SRPX, SCARA5, RECK, TPR, NRG1, EXT1, IFITM3, COL6A1, RGS5, TIMP1, SDC2, MCAM, ENPP2, AGT, TIMP3, DPP4, VCAM1, RNASE3, COL6A2, ATRX, CD36, N4BP1, SERPINE2, STRA6, PMP22, NTRK2, NT5E, SPARC, MAF, MSX1, HES1, TNXB, PCOLCE, IKZF2, SLC26A3, CTSS, ABCC1, FIGF, ANGPT4, ZBTB20, LYVE1, WNT5B, TIMP2, SFRP4, GUCY1A3, MITF, DCN, GSTM3, TUBB2A, MMP2, THBD, NEDD4, SPON2, COL3A1, SPTBN1, FYN, ITGBL1, FN1, MXRA8, BMPR2, CES1, VCAN, CDH11, SELENBP1, CA3, KLF9, IGF1, FGF18, PPAP2B, PRRX1, HLA-DRA, PDGFRA, GDF10, CTSK, MYLPF, FAM3B, STXBP6, CYP1B1, LTBP1, KITLG, TRIO, LSP1, S1PR1, PLAU, RBBP6, CRIP1, SDPR, POSTN, IGFBP6, FST, CXCL9, LRRC17, FGFR1, C1S, IFNGR1, GSN, BST2, PAPSS2, IL33, CD3G, CBL, PRSS23, CXCR7, LOXL1, C2orf40, TGFB3, FBN1, COL7A1, AOC3, BLNK, MMP14, LOXL2, COL1A2, AEBP1, GNG11, ANGPTL4, CFB, C7, CYGB, LTBP4, MARCKS, ALPL, CKM, COL1A1, ACOT2, SLC16A1, CXCL12, C4B (includes others), CAPN9, GAP43, CLEC10A
Connective Tissue Disorders	125ppm	NFIX, MMP14, ASPN, FBN1, AGTR1, AGT, TNFRSF11B
	500ppm	MRC1/MRC1L1, SLIT3, COL14A1, MMP16, XDH, SERPINA3, C1QA, TNXB, FGG, G0S2, CTSS, POSTN, AIF1, ADAMTS5, ADAMTS16, ACTA1, TIMP2, TNFRSF11B, HLA-C, PTGIS, CXCL9, C1S, GSN, IL33, C1qtnf6, CLIC2, TPST1, MATN2, CES5A, FBN1, TNFAIP6, TNS1, AGTR1, C2, RBP4, ARG1, COL3A1, APOE, LOX, FYN, FN1, NFIX, GALNTL1, RECK, HLA-DQA1, ADIPOQ, SELENBP1, C1R, LHFP, COL6A1, IGF1, SDC2, ANXA1, PDGFRA, CFB, ASPN, ENPP2, GBP2, HSPB6, AGT, TIMP3, DPP4, COL5A2, VCAM1, FCGR2A, TUBB2C, CD36, C7orf58, VIM, F13A1, SPATS2L, CSGALNACT1, STXBP6, GRB10, LTBP1, COL5A3, PMP22, GHR, NTRK2, CXCL12, TNFSF13, C4B (includes others), SPARC, GAP43, PLAU, EFEMP1, ACSL1, MAOA

	2500ppm	SLIT3, MRC1/MRC1L1, DPYSL2, COL14A1, XDH, SERPINA3, HLA-DMB, C1QA, TNXB, ADAM8, EGR2, CTSS, ZBTB20, AIF1, ADAMTS16, WNT5B, TIMP2, PRKCQ, TUBB2A, IGFBP5, MMP2, TPST1, CES5A, MS4A7, CFLAR, COL3A1, FYN, FN1, FAM63B, LRP6, ADIPOQ, CDH11, SELENBP1, C1R, COL5A1, LHFP, IGF1, HLA-DRA, PDGFRA, TUBB2C, FCGR2A, VIM, SPATS2L, STXBP6, LTBP1, COL5A3, PGCP, TNFSF13, FCER1G, S1PR1, P2RY12, PLAU, PSEN1, MMP3, C13orf15, MMP13, FMNL2, LATS2, G0S2, POSTN, ADAMTS5, ACTA1, TNFRSF11B, HLA-C, CXCL9, C1S, FGFR1, IFNGR1, GSN, PAPSS2, IL33, CLIC2, MATN2, FBN1, PRRC2C, TNS1, AGTR1, C2, COL7A1, KIAA1370, RBP4, BLNK, LOX, NFIX, GALNTL1, MMP14, RECK, PHLDB2, COL1A2, COL6A1, RGS5, TIMP1, SDC2, ASPN, CFB, ENPP2, ALPL, AGT, TIMP3, DPP4, VCAM1, COL5A2, COL6A2, EFEMP2, CD36, C7orf58, F13A1, GRB10, RCOR1, COL1A1, EBF1, PMP22, NTRK2, CXCL12, C4B (includes others), SPARC, GAP43, ACSL1
Genetic Disorder	125ppm	MRC1/MRC1L1, SLIT3, NFIX, EMILIN2, MMP14, MSX1, SERPINA3, MSLN, VCAN, C1R, FSTL1, GPX3, CTSS, TNNT3, PROS1, HLA-DRA, ASPN, CAV1, CYGB, FIGF, ACTA1, AGT, TNFRSF11B, PVALB, TIMP3, TTR, NBL1, GUCY1A3, CXCR4, FGFR1, LAMA2, VIM, IGFBP5, MFAP4, THBD, ANGPTL1, MYL1, OGN, NTRK2, CXCL12, FBN1, PLTP, PLAU, AGTR1
	500ppm	SLIT3, DBN1, COL14A1, GAS6, PTPLA, XDH, CLMP, SERPINA3, CP, RBFOX3, FGG, SLC39A8, SRPX2, CAV1, MGP, ADAMTS16, PTGIS, WT1, ACAA1, MFAP5, CIDEC, SPOCK2, NDN, CES5A, PLTP, TNFAIP6, PCBD1, APOD, APOE, SERPING1, FHL1, HTR4, GDF15, PTPN14, ADIPOQ, HLA-DQA1, C1R, LHFP, AR, PTPRJ, SORBS1, PROS1, C9orf150, PLA2G16, TUBB2C, FCGR2A, FUCA2, SERPINF1, VIM, SPATS2L, CSGALNACT1, MMD, LAMB2, MYOC, FAM114A1, SULT1A1, ATP1A2, SYNGR1, MAOA, RTN1, BNC2, GPC3, PLBD1, GPX3, ENTPD5, LPL, NUPR1, COQ6, CAST, ADAMTS5, HLA-C, TNFRSF11B, GULP1, AQP7, LAMA2, PCSK6, FXYD1, RDX, ANGPTL1, MAMDC2, OGN, MATN2, PNOC, TMEM176B, TNS1, AGTR1, C2, RBP4, PBRM1, LOX, TPM1, IFI27, SRPX, NEFL, SCARA5, RECK, PKHD1L1, CLIC4, COL6A1, DDR2, SDC2, ENPP2, AGT, DPP4, TIMP3, VCAM1, RNASE3, NBL1, AP1S2, CD36, LOXL3, EGFL7, SEPP1, PMP22, CIDEA, NTRK2, P2RY14, GHR, NT5E, SPARC, C5orf13, ACSL1, MRC1/MRC1L1, GPD1, CA12, MSX1, TNXB, TIPARP, MYLK, KRT13, CTSS, CASQ1, FIGF, TIMP2, GUCY1A3, PCSK5, DCN, OAT, THBD, GPM6A,

		SFRP1, CAPRIN1, COL3A1, FYN, ITGBL1, FN1, EMILIN2, MSLN, VCAN, SELENBP1, CA3, FSTL1, IGF1, FGF18, PDLIM5, PDGFRA, FXYD2, SMPD3, LIMCH1, FMO3, CTSK, FAM3B, MFAP4, RAMP1, AXL, F3, STXBP6, MYL1, LTBP1, COL5A3, TF, ANK2, BNC1, TNFSF13, IHH, PLAU, MMP16, MAP1B, G0S2, CRIP1, TNNT3, POSTN, TSPAN4, ACTA1, NMBR, IGFBP6, FST, CXCL9, CD302, LRRC17, C1S, MACROD1, GCNT2, GSN, BST2, IL33, PRSS23, LOXL1, S100B, TGFB3, C2orf40, FBN1, AKR1B1, ARG1, AOC3, NFIX, PTGER3, PPP1R1A, AEBP1, PHYH, ANXA1, ASPN, CFB, C7, CYGB, CCRL1, GBP2, PVALB, COL5A2, CKM, CD48, C7orf58, F13A1, GRB10, CLDN1, SLC16A1, CXCL12, C4B (includes others), FBLN2, EFEMP1, GAP43
	2500ppm	SLIT3, DPYSL2, DBN1, COL14A1, GAS6, XDH, CHRNB1, CLMP, SERPINA3, CP, SPDEF, ZFYVE1, EGR2, CAV1, DMXL2, MGP, TCERG1, ARHGEF26, ADAMTS16, ALDH3A1, HSD17B3, PRKCQ, MED1, MFAP5, CIDEC, IGFBP5, ZEB1, NDN, CES5A, CFLAR, PLTP, WASF2, APOD, SERPING1, HTR4, HNRNPA2B1, ADIPOQ, C1R, SPON1, LHFP, DUSP5, PROS1, MXD1, LY6E, CYP1A1, ENTPD1, TUBB2C, FCGR2A, SERPINF1, VIM, SPATS2L, ID3, MMD, MYOC, FAM114A1, SULT1A1, ATP1A2, EBF3, PSEN1, FNDC1, QPCT, CFD, MMP3, RTN1, EML4, C13orf15, MMP13, GPC3, CD163, PLBD1, MPP6, GPX3, LPL, ARHGAP20, STAB1, CAST, ADAMTS5, TEK, HLA-C, TNFRSF11B, GULP1, AQP7, GM2A, LAMA2, PCSK6, RDX, FXYD1, ANGPTL1, TBL1X, OGN, HMGXB4, MATN2, IGFBP3, ANKRD11, PPP1R12A, MAP2, TNS1, TMEM176B, AGTR1, C2, RBP4, KIAA1370, PBRM1, LOX, MANEA, SRPX, SCARA5, NEFL, RECK, SLC35D3, NRG1, EXT1, CLIC4, PHLDB2, COL6A1, RGS5, DDR2, SDC2, TIMP1, MCAM, ENPP2, AGT, KDM4C, DPP4, TIMP3, VCAM1, RNASE3, COL6A2, NBL1, XRN2, AP1S2, ATRX, CD36, SERPINE2, STRA6, PMP22, NRTN, NTRK2, SLC14A1, NT5E, SPARC, C5orf13, ACSL1, MRC1/MRC1L1, CADM3, GPD1, MAF, MSX1, HLA-DMB, HES1, TNXB, PTPRO, CTSS, PRPF4B, ABCC1, CASQ1, ZBTB20, PRPF40A, FIGF, CRIM1, WNT5B, TIMP2, DBP, GUCY1A3, MITF, PCSK5, DCN, TUBB2A, MMP2, PCK1, THBD, NEDD4, SPON2, NR1D1, MS4A7, COL3A1, SPTBN1, FYN, ITGBL1, FN1, EMILIN2, MXRA8, LRP6, BMPR2, GBF1, CDH11, VCAN, SELENBP1, COL5A1, FSTL1, CA3, YY1, RIF1, IGF1, FGF18, TTC7B, LRRFIP1, PDLIM5, HLA-DRA, PDGFRA, FXYD2, LIMCH1, RRP1B, FMO3, CTSK, FAM3B, MFAP4, STXBP6, MYL1, CYP1B1, LTBP1, KITLG, PGCP, COL5A3, TRIO, GLIS2, VPS13C, TNFSF13, FCER1G, S1PR1,

		P2RY12, PLAU, SERPINI1, FMNL2, LATS2, NID1, ZC3H11A, SSR3, G0S2, CRIP1, POSTN, DKK2, NIPBL, KLF2, ACTA1, IGFBP6, TRIOBP, FST, CXCL9, CD302, LRRC17, C1S, FGFR1, GCNT2, IFNGR1, GSN, BST2, PAPSS2, EPRS, GRHPR, IL33, CD3G, RPS6KA6, CBL, PRSS23, CXCR7, S100B, LOXL1, TGFB3, C2orf40, FBN1, ELF5, COL7A1, AOC3, BLNK, POU3F1, NFIX, PTGER3, MMP14, COL1A2, AEBP1, ANGPTL4, PHYH, ASPN, CFB, C7, CYGB, TULP4, MARCKS, ALPL, PVALB, COL5A2, CKM, EFEMP2, C7orf58, F13A1, MSI2, GRB10, COL1A1, EBF1, CNN3, SLC16A1, CXCL12, C4B (includes others), FBLN2, GAP43, AKAP9
Organismal Development	125ppm	AOC3, TIMP3, GUCY1A3, CXCR4, MMP14, FGFR1, SERPINF1, ANPEP, ANGPTL1, TIPARP, LAMC1, AEBP1, NTRK2, CTSS, CXCL12, PPAP2B, CAV1, FIGF, PLAU, AGTR1, AGT
	500ppm	GAS6, TIPARP, MFAP2, CTSS, LPL, CAV1, FIGF, TIMP2, IGFBP6, AQP7, WT1, FST, GUCY1A3, ANGPTL1, IL33, TPST1, AGTR1, COL3A1, AOC3, LOX, APOE, FN1, PTGER3, RECK, ADIPOQ, ANPEP, AR, IGF1, PTPRJ, FGF18, PHYH, PPAP2B, PRRX1, AGT, TIMP3, VCAM1, MYLPF, CD36, SERPINF1, AXL, F3, LAMB2, GHR, NTRK2, CXCL12, ATP1A2, SPARC, IHH, PLAU
	2500ppm	GAS6, MSX1, HES1, SPAG9, SPDEF, PCOLCE, LAMC1, CTSS, ABCC1, CAV1, FIGF, ANGPT4, ZBTB20, AIF1, TIMP2, GUCY1A3, MED1, PCSK5, MITF, MMP2, IGFBP5, ZEB1, THBD, NEDD4, PATZ1, MYST3, WASF2, COL3A1, FN1, LRP6, ADIPOQ, ANPEP, VCAN, COL5A1, YY1, IGF1, FGF18, PPAP2B, PRRX1, PDLIM5, MXD1, PDGFRA, LY6E, SERPINF1, ID3, CYP1B1, KITLG, SERPINH1, S1PR1, PLAU, PSEN1, MMP3, NR2F2, MMP13, GPC3, POSTN, STAB1, NIPBL, KLF2, TEK, TNFRSF11B, FST, FGFR1, GCNT2, LAMA2, PCSK6, GSN, ANGPTL1, BST2, IL33, CBL, ANKRD11, IGFBP3, TGFB3, AGTR1, RBP4, AOC3, LOX, PTGER3, MMP14, RECK, NRG1, EXT1, COL1A2, AEBP1, ANGPTL4, RGS5, TIMP1, LTBP4, MARCKS, AGT, TIMP3, VCAM1, S1PR2, NBL1, EFEMP2, CD36, GRB10, COL1A1, NTRK2, SLC14A1, CXCL12, BIK, SPARC

Cell-To-Cell Signaling and Interaction	125ppm	AOC3, MRC1/MRC1L1, TPM1, MMP14, PTPN14, VCAN, NID1, LAMC1, SDC2, PPAP2B, PROS1, HLA-DRA, CAV1, FIGF, TNFRSF11B, AGT, TIMP3, TTR, CXCR4, FGFR1, LAMA2, SERPINF1, VIM, IGFBP5, THBD, ANGPTL1, CD3G, MYOC, CXCL12, LSP1, CD248, PLTP, PLAU, TFPI, CERCAM
	500ppm	MRC1/MRC1L1, RARRES2, GAS6, CDH22, MMP16, XDH, C1QA, MMRN1, TNXB, GPC3, FGG, SRPX2, LPL, CAV1, POSTN, FIGF, LYVE1, FXYD5, HLA-C, TNFRSF11B, TIMP2, CXCL9, DCN, LAMA2, THBD, GSN, ANGPTL1, NDN, IL33, S100B, TGFB3, CD248, PLTP, TNFAIP6, COL3A1, AOC3, TPM1, FYN, LOX, APOE, SERPING1, FN1, PTGER3, PPP1R1A, NID2, SCARA5, PTPN14, HLA-DQA1, ADIPOQ, MSLN, CLIC4, ANPEP, LOXL2, SOD3, VCAN, SSPN, VNN1, AR, PTPRJ, IGF1, SORBS1, SDC2, PPAP2B, ANXA1, PROS1, PDGFRA, AGT, TIMP3, Mcpt1, DPP4, VCAM1, RNASE3, FCGR2A, CD36, SERPINF1, CD48, VIM, F13A1, RAMP1, AXL, F3, LTBP1, LAMB2, COL5A3, GHR, MYOC, CLDN1, NT5E, TNFSF13, CXCL12, LSP1, C4B (includes others), SPARC, PLAU, GAP43, CLEC10A
	2500ppm	MRC1/MRC1L1, CADM3, GAS6, XDH, MAF, HLA-DMB, C1QA, HES1, TNXB, ADAM8, LAMC1, EGR2, CAV1, FIGF, LYVE1, TIMP2, PRKCQ, DCN, FERMT2, MMP2, IGFBP5, ZEB1, THBD, NDN, SPON2, PLTP, ADIPOR2, COL3A1, FYN, SERPING1, FN1, NID2, LRP6, ADIPOQ, SOD3, CDH11, VCAN, COL5A1, IGF1, PROS1, PPAP2B, HLA-DRA, PDGFRA, ENTPD1, FCGR2A, SERPINF1, VIM, LTBP1, KITLG, COL5A3, MYOC, TNFSF13, LSP1, S1PR1, FCER1G, P2RY12, PLAU, PSEN1, RARRES2, SERPINI1, CDH22, MMP13, MMRN1, CD163, GPC3, NID1, LPL, POSTN, KLF2, TEK, HLA-C, TNFRSF11B, ASGR2, CXCL9, FGFR1, LAMA2, IFNGR1, GSN, ANGPTL1, IL33, CD3G, CBL, S100B, IGFBP3, CD248, COL7A1, AOC3, LOX, PTGER3, SCARA5, MMP14, NRG1, CLIC4, LOXL2, SSPN, VNN1, SDC2, TIMP1, MCAM, MARCKS, AGT, Mcpt1, DPP4, TIMP3, VCAM1, RNASE3, CD36, F13A1, SERPINE2, EBF1, ENTPD2, NT5E, CXCL12, C4B (includes others), SPARC, CLEC10A, CERCAM
Tissue Development	125ppm	AOC3, SLIT3, TPM1, NFIX, MMP14, PTPN14, MSX1, VCAN, NID1, TIPARP, LAMC1, AEBP1, SDC2, PPAP2B, CAV1, FIGF, LTBP4, TNFRSF11B, AGT, TIMP3, CXCR4, FGFR1, MYLPF, LAMA2, PCSK6, SERPINF1, IGFBP5, THBD, ANGPTL1, MYOC, NTRK2, CXCL12, PLTP, PLAU, TFPI,

		ADAMTSL4, IGSF10, CCDC80, CERCAM
	500ppm	SLIT3, COL14A1, GAS6, XDH, MSX1, CLMP, CP, C1QA, TNXB, TIPARP, FGG, MFAP2, SRPX2, CAV1, FIGF, LYVE1, TIMP2, WT1, GUCY1A3, PCSK5, DCN, SPOCK2, FMOD, THBD, SFRP1, PLTP, ADAMTSL4, TNFAIP6, IGSF10, COL3A1, APOE, FYN, SERPING1, FN1, NID2, PTPN14, ADIPOQ, VCAN, AR, IGF1, PTPRJ, SORBS1, FGF18, PRRX1, PPAP2B, PDGFRA, TBX2, CTSK, FCGR2A, MYLPF, SERPINF1, AXL, F3, COL5A3, MYOC, TNFSF13, IHH, PLAU, RARRES2, MMP16, CDH22, MAP1B, MMRN1, GPC3, POSTN, CAST, FXYD5, TNFRSF11B, CXCL9, FST, PCSK6, LAMA2, GSN, ANGPTL1, IL33, TGFB3, AKR1B1, CCDC80, RBP4, PBRM1, AOC3, LOX, TPM1, NFIX, PTGER3, RECK, CLIC4, LOXL2, SSPN, AEBP1, VNN1, SDC2, ANXA1, C7, ENPP2, LTBP4, AGT, TIMP3, VCAM1, CD36, CD48, F13A1, EGFL7, GHR, NTRK2, CLDN1, CXCL12, C4B (includes others), SPARC, GAP43
	2500ppm	SLIT3, CADM3, COL14A1, GAS6, XDH, MAF, MSX1, CLMP, C1QA, CP, HES1, TNXB, ADAM8, LAMC1, MFAP2, EGR2, CAV1, FIGF, ANGPT4, LYVE1, TIMP2, PRKCQ, GUCY1A3, PCSK5, MED1, MITF, DCN, FERMT2, IGFBP5, MMP2, ZEB1, FMOD, THBD, SPON2, PLTP, IGSF10, COL3A1, FYN, SERPING1, FN1, NID2, LRP6, HNRNPA2B1, ADIPOQ, BMPR2, VCAN, CDH11, COL5A1, IGF1, FGF18, PRRX1, PPAP2B, PDGFRA, LY6E, CTSK, ENTPD1, FCGR2A, MYLPF, SERPINF1, KITLG, TRIO, COL5A3, MYOC, TNFSF13, S1PR1, FCER1G, P2RY12, PLAU, PSEN1, SERPINI1, RARRES2, MMP3, CDH22, NR2F2, MMP13, MMRN1, GPC3, NID1, POSTN, NIPBL, CAST, KLF2, TEK, TNFRSF11B, CXCL9, FST, FGFR1, PCSK6, LAMA2, IFNGR1, GSN, ANGPTL1, PAPSS2, IL33, CBL, IGFBP3, TGFB3, ANKRD11, CCDC80, ELF5, COL7A1, RBP4, AOC3, PBRM1, POU3F1, LOX, NFIX, PTGER3, MMP14, RECK, NRG1, EXT1, CLIC4, LOXL2, SSPN, AEBP1, VNN1, SDC2, TIMP1, MCAM, C7, LTBP4, ENPP2, MARCKS, AGT, TIMP3, VCAM1, EFEMP2, CD36, F13A1, SERPINE2, NTRK2, NRTN, CXCL12, C4B (includes others), SPARC, GAP43, CERCAM

Cellular Growth and Proliferation	125ppm	SLIT3, NAB2, ATP2B1, MSX1, LAMC1, GPX3, CRIP1, IKZF2, KIF13A, CTSS, CAV1, Cyss (includes others), FIGF, TNFRSF11B, SFRP4, GUCY1A3, FGFR1, PCSK6, LAMA2, IGFBP5, THBD, ANGPTL1, BST2, CD3G, JDP2, LOC100506736/SLFN12L, FBN1, NGFRAP1, CD248, TFPI, AGTR1, TPM1, KLK1, NFIX, EMILIN2, MMP14, PTPN14, MSLN, IFITM3, VCAN, KLF9, AEBP1, DPT, DDR2, SDC2, BRD4, CYGB, LTBP4, AGT, PLA2G16, TIMP3, CXCR4, SERPINF1, VIM, Tsc22d3, PMP22, NTRK2, NOV, SERPINH1, CXCL12, PLAU, HRASLS
	500ppm	SLIT3, DBN1, COL14A1, GAS6, XDH, MSX1, MYLK, MFAP2, SLC26A3, CTSS, CAV1, MGP, FIGF, AIF1, TIMP2, WT1, SFRP4, GUCY1A3, DCN, THBD, NDN, JDP2, SFRP1, CAPRIN1, TNFAIP6, STEAP3, APOE, FYN, FHL1, EMILIN2, FN1, HTR4, PTPN14, GDF15, ADIPOQ, FOLR2, MSLN, VCAN, CA3, KLF9, AR, PTPRJ, IGF1, DPT, FGF18, PRRX1, PDGFRA, TBX2, FXYD2, CAV2, PLAC8, APOBEC1, EMP3, SERPINF1, VIM, AXL, F3, LTBP1, LAMB2, NOV, TF, SERPINH1, TNFSF13, BNC1, IHH, PLAU, FGL2, GPC3, GPX3, CRIP1, ENTPD5, POSTN, NUPR1, CAST, TNFRSF11B, IGFBP6, AQP7, FST, CXCL9, PCSK6, LAMA2, FXYD1, MAGED2, GSN, ANGPTL1, BST2, IL33, S100B, TGFB3, FBN1, CD248, AKR1B1, AGTR1, RBP4, ARG1, TPM1, LOX, NFIX, RECK, IFITM3, AEBP1, COL6A1, SDC2, DDR2, ANXA1, CFB, CYGB, ENPP2, LTBP4, GBP2, AGT, DPP4, TIMP3, ST3GAL2, VCAM1, RNASE3, CD36, CD48, EGFL7, GRB10, Tsc22d3, PMP22, GHR, NTRK2, NT5E, CXCL12, SPARC, NFIB, GAP43, C5orf13, CLEC10A
	2500ppm	SLIT3, DBN1, COL14A1, GAS6, XDH, MSX1, HES1, SPDEF, LAMC1, MFAP2, EGR2, SLC26A3, IKZF2, PTPRO, CTSS, ABCC1, CAV1, MGP, FIGF, AIF1, SLC12A4, ALDH3A1, WNT5B, TIMP2, SFRP4, PRKCQ, GUCY1A3, MED1, MITF, DCN, IGFBP5, MMP2, ZEB1, THBD, NDN, PATZ1, NR1D1, JDP2, CFLAR, WASF2, ADIPOR2, STEAP3, SPTBN1, FYN, EMILIN2, FN1, HTR4, HNRNPA2B1, LRP6, ADIPOQ, FOLR2, BMPR2, GBF1, EIF4G1, CDH11, VCAN, CA3, KLF9, DUSP5, YY1, IGF1, DPT, FGF18, PRRX1, MXD1, PDGFRA, FXYD2, PLAC8, CYP1A1, APOBEC1, ENTPD1, EMP3, SERPINF1, VIM, SCAF11, ID3, CYP1B1, LTBP1, KITLG, TRIO, NOV, SERPINH1, TNFSF13, S1PR1, FCER1G, PLAU, RBBP6, HRASLS, PSEN1, MMP3, SCAMP2, FGL2, NR2F2, CD163, LATS2, GPC3, GPX3, CRIP1, POSTN, CAST, KLF2, TEK, TNFRSF11B, AQP7, IGFBP6, FST, CXCL9, FGFR1, LAMA2, PCSK6, FXYD1, IFNGR1, GSN, BST2, ANGPTL1, IL33, CD3G, CBL, CXCR7, S100B, IGFBP3,

		TGFB3, FBN1, CD248, PRRC2C, AGTR1, ELF5, RBP4, BLNK, LOX, NFIX, RECK, MMP14, NRG1, TPR, IFITM3, COL1A2, AEBP1, COL6A1, ANGPTL4, TIMP1, DDR2, SDC2, MCAM, CFB, CYGB, ENPP2, LTBP4, AGT, KDM4C, DPP4, TIMP3, ST3GAL2, VCAM1, RNASE3, S1PR2, COL6A2, EFEMP2, XRN2, CD36, MSI2, GRB10, SERPINE2, COL1A1, Tsc22d3, PMP22, NTRK2, NT5E, CXCL12, SPARC, GAP43, C5orf13, CLEC10A
Cellular Development	125ppm	SLIT3, NAB2, TPM1, EMILIN2, MMP14, PTPN14, MSX1, SERPINA3, ANPEP, NID1, VCAN, LAMC1, KLF9, KIF13A, SDC2, CAV1, GDF10, ASPN, FIGF, LTBP4, TNFRSF11B, AGT, TIMP3, SFRP4, NBL1, CXCR4, LRRC17, FGFR1, LAMA2, PCSK6, SERPINF1, VIM, IGFBP5, THBD, CD3G, PMP22, NOV, NTRK2, MYOC, JDP2, CXCL12, FBN1, PLAU, CCDC80, AGTR1
	500ppm	SLIT3, COL14A1, GAS6, XDH, MSX1, SERPINA3, C1QC, TIPARP, MYLK, SLC26A3, SRPX2, CAV1, MGP, FIGF, AIF1, TIMP2, WT1, SFRP4, DCN, THBD, NDN, JDP2, SFRP1, STEAP3, APOE, FYN, EMILIN2, FN1, HTR4, NID2, GDF15, PTPN14, HLA-DQA1, ADIPOQ, ANPEP, VCAN, SELENBP1, CA3, KLF9, AR, IGF1, SORBS1, FGF18, PRRX1, GDF10, TBX2, PLAC8, CTSK, FCGR2A, SERPINF1, VIM, CDO1, AXL, LTBP1, LAMB2, COL5A3, NOV, MYOC, ILDR2, BNC1, TNFSF13, IHH, PLAU, RARRES2, MAP1B, GPC3, ENTPD5, POSTN, CAST, TNFRSF11B, HLA-C, IGFBP6, FST, LRRC17, LAMA2, GSN, IL33, S100B, TGFB3, FBN1, AKR1B1, CCDC80, AGTR1, LOX, TPM1, PTGER3, CLIC4, LOXL2, VNN1, SDC2, ANXA1, ASPN, LTBP4, GBP2, AGT, TIMP3, DPP4, VCAM1, NBL1, Tsc22d3, PMP22, NTRK2, GHR, CXCL12, SPARC, GAP43, 1100001G20Rik, C5orf13, CLEC10A

	2500ppm	SLIT3, DPYSL2, COL14A1, GAS6, XDH, CHRNB1, MAF, MSX1, SERPINA3, C1QC, HES1, SPAG9, SPDEF, LAMC1, EGR2, SLC26A3, PTPRO, CAV1, MGP, FIGF, AIF1, WNT5B, TIMP2, SFRP4, PRKCQ, MITF, MED1, DCN, IGFBP5, MMP2, ZEB1, THBD, NDN, PATZ1, NR1D1, JDP2, MYST3, WASF2, CFLAR, STEAP3, FYN, EMILIN2, FN1, HTR4, NID2, LRP6, HNRNPA2B1, ADIPOQ, BMPR2, ANPEP, CDH11, VCAN, SELENBP1, CA3, KLF9, DUSP5, YY1, IGF1, FGF18, PRRX1, MXD1, GDF10, LY6E, PLAC8, CYP1A1, CTSK, FCGR2A, SERPINF1, VIM, CDO1, ID3, LTBP1, KITLG, COL5A3, NOV, ILDR2, MYOC, TNFSF13, S1PR1, FCER1G, P2RY12, EBF3, PLAU, RBBP6, PSEN1, RARRES2, MMP3, MMP13, GPC3, NID1, POSTN, NIPBL, CAST, KLF2, TEK, HLA-C, TNFRSF11B, IGFBP6, FST, LRRC17, FGFR1, LAMA2, IFNGR1, GSN, TBL1X, IL33, CD3G, CBL, CXCR7, S100B, IGFBP3, TGFB3, FBN1, CCDC80, ELF5, AGTR1, BLNK, POU3F1, LOX, PTGER3, CHD4, MMP14, NRG1, EXT1, CLIC4, LOXL2, VNN1, SDC2, TIMP1, MCAM, ASPN, LTBP4, MARCKS, AGT, DPP4, TIMP3, VCAM1, S1PR2, NBL1, EFEMP2, MSI2, SERPINE2, COL1A1, Tsc22d3, EBF1, PMP22, NTRK2, NRTN, CXCL12, SPARC, GAP43, 1100001G20Rik, C5orf13, CLEC10A
Skeletal and Muscular System Development and Function	125ppm	NAB2, SLIT3, TPM1, NFIX, ATP2B1, MMP14, MSX1, SERPINA3, VCAN, TIPARP, LAMC1, AEBP1, CTSS, TNNT3, CASQ1, GDF10, ASPN, CAV1, ACTA1, AGT, TNFRSF11B, TIMP3, PVALB, GUCY1A3, CXCR4, FGFR1, MYLPF, LAMA2, IGFBP5, THBD, MYL1, Tsc22d3, NOV, JDP2, CXCL12, FBN1, PLAU, TFPI, IGSF10
	500ppm	GAS6, XDH, C1QA, MYLK, CTSS, TNNT3, CASQ1, MGP, POSTN, CAV1, CAST, AIF1, ACTA1, TNFRSF11B, FST, PCSK5, FXYD1, FMOD, THBD, TGFB3, SFRP1, AKR1B1, IGSF10, RBP4, ARG1, APOE, TPM1, FHL1, NFIX, FN1, ADIPOQ, CLIC4, VCAN, SSPN, AR, IGF1, FGF18, SORBS1, PRRX1, ASPN, HSPB6, AGT, TIMP3, MYLPF, F3, EGFL7, MYL1, GRB10, Tsc22d3, GHR, NOV, ANK2, ATP1A2, C4B (includes others), SPARC, PLAU
	2500ppm	MMP3, GAS6, XDH, MSX1, MMP13, C1QA, HES1, GPC3, EGR2, CTSS, LPL, CAV1, MGP, POSTN, DKK2, NIPBL, AIF1, KLF2, TEK, TNFRSF11B, FST, MITF, PCSK5, FGFR1, LAMA2, MMP2, IGFBP5, ZEB1, GSN, THBD, FMOD, PAPSS2, IL33, PRELP, TGFB3, IGFBP3, ANKRD11, FBN1, IGSF10, RBP4, LOX, NFIX, FN1, MMP14, LRP6, ADIPOQ, EXT1, BMPR2, CLIC4, VCAN, CDH11, COL1A2, AEBP1, IGF1, TIMP1, FGF18, PRRX1, ASPN, GDF10, PDGFRA, ALPL, AGT, TIMP3, CTSK, VCAM1,

		COL5A2, S1PR2, COL1A1, TRIO, Tsc22d3, NOV, FCER1G, S1PR1, SPARC, PLAU, PSEN1
Inflammatory Response	125ppm	AOC3, MRC1/MRC1L1, MMP14, SERPINA3, C1QB, ANPEP, IFITM3, SOD3, VCAN, C1R, CTSS, PROS1, HLA-DRA, CAV1, FIGF, AGT, TNFRSF11B, TIMP3, NBL1, CXCR4, LAMA2, SERPINF1, THBD, BST2, CD3G, TPST1, CXCL12, LSP1, PLAU, TFPI, AGTR1
	500ppm	MRC1/MRC1L1, RARRES2, GAS6, XDH, C1QA, SERPINA3, C1QB, GPC3, FGG, MYLK, CTSS, NUPR1, CAV1, FIGF, AIF1, CAST, GULP1, TNFRSF11B, HLA-C, TIMP2, WT1, CXCL9, GUCY1A3, DCN, LAMA2, THBD, FMOD, GSN, BST2, IL33, TPST1, S100B, PNOC, PLTP, TNFAIP6, AKR1B1, AGTR1, C2, COL3A1, AOC3, APOE, FYN, SERPING1, FN1, PTGER3, HLA-DQA1, ADIPOQ, IFITM3, ANPEP, SOD3, VCAN, C1R, VNN1, PTPRJ, IGF1, PROS1, ANXA1, CFB, C7, CCRL1, GBP2, AGT, DPP4, Mcpt1, TIMP3, VCAM1, NBL1, FCGR2A, CD48, SERPINF1, CD36, F13A1, CDO1, AXL, F3, LTBP1, P2RY14, TF, NT5E, CXCL12, TNFSF13, LSP1, C4B (includes others), PLAU, CLEC10A
	2500ppm	MRC1/MRC1L1, GAS6, XDH, MAF, C1QA, HLA-DMB, SERPINA3, C1QB, ADAM8, EGR2, CTSS, ABCC1, CAV1, FIGF, AIF1, TIMP2, PRKCQ, GUCY1A3, DCN, MMP2, ZEB1, THBD, FMOD, SPON2, TPST1, ADIPOR2, COL3A1, FYN, SERPING1, FN1, ADIPOQ, ANPEP, VCAN, SOD3, C1R, IGF1, PROS1, HLA-DRA, ENTPD1, FCGR2A, SERPINF1, CDO1, LTBP1, KITLG, GNAI3, TNFSF13, LSP1, S1PR1, FCER1G, P2RY12, PLAU, PSEN1, RARRES2, MMP3, CD163, STAB1, CAST, KLF2, HLA-C, TNFRSF11B, GULP1, CXCL9, GM2A, LAMA2, IFNGR1, GSN, BST2, IL33, CD3G, CXCR7, S100B, C2, AGTR1, AOC3, BLNK, PTGER3, MMP14, IFITM3, VNN1, TIMP1, MCAM, CFB, C7, AGT, TIMP3, DPP4, Mcpt1, VCAM1, NBL1, CD36, SERPINE2, COL1A1, EBF1, NT5E, ENTPD2, CXCL12, C4B (includes others)
Inflammatory Disease	125ppm	NFIX, CTSS, MMP14, ASPN, FBN1, LTBP4, AGTR1

	500ppm	MRC1/MRC1L1, SLIT3, GPD1, GAS6, XDH, CA12, C1QA, SERPINA3, TNXB, RBFOX3, FGG, MYLK, OSTalpha, CTSS, AIF1, ADAMTS16, TIMP2, PTGIS, WT1, GUCY1A3, PCSK5, THBD, TPST1, CES5A, TNFAIP6, COL3A1, FYN, APOE, SERPING1, FN1, ADIPOQ, HLA-DQA1, FOLR2, ANPEP, SELENBP1, C1R, CA3, LHFP, AR, IGF1, PDGFRA, C9orf150, TUBB2C, FCGR2A, VIM, SPATS2L, RAMP1, CSGALNACT1, AXL, F3, STXBP6, LTBP1, TF, FAM114A1, TNFSF13, BNC1, ANK2, ATP1A2, PLAU, MAOA, RARRES2, MMP16, G0S2, LPL, POSTN, ADAMTS5, ACTA1, TNFRSF11B, HLA-C, IGFBP6, CXCL9, FST, C1S, MACROD1, LAMA2, GSN, IL33, C1qtnf6, CLIC2, MATN2, TGFB3, FBN1, TNS1, C2, AGTR1, ARG1, RBP4, LOX, NFIX, IFI27, GALNTL1, PTGER3, RECK, IFITM3, COL6A1, SDC2, ANXA1, CFB, ASPN, LTBP4, ENPP2, CCRL1, GBP2, AGT, DPP4, TIMP3, VCAM1, RNASE3, CD36, CD48, C7orf58, F13A1, LOXL3, GRB10, PMP22, GHR, NTRK2, NT5E, CXCL12, C4B (includes others), SPARC, GAP43, EFEMP1, ACSL1
	2500ppm	DPYSL2, MRC1/MRC1L1, SLIT3, GPD1, GAS6, XDH, SERPINA3, C1QA, HLA-DMB, TNXB, ADAM8, EGR2, CTSS, OSTalpha, ABCC1, ZBTB20, AIF1, ADAMTS16, WNT5B, TIMP2, PRKCQ, GUCY1A3, MED1, PCSK5, TUBB2A, IGFBP5, MMP2, ZEB1, THBD, SPON2, TPST1, CES5A, MS4A7, CFLAR, ADIPOR2, COL3A1, FYN, SERPING1, FN1, FAM63B, LRP6, ADIPOQ, FOLR2, ANPEP, CDH11, SELENBP1, COL5A1, SPON1, C1R, CA3, LHFP, DUSP5, RIF1, IGF1, HLA-DRA, MXD1, PDGFRA, CYP1A1, RRP1B, ENTPD1, FCGR2A, TUBB2C, VIM, SPATS2L, STXBP6, LTBP1, KITLG, PGCP, FAM114A1, TNFSF13, ATP1A2, S1PR1, FCER1G, P2RY12, PLAU, QPCT, PSEN1, CFD, SERPINI1, RARRES2, MMP3, C13orf15, FMNL2, MMP13, LATS2, CD163, G0S2, LPL, ARHGAP20, POSTN, NIPBL, ADAMTS5, KLF2, ACTA1, TEK, HLA-C, TNFRSF11B, IGFBP6, TRIOBP, CXCL9, FST, FGFR1, C1S, LAMA2, IFNGR1, GSN, PAPSS2, IL33, CD3G, CLIC2, MATN2, IGFBP3, TGFB3, FBN1, PRRC2C, TNS1, C2, AGTR1, RBP4, KIAA1370, BLNK, LOX, NFIX, PTGER3, GALNTL1, MMP14, RECK, NRG1, IFITM3, PHLDB2, COL6A1, RGS5, TIMP1, SDC2, MCAM, CFB, ASPN, LTBP4, ENPP2, ALPL, AGT, DPP4, TIMP3, KDM4C, VCAM1, RNASE3, EFEMP2, CD36, C7orf58, F13A1, MSI2, GRB10, SERPINE2, RCOR1, COL1A1, EBF1, PMP22, NTRK2, NT5E, CNN3, CXCL12, C4B (includes others), BIK, SPARC, GAP43, ACSL1

Cellular Assembly and Organization	125ppm	TPM1, NFIX, TPPP3, MMP14, PTPN14, SERPINA3, SLC9A4, ANPEP, VCAN, LAMC1, KLF9, SDC2, SDPR, TNFRSF11B, AGT, TTR, CXCR4, LAMA2, SERPINF1, VIM, BST2, PMP22, NTRK2, SERPINH1, CXCL12, PLAU
	500ppm	DBN1, GAS6, MAP1B, SERPINA3, TNXB, MYLK, POSTN, CAV1, CAST, LYVE1, ACTA1, WT1, CXCL9, DCN, LAMA2, RDX, SPOCK2, GSN, FMOD, BST2, NDN, S100B, TGFB3, GPM6A, PNOC, COL3A1, ARG1, APOE, FYN, LOX, TPM1, FHL1, FN1, NFIX, NEFL, NID2, RECK, PTPN14, ADIPOQ, ANPEP, VCAN, AR, IGF1, SDC2, SORBS1, DPT, FGF18, CAV2, TMOD2, AGT, COL5A2, VCAM1, FCGR2A, SERPINF1, VIM, AXL, PMP22, COL5A3, GHR, NTRK2, CXCL12, SERPINH1, SPARC, NFIB, GAP43, PLAU, SYNGR1, MAOA
	2500ppm	DPYSL2, SLIT3, DBN1, GAS6, SERPINA3, TNXB, NID1, LAMC1, ARHGAP20, POSTN, CAV1, LYVE1, CAST, KLF2, ACTA1, TEK, PRKCQ, CXCL9, DCN, FGFR1, LAMA2, RDX, MMP2, GSN, BST2, NDN, S100B, IGFBP3, MAP2, COL3A1, LOX, POU3F1, FYN, FN1, NFIX, NID2, NEFL, RECK, MMP14, TPR, NRG1, EFHD1, EXT1, VCAN, COL1A2, COL5A1, IGF1, TIMP1, FGF18, DPT, MARCKS, AGT, COL5A2, VCAM1, S1PR2, NBL1, FCGR2A, VIM, SERPINE2, KITLG, COL1A1, COL5A3, TRIO, PMP22, NRTN, NTRK2, CXCL12, SERPINH1, S1PR1, SPARC, GAP43, PLAU, SEPT2, PSEN1
Cellular Function and Maintenance	125ppm	CXCR4, CXCL12, CAV1, AGTR1, AGT
	500ppm	MRC1/MRC1L1, DBN1, LOX, APOE, FYN, FN1, NEFL, GAS6, ADIPOQ, C1QA, TNXB, GPC3, AR, IGF1, SORBS1, DPT, ANXA1, PROS1, CAV1, CAV2, TMOD2, GULP1, VCAM1, COL5A2, CXCL9, FCGR2A, DCN, RDX, CD36, VIM, AXL, BST2, F3, GHR, CXCL12, SERPINH1, TGFB3, PLAU, COL3A1
	2500ppm	MRC1/MRC1L1, DBN1, LOX, FYN, FN1, NEFL, ADIPOQ, C1QA, TNXB, GPC3, CD163, COL5A1, COL1A2, DPT, PROS1, CAV1, KLF2, GULP1, VCAM1, COL5A2, FCGR2A, DCN, RDX, CD36, VIM, NEDD4, CD3G, COL1A1, CBL, CXCL12, SERPINH1, FCER1G, TGFB3, PLAU, COL3A1
Skeletal and Muscular Disorders	125ppm	TIMP3, NFIX, CXCR4, MMP14, LAMA2, MSX1, IFITM3, MYL1, TNNT3, HLA-DRA, ASPN, CAV1,

		FBN1, PLAU, ACTA1, AGTR1, TNFRSF11B, AGT
	500ppm	MRC1/MRC1L1, SLIT3, GPD1, XDH, MSX1, CA12, SERPINA3, C1QA, CP, TNXB, FGG, MFAP2, CTSS, CASQ1, MGP, AIF1, ADAMTS16, PTGIS, GUCY1A3, TPST1, CES5A, TNFAIP6, APOD, COL3A1, FYN, APOE, SERPING1, FHL1, FN1, HLA-DQA1, ADIPOQ, VCAN, SELENBP1, C1R, CA3, LHFP, AR, IGF1, SMPD3, CTSK, TUBB2C, FCGR2A, VIM, SPATS2L, CSGALNACT1, AXL, F3, STXBP6, MYL1, LTBP1, TNFSF13, ATP1A2, IHH, PLAU, MAOA, RTN1, MMP16, MAP1B, GPC3, G0S2, TNNT3, LPL, CAST, ADAMTS5, ACTA1, TNFRSF11B, HLA-C, CXCL9, FST, C1S, GCNT2, LAMA2, GSN, IL33, C1qtnf6, CLIC2, MATN2, LOXL1, S100B, C2orf40, FBN1, TNS1, AGTR1, C2, ARG1, RBP4, LOX, NFIX, SRPX, PPP1R1A, NEFL, GALNTL1, RECK, AEBP1, COL6A1, SDC2, ANXA1, C7, ASPN, CFB, ENPP2, GBP2, AGT, PVALB, TIMP3, DPP4, VCAM1, COL5A2, AP1S2, C7orf58, CD36, F13A1, GRB10, PMP22, NTRK2, GHR, SLC16A1, CXCL12, C4B (includes others), SPARC, EFEMP1, GAP43, C5orf13, ACSL1
	2500ppm	DPYSL2, MRC1/MRC1L1, SLIT3, GPD1, XDH, CHRNB1, MSX1, CP, SERPINA3, C1QA, HLA-DMB, TNXB, ADAM8, MFAP2, EGR2, CTSS, CASQ1, MGP, TCERG1, ZBTB20, AIF1, CRIM1, ADAMTS16, WNT5B, PRKCQ, DBP, GUCY1A3, TUBB2A, IGFBP5, MMP2, NR1D1, TPST1, MS4A7, CES5A, CFLAR, APOD, COL3A1, FYN, SERPING1, FN1, FAM63B, LRP6, ADIPOQ, VCAN, CDH11, SELENBP1, C1R, COL5A1, CA3, LHFP, DUSP5, IGF1, MXD1, HLA-DRA, PDGFRA, RRP1B, CTSK, FCGR2A, TUBB2C, VIM, SPATS2L, ID3, STXBP6, MYL1, LTBP1, PGCP, TNFSF13, ATP1A2, S1PR1, FCER1G, P2RY12, PLAU, PSEN1, SERPINI1, MMP3, RTN1, C13orf15, FMNL2, MMP13, GPC3, LATS2, SSR3, G0S2, LPL, DKK2, CAST, ADAMTS5, ACTA1, TNFRSF11B, HLA-C, CXCL9, C1S, FGFR1, LAMA2, GCNT2, IFNGR1, GSN, PAPSS2, IL33, CLIC2, MATN2, S100B, LOXL1, C2orf40, ANKRD11, FBN1, MAP2, PRRC2C, TNS1, AGTR1, C2, KIAA1370, RBP4, BLNK, POU3F1, LOX, NFIX, SRPX, NEFL, GALNTL1, SLC35D3, RECK, MMP14, NRG1, EXT1, PHLDB2, COL1A2, AEBP1, COL6A1, RGS5, SDC2, TIMP1, C7, ASPN, CFB, ENPP2, ALPL, AGT, PVALB, KDM4C, DPP4, TIMP3, COL5A2, VCAM1, COL6A2, EFEMP2, AP1S2, C7orf58, CD36, F13A1, GRB10, RCOR1, COL1A1, EBF1, PMP22, NTRK2, SLC14A1, SLC16A1, CXCL12, C4B (includes others), SPARC, GAP43,

		C5orf13, ACSL1
Organismal Injury and Abnormalities	125ppm	KLK1, SFRP4, TPM1, CXCR4, FGFR1, MMP14, VIM, THBD, ANPEP, SOD3, NTRK2, CTSS, CXCL12, HLA-DRA, CAV1, PLAU, ACSL1, AGTR1, ACTA1, TNFRSF11B, AGT
	500ppm	XDH, CA12, C1QA, CTSS, LPL, NUPR1, CAV1, POSTN, LYVE1, ACTA1, TIMP2, TNFRSF11B, PTGIS, SFRP4, CXCL9, C1S, RDX, THBD, GSN, IL33, TNFAIP6, C2, AGTR1, ARG1, COL3A1, APOE, TPM1, FYN, SERPING1, FN1, IFI27, PTGER3, ADIPOQ, CES1, ANPEP, SOD3, C1R, CA3, VNN1, AR, IGF1, ANXA1, CFB, PDGFRA, PLAC8, HSPB6, PON3, AGT, VCAM1, FCGR2A, VIM, F3, TF, NT5E, CXCL12, ATP1A2, C4B (includes others), PLAU, ACSL1
	2500ppm	SERPINI1, MMP3, XDH, CHRNB1, MMP13, C1QA, ABCC1, LPL, CAV1, POSTN, LYVE1, KLF2, ACTA1, TNFRSF11B, TIMP2, SFRP4, CXCL9, MED1, FGFR1, C1S, RDX, IFNGR1, MMP2, THBD, GSN, IGFBP3, FBN1, AGTR1, C2, COL3A1, FYN, SERPING1, PTGER3, MMP14, ADIPOQ, BMPR2, ANPEP, SOD3, COL1A2, C1R, VNN1, RGS5, IGF1, TIMP1, HLA-DRA, PDGFRA, CFB, PLAC8, AGT, VCAM1, S1PR2, ENTPD1, FCGR2A, ID3, SERPINE2, COL1A1, GLIS2, NT5E, CXCL12, S1PR1, C4B (includes others), P2RY12, PLAU, ACSL1, PSEN1
Organ Development	125ppm	CXCR4, MMP14, FGFR1, PCSK6, SERPINF1, MSX1, IGFBP5, SOD3, TIPARP, VCAN, NTRK2, DPT, CXCL12, CAV1, FIGF, FBN1, PLAU, AGTR1, AGT

	500ppm	PBRM1, LOX, FN1, PTGER3, ADIPOQ, MSX1, GPC3, ANPEP, VCAN, TIPARP, AR, IGF1, PTPRJ, FGF18, DPT, MGP, PDGFRA, CAV1, TBX2, FIGF, WT1, COL5A2, VCAM1, FST, PCSK5, PCSK6, SERPINF1, CXCL12, TGFB3, SPARC, FBN1, IHH, NFIB, SFRP1, PLAU, COL3A1, RBP4
	2500ppm	SLIT3, NR2F2, MSX1, HES1, GPC3, EGR2, MGP, CAV1, FIGF, NIPBL, KLF2, WNT5B, TIMP2, HSD17B3, FST, MITF, MED1, PCSK5, DCN, FGFR1, PCSK6, MMP2, IGFBP5, PATZ1, IGFBP3, TGFB3, FBN1, CFLAR, TMEM176B, AGTR1, ELF5, COL3A1, RBP4, SPTBN1, PBRM1, LOX, POU3F1, FYN, FN1, PTGER3, MMP14, LRP6, NRG1, ADIPOQ, EXT1, ANPEP, VCAN, COL1A2, COL5A1, AEBP1, YY1, IGF1, FGF18, TIMP1, DPT, PDGFRA, LY6E, MARCKS, AGT, COL5A2, VCAM1, S1PR2, ATRX, SERPINF1, ID3, COL1A1, ILDR2, CXCL12, BIK, S1PR1, SPARC, PLAU, PSEN1
Immunological Disease	125ppm	CXCR4
	500ppm	MRC1/MRC1L1, SLIT3, COL14A1, GPD1, SERPINA3, C1QA, TNXB, MYLK, CTSS, AIF1, SFRP4, SPOCK2, THBD, FAM102B, TPST1, CES5A, TNFAIP6, COL3A1, FYN, APOE, SERPING1, FN1, PTPN14, ADIPOQ, HLA-DQA1, FOLR2, VCAN, SELENBP1, C1R, LHFP, CA3, AR, IGF1, PTPRJ, PDLIM5, PDGFRA, SESTD1, FCGR2A, TUBB2C, VIM, SPATS2L, CSGALNACT1, AXL, F3, STXBP6, LTBP1, ANK2, TNFSF13, ATP1A2, BNC2, G0S2, LPL, ADAMTS5, ACTA1, HLA-C, TNFRSF11B, IGFBP6, CXCL9, C1S, LAMA2, GSN, IL33, MAMDC2, C1qtnf6, CLIC2, MATN2, FBN1, TNS1, C2, AGTR1, ARG1, RBP4, LOX, IFI27, PTGER3, GALNTL1, RECK, CLIC4, IFITM3, SDC2, ANXA1, CFB, CCRL1, ENPP2, GBP2, AGT, DPP4, VCAM1, RNASE3, C7orf58, CD36, F13A1, GRB10, PMP22, NTRK2, GHR, NT5E, CXCL12, C4B (includes others), EFEMP1, GAP43, ACSL1

	2500ppm	DPYSL2, MRC1/MRC1L1, SLIT3, COL14A1, GPD1, CHRNB1, HLA-DMB, SERPINA3, C1QA, TNXB, ADAM8, EGR2, CTSS, PTPRO, ABCC1, ZBTB20, AIF1, SFRP4, PRKCQ, TUBB2A, MMP2, IGFBP5, THBD, FAM102B, TPST1, MS4A7, CES5A, CFLAR, COL3A1, FYN, SERPING1, FN1, FAM63B, LRP6, ADIPOQ, FOLR2, CDH11, VCAN, SELENBP1, C1R, SPON1, CA3, LHFP, IGF1, PDLIM5, HLA-DRA, PDGFRA, CYP1A1, TUBB2C, FCGR2A, VIM, SPATS2L, STXBP6, LTBP1, KITLG, PGCP, TNFSF13, ATP1A2, FCER1G, S1PR1, P2RY12, PSEN1, CFD, MMP3, C13orf15, FMNL2, MMP13, LATS2, G0S2, LPL, ARHGAP20, CHD2, KLF2, ADAMTS5, TEK, ACTA1, TNFRSF11B, HLA-C, IGFBP6, TRIOBP, CXCL9, FGFR1, GM2A, C1S, LAMA2, IFNGR1, GSN, PAPSS2, IL33, CD3G, CLIC2, MATN2, IGFBP3, FBN1, PRRC2C, TNS1, AGTR1, C2, COL7A1, KIAA1370, RBP4, BLNK, LOX, PTGER3, GALNTL1, RECK, NRG1, CLIC4, IFITM3, PHLDB2, COL1A2, RGS5, SDC2, TIMP1, MCAM, CFB, ENPP2, TULP4, ALPL, AGT, KDM4C, DPP4, VCAM1, RNASE3, C7orf58, CD36, F13A1, MSI2, GRB10, RCOR1, COL1A1, PMP22, EBF1, NRTN, NTRK2, CNN3, NT5E, CXCL12, C4B (includes others), GAP43, ACSL1
Cell Morphology	125ppm	SLIT3, NAB2, TPM1, MMP14, PTPN14, SERPINA3, ANPEP, SDC2, CAV1, ASPN, BRD4, FIGF, AGT, TIMP3, FGFR1, PCSK6, LAMA2, VIM, THBD, CD3G, PMP22, NTRK2, MYOC, CXCL12, LSP1, FBN1, PLAU, AGTR1
	500ppm	SLIT3, GAS6, MAP1B, SERPINA3, MYLK, SRPX2, ENTPD5, LPL, CAV1, POSTN, FIGF, AIF1, CAST, FST, CXCL9, DCN, LAMA2, RDX, SPOCK2, GSN, THBD, BST2, NDN, IL33, S100B, TGFB3, FBN1, PNOC, SFRP1, TNS1, AGTR1, ARG1, APOE, FYN, TPM1, NFIX, FN1, HTR4, PTGER3, NEFL, RECK, GDF15, PTPN14, CLIC4, ANPEP, VCAN, AR, IGF1, FGF18, SDC2, SORBS1, ANXA1, ASPN, GBP2, HSPB6, AGT, DPP4, TIMP3, VCAM1, FCGR2A, AP1S2, VIM, AXL, LTBP1, LAMB2, PMP22, COL5A3, NTRK2, MYOC, ANK2, CXCL12, BNC1, LSP1, IHH, SPARC, GAP43, PLAU, SYNGR1
	2500ppm	DPYSL2, SLIT3, GAS6, SERPINA3, HES1, SPDEF, ARHGAP20, LPL, POSTN, MGP, CAV1, DKK2, FIGF, CAST, AIF1, KLF2, TEK, FST, CXCL9, MITF, FGFR1, DCN, LAMA2, FERMT2, GSN, THBD, NEDD4, NDN, IL33, CD3G, CBL, S100B, IGFBP3, FBN1, WASF2, CFLAR, MAP2, TNS1, FYN, NFIX, FN1, HTR4, PTGER3, NEFL, RECK, MMP14, NRG1, TPR, EXT1, CLIC4, ANPEP, VCAN, CDH11, ANGPTL4, IGF1, TIMP1, FGF18, SDC2, ASPN, MARCKS, ALPL, AGT, TIMP3, DPP4, VCAM1,

		S1PR2, FCGR2A, AP1S2, SERPINF1, VIM, SERPINE2, LTBP1, KITLG, GNAI3, COL1A1, PMP22, COL5A3, TRIO, MYOC, NTRK2, NRTN, CXCL12, LSP1, S1PR1, P2RY12, SPARC, PLAU, GAP43, PSEN1
Hematological Disease	125ppm	PLAU, THBD, TFPI
	500ppm	APOE, GAS6, FCGR2A, PTGER3, C1QA, THBD, AXL, F3, PROS1, PDGFRA, CFB, PLAU, C2
	2500ppm	SLIT3, GPD1, GAS6, XDH, CHRNB1, CLMP, C1QA, MFAP2, PTPRO, CTSS, ABCC1, CAV1, ZBTB20, ADAMTS16, WNT5B, PRKCQ, GUCY1A3, PCSK5, TUBB2A, MMP2, THBD, MYST3, SPTBN1, FYN, FN1, LRP6, ADIPOQ, BMPR2, SELENBP1, SPON1, COL5A1, RIF1, IGF1, LRRFIP1, PROS1, PDGFRA, LIMCH1, CYP1A1, FCGR2A, TUBB2C, CYP1B1, LTBP1, MMD, KITLG, TRIO, PGCP, FAM114A1, ATP1A2, FCER1G, P2RY12, PLAU, FNDC1, PSEN1, CD163, ZC3H11A, LPL, ARHGAP20, POSTN, CAST, KLF2, TNFRSF11B, CXCL9, CD302, FGFR1, GM2A, LRRC17, LAMA2, IFNGR1, GSN, IL33, CD3G, CBL, HMGXB4, MATN2, S100B, IGFBP3, TNS1, C2, ELF5, AGTR1, KIAA1370, BLNK, PTGER3, NRG1, EXT1, DDR2, CFB, AGT, KDM4C, DPP4, COL5A2, RNASE3, XRN2, ATRX, CD36, F13A1, MSI2, SERPINE2, GRB10, NTRK2, CXCL12, ACSL1
Metabolic Disease	125ppm	TTR, PPAP2B, FGFR1, CXCL12, Dclk1, SERPINA3, IGFBP5, IFITM3, AGT
	500ppm	SLIT3, GPD1, PTPLA, XDH, GSTA2, CA12, CLMP, Dclk1, SERPINA3, CP, TNXB, MYLK, AIF1, ADAMTS16, SFRP4, ACAA1, PCSK5, CIDEC, FAM102B, GPM6A, SFRP1, PCBD1, COL3A1, FYN, APOE, SERPING1, FN1, ITGBL1, HTR4, GDF15, PTPN14, ADIPOQ, HLA-DQA1, VCAN, LHFP, CA3, AR, IGF1, PTPRJ, SORBS1, PPAP2B, PDLIM5, PDGFRA, SMPD3, LIMCH1, SESTD1, FMO3, FCGR2A, TUBB2C, SERPINF1, CSGALNACT1, LAMB2, TF, FAM114A1, ANK2, ATP1A2, MAOA, MMP16, BNC2, LPL, ADAMTS5, HLA-C, TNFRSF11B, GULP1, AQP7, C1S, LAMA2, GSN, MAMDC2, MATN2, FBN1, AKR1B1, TNS1, C2, AGTR1, ARG1, RBP4, AOC3, PTGER3, CLIC4, IFITM3, PHYH, ANXA1, CFB, C7, CCRL1, GBP2, AGT, DPP4, TIMP3, VCAM1, COL5A2, CKM, C7orf58, CD48, CD36, F13A1, GRB10, PMP22, P2RY14, NTRK2, GHR, CXCL12, EFEMP1, GAP43,

		ACSL1
	2500ppm	DPYSL2, SLIT3, GPD1, XDH, GSTA2, CHRNB1, CLMP, Dclk1, SERPINA3, CP, HES1, TNXB, PTPRO, DMXL2, ZBTB20, AIF1, ADAMTS16, SFRP4, PCSK5, TUBB2A, CIDEC, IGFBP5, MMP2, PCK1, ZEB1, FAM102B, MS4A7, WASF2, ADIPOR2, COL3A1, SPTBN1, FYN, SERPING1, FN1, ITGBL1, HTR4, HNRNPA2B1, LRP6, ADIPOQ, GBF1, VCAN, COL5A1, SPON1, LHFP, CA3, RIF1, IGF1, TTC7B, PDLIM5, PPAP2B, HLA-DRA, PDGFRA, LIMCH1, FMO3, FCGR2A, TUBB2C, SERPINF1, TRIO, PGCP, FAM114A1, VPS13C, ATP1A2, EBF3, P2RY12, PSEN1, CFD, LATS2, NID1, CHD2, ARHGAP20, LPL, DKK2, ADAMTS5, GULP1, TNFRSF11B, HLA-C, AQP7, C1S, FGFR1, GM2A, LAMA2, IFNGR1, GSN, CXCR7, MATN2, IGFBP3, PPP1R12A, FBN1, TNS1, C2, AGTR1, RBP4, KIAA1370, BLNK, AOC3, PTGER3, NRG1, EXT1, CLIC4, IFITM3, PHLDB2, COL1A2, ANGPTL4, RGS5, TIMP1, PHYH, C7, CFB, TULP4, ALPL, AGT, TIMP3, DPP4, KDM4C, COL5A2, VCAM1, CKM, C7orf58, CD36, F13A1, MSI2, GRB10, COL1A1, PMP22, EBF1, NTRK2, CXCL12, GAP43, AKAP9, ACSL1
Endocrine System Disorders	125ppm	TTR, PPAP2B, FGFR1, Dclk1, SERPINA3, IFITM3, AGT
	500ppm	SLIT3, GPD1, PTPLA, MMP16, CLMP, BNC2, CA12, Dclk1, CP, SERPINA3, TNXB, MYLK, LPL, AIF1, ADAMTS5, ADAMTS16, GULP1, TNFRSF11B, HLA-C, AQP7, SFRP4, FST, PCSK5, C1S, LAMA2, CIDEC, MAMDC2, FAM102B, MATN2, FBN1, GPM6A, SFRP1, AKR1B1, TNS1, AGTR1, C2, RBP4, AOC3, APOE, FYN, SERPING1, ITGBL1, FN1, HTR4, PTGER3, PTPN14, GDF15, HLA-DQA1, ADIPOQ, CLIC4, IFITM3, VCAN, CA3, LHFP, AR, PTPRJ, IGF1, SORBS1, PDLIM5, ANXA1, PPAP2B, C7, CFB, PDGFRA, CCRL1, GBP2, SMPD3, LIMCH1, SESTD1, AGT, TIMP3, DPP4, COL5A2, VCAM1, CKM, TUBB2C, CD36, CD48, C7orf58, SERPINF1, F13A1, CSGALNACT1, GRB10, PMP22, GHR, NTRK2, P2RY14, FAM114A1, TF, ANK2, ATP1A2, GAP43, EFEMP1, ACSL1,

		MAOA
	2500ppm	DPYSL2, SLIT3, GPD1, CHRNB1, CLMP, Dclk1, SERPINA3, CP, HES1, TNXB, PTPRO, DMXL2, ZBTB20, AIF1, ADAMTS16, SFRP4, HSD17B3, PCSK5, TUBB2A, CIDEC, MMP2, PCK1, ZEB1, FAM102B, MS4A7, WASF2, ADIPOR2, SPTBN1, FYN, SERPING1, FN1, ITGBL1, HTR4, LRP6, ADIPOQ, GBF1, VCAN, SPON1, LHFP, CA3, RIF1, IGF1, TTC7B, PDLIM5, PPAP2B, HLA-DRA, PDGFRA, LIMCH1, CYP1A1, TUBB2C, SERPINF1, CYP1B1, TRIO, PGCP, FAM114A1, VPS13C, ATP1A2, EBF3, P2RY12, PSEN1, LATS2, NID1, CHD2, ARHGAP20, LPL, DKK2, ADAMTS5, GULP1, TNFRSF11B, HLA-C, FST, C1S, FGFR1, GM2A, LAMA2, IFNGR1, CXCR7, MATN2, IGFBP3, PPP1R12A, FBN1, TNS1, C2, AGTR1, KIAA1370, BLNK, AOC3, PTGER3, NRG1, EXT1, CLIC4, IFITM3, PHLDB2, COL1A2, RGS5, TIMP1, C7, CFB, TULP4, ALPL, AGT, TIMP3, KDM4C, DPP4, VCAM1, CKM, ATRX, C7orf58, CD36, F13A1, MSI2, GRB10, PMP22, EBF1, NTRK2, GAP43, AKAP9, ACSL1
Hematological System Development and Function	125ppm	AOC3, TIMP3, CXCR4, MMP14, SERPINF1, SERPINA3, THBD, ANPEP, SOD3, CTSS, PROS1, CXCL12, LSP1, CAV1, FIGF, PLTP, PLAU, TFPI, CERCAM, TNFRSF11B, AGT
	500ppm	MRC1/MRC1L1, RARRES2, GAS6, XDH, C1QA, SERPINA3, GPC3, FGG, MYLK, CTSS, CAV1, FIGF, CAST, HLA-C, TIMP2, TNFRSF11B, CXCL9, GUCY1A3, DCN, THBD, GSN, IL33, S100B, PNOC, PLTP, AKR1B1, C2, AOC3, FYN, APOE, SERPING1, FN1, PTGER3, HLA-DQA1, ADIPOQ, MSLN, ANPEP, VCAN, SOD3, PTPRJ, IGF1, PROS1, ANXA1, C7, CFB, AGT, Mcpt1, DPP4, TIMP3, VCAM1, FCGR2A, SERPINF1, CD48, CD36, F13A1, AXL, F3, LTBP1, NT5E, TNFSF13, CXCL12, LSP1, C4B (includes others), PLAU, CLEC10A

	2500ppm	RARRES2, MMP3, GAS6, XDH, MAF, HLA-DMB, C1QA, SERPINA3, C1QC, CD163, GPC3, EGR2, CTSS, CAV1, FIGF, CAST, KLF2, TEK, TIMP2, TNFRSF11B, HLA-C, CXCL9, FST, PRKCQ, GUCY1A3, MED1, MMP2, IFNGR1, ZEB1, GSN, THBD, PAPSS2, SPON2, IL33, CD3G, PATZ1, CBL, CXCR7, MYST3, S100B, PLTP, CFLAR, C2, AOC3, BLNK, FYN, SERPING1, FN1, PTGER3, CHD4, MMP14, ADIPOQ, BMPR2, ANPEP, VCAN, SOD3, YY1, DUSP5, IGF1, TIMP1, MCAM, PROS1, HLA-DRA, CFB, C7, AGT, Mcpt1, TIMP3, DPP4, VCAM1, ENTPD1, FCGR2A, CD36, SERPINF1, F13A1, ID3, LTBP1, SERPINE2, KITLG, COL1A1, GNAI3, EBF1, ENTPD2, NT5E, TNFSF13, CXCL12, LSP1, C4B (includes others), S1PR1, FCER1G, P2RY12, PLAU, CERCAM, CLEC10A, PSEN1
Immune Cell Trafficking	125ppm	AOC3, TIMP3, NBL1, CXCR4, MMP14, SERPINA3, THBD, SOD3, CTSS, CXCL12, LSP1, FIGF, PLTP, PLAU, CERCAM, TNFRSF11B, AGT
	500ppm	RARRES2, GAS6, XDH, SERPINA3, C1QA, GPC3, FGG, MYLK, CTSS, FIGF, CAST, HLA-C, TIMP2, TNFRSF11B, CXCL9, GSN, THBD, IL33, S100B, PNOC, PLTP, C2, AOC3, APOE, FYN, SERPING1, FN1, PTGER3, HLA-DQA1, ADIPOQ, VCAN, SOD3, PTPRJ, IGF1, PROS1, ANXA1, CFB, C7, AGT, TIMP3, Mcpt1, DPP4, VCAM1, NBL1, FCGR2A, CD48, CD36, F13A1, AXL, F3, LTBP1, NT5E, TNFSF13, CXCL12, LSP1, C4B (includes others), PLAU
Immune Cell Trafficking	2500ppm	DPYSL2, RARRES2, MMP3, GAS6, XDH, MAF, HLA-DMB, C1QA, SERPINA3, CD163, GPC3, EGR2, CTSS, ABCC1, FIGF, CAST, KLF2, HLA-C, TIMP2, TNFRSF11B, CXCL9, PRKCQ, MMP2, IFNGR1, THBD, GSN, SPON2, IL33, CD3G, CXCR7, S100B, PLTP, C2, AOC3, FYN, SERPING1, FN1, PTGER3, MMP14, ADIPOQ, BMPR2, VCAN, SOD3, IGF1, TIMP1, PROS1, MCAM, HLA-DRA, C7, CFB, AGT, Mcpt1, TIMP3, DPP4, VCAM1, NBL1, FCGR2A, CD36, F13A1, LTBP1, KITLG, GNAI3, COL1A1, EBF1, NT5E, TNFSF13, CXCL12, LSP1, FCER1G, S1PR1, C4B (includes others), PLAU, CERCAM
Hematopoiesis	125ppm	CXCR4, MMP14, CXCL12
	500ppm	FYN, VCAM1, CXCL9, CD48, CD36, IL33, CXCL12, ANXA1, LSP1, C4B (includes others), CFB, CAST, C2, AGT

	2500ppm	FYN, VCAM1, CXCL9, PRKCQ, FCGR2A, MMP14, CD36, IL33, KITLG, CD3G, CXCL12, LSP1, C4B (includes others), FCER1G, CFB, CAST, C2, AGT
Lymphoid Tissue Structure and Development	125ppm	CXCL12, MMP14, FBN1, PLAU, TFPI, AGT
	500ppm	FYN, APOE, VCAM1, IGF1, CXCL12, PLAU, AGT
	2500ppm	KITLG, FYN, VCAM1, MMP14, CXCL12
Post-Translational Modification	125ppm	MMP14, PCSK6, PLAU
	500ppm	APOE, FYN, LOX, CTSK, PCSK5, C1S, OAT, PCSK6, ADIPOQ, CP, TIPARP, MYLK, GHR, IGF1, PPAP2B, C4B (includes others), PDGFRA, PLAU, EFEMP1, AGT, ARG1
	2500ppm	CTSK, MMP3, PCSK5, CTSS, C1S, MMP14, PCSK6, C4B (includes others), MMP13, MMP2, PLAU
Tissue Morphology	125ppm	TIMP3, TPM1, PVALB, GUCY1A3, CXCR4, MYLPF, MMP14, VIM, IGFBP5, MYL1, SOD3, DPT, KIF13A, CTSS, TNNT3, SERPINH1, CASQ1, CAV1, BRD4, PLAU, AGTR1, ACTA1, AGT, TNFRSF11B
	500ppm	GAS6, XDH, C1QA, FGG, PCOLCE, MYLK, CTSS, TNNT3, LPL, CASQ1, CAV1, CAST, ACTA1, TNFRSF11B, AQP7, FST, FXYD1, GSN, IL33, TGFB3, PNOC, AGTR1, LOX, FYN, APOE, TPM1, NFIX, ADIPOQ, SSPN, AR, IGF1, SORBS1, PRRX1, ANXA1, PDGFRA, TBX2, LTBP4, HSPB6, AGT, TIMP3, Mcpt1, CTSK, VCAM1, MYLPF, VIM, AXL, MYL1, GRB10, CIDEA, GHR, NT5E, SERPINH1, CXCL12, ANK2, ATP1A2, C4B (includes others), IHH, SPARC, PLAU, MAOA
	2500ppm	SERPINI1, MMP3, GAS6, XDH, MMP13, C1QA, HES1, PCOLCE, LAMC1, EGR2, CTSS, CAV1, KLF2, TEK, TNFRSF11B, IGFBP6, FST, MITF, MED1, FGFR1, DCN, MMP2, IFNGR1, IGFBP5, GSN, SPON2, IL33, CD3G, CBL, IGFBP3, TGFB3, CFLAR, AGTR1, BLNK, AOC3, FYN, POU3F1, SERPING1, NFIX, FN1, HTR4, NEFL, MMP14, LRP6, NRG1, BMPR2, CES1, SOD3, CA3, IGF1, TIMP1, FGF18, PRRX1, MXD1, PDGFRA, LTBP4, AGT, TIMP3, CTSK, VCAM1, S1PR2, FCGR2A, EFEMP2, ATRX, SERPINE2, KITLG, NRTN, NTRK2, NT5E, TNFSF13, CXCL12, SERPINH1, LSP1, C4B

		(includes others), FCER1G, S1PR1, BIK, SPARC, PLAU, GAP43, HRASLS, PSEN1
Connective Tissue Development and Function	125ppm	TPM1, SFRP4, CXCR4, LRRC17, FGFR1, SERPINF1, IGFBP5, VCAN, AEBP1, NOV, DDR2, CXCL12, GDF10, CAV1, FBN1, FIGF, PLAU, AGTR1, TNFRSF11B, AGT
	500ppm	APOE, COL14A1, NFIX, FN1, PTGER3, GAS6, RECK, XDH, ADIPOQ, VCAN, MFAP2, AEBP1, AR, IGF1, SDC2, SORBS1, DDR2, FGF18, POSTN, MGP, ASPN, CAV1, NUPR1, PDGFRA, GBP2, CAST, AIF1, AGT, TNFRSF11B, IGFBP6, VCAM1, DCN, VIM, GSN, NDN, CIDEA, GHR, TF, CXCL12, IHH, SPARC, CD248, PLAU, SFRP1, GAP43
	2500ppm	COL14A1, RARRES2, MMP3, GAS6, XDH, MMP13, HES1, GPC3, MFAP2, EGR2, CTSS, MGP, CAV1, POSTN, DKK2, NIPBL, AIF1, CAST, KLF2, WNT5B, TNFRSF11B, IGFBP6, FST, MITF, PCSK5, MED1, DCN, MMP2, GSN, TBL1X, NDN, PAPSS2, IL33, ANKRD11, IGFBP3, CD248, WASF2, NFIX, FN1, PTGER3, RECK, MMP14, LRP6, ADIPOQ, BMPR2, VCAN, SELENBP1, YY1, AEBP1, IGF1, SDC2, FGF18, DDR2, TIMP1, ASPN, PDGFRA, ENPP2, ALPL, AGT, TIMP3, CTSK, VCAM1, SERPINF1, COL1A1, EBF1, NT5E, FCER1G, S1PR1, SPARC, PLAU, 1100001G20Rik
Embryonic Development	125ppm	NFIX, CXCR4, CXCL12, LAMA2, BRD4, IGFBP5, PLAU, AGTR1, VCAN, AGT
	500ppm	TIMP3, CTSK, FST, FN1, GAS6, XDH, ADIPOQ, AXL, GSN, FGG, IL33, AR, IGF1, CXCL12, POSTN, TGFB3, SPARC, IHH, SFRP1, PLAU, AGTR1, AGT, TNFRSF11B
	2500ppm	NFIX, FN1, GAS6, MMP14, XDH, NRG1, LRP6, ADIPOQ, BMPR2, HES1, VCAN, IGF1, POSTN, ENPP2, TNFRSF11B, TIMP2, TIMP3, VCAM1, CTSK, FST, MITF, IGFBP5, MMP2, GSN, KITLG, IL33, NRTN, CXCL12, FCER1G, SPARC, PSEN1
Renal and Urological Disease	125ppm	KLK1, AGTR1, TNFRSF11B, AGT

	500ppm	FYN, APOE, FN1, PTGER3, GAS6, XDH, CA12, ADIPOQ, C1QA, SERPINA3, CA3, COL6A1, AR, IGF1, LPL, CFB, FXYD2, FXYD5, TIMP2, AGT, PTGIS, PVALB, WT1, DPP4, VCAM1, PCSK5, FCGR2A, TUBB2C, AXL, LAMB2, GHR, C4B (includes others), SPARC, C2, AGTR1
	2500ppm	CFD, FYN, FN1, PTGER3, GAS6, MMP14, XDH, ADIPOQ, SERPINA3, C1QA, LAMC1, CA3, COL6A1, IGF1, TIMP1, ABCC1, LPL, CFB, FXYD2, TIMP2, AGT, TIMP3, DPP4, PVALB, VCAM1, CYP1A1, PCSK5, TUBB2C, TUBB2A, IFNGR1, MMP2, CYP1B1, GRHPR, GLIS2, FCER1G, C4B (includes others), SPARC, P2RY12, CPXM1, C2, AGTR1, PSEN1
Developmental Disorder	125ppm	TPM1, GUCY1A3, CXCL12, CAV1, MSX1, FIGF, FBN1, MFAP4, AGTR1, AGT
	500ppm	MAP1B, CA12, MSX1, GPC3, GPX3, MFAP2, SRPX2, CAV1, POSTN, NUPR1, FIGF, TNFRSF11B, PTGIS, WT1, FST, GUCY1A3, PCSK5, PCSK6, GSN, NDN, IL33, TGFB3, FBN1, AGTR1, ARG1, PBRM1, TPM1, APOE, NFIX, ADIPOQ, CA3, AR, IGF1, PDGFRA, C7, SMPD3, AGT, DPP4, CTSK, AP1S2, MFAP4, GHR, NTRK2, TF, NT5E, CXCL12, ANK2, ATP1A2, IHH, NFIB, GAP43, PLAU
	2500ppm	MMP3, NR2F2, MSX1, MMP13, HES1, GPC3, LAMC1, GPX3, MFAP2, POSTN, CAV1, FIGF, NIPBL, WNT5B, TNFRSF11B, FST, GUCY1A3, PCSK5, MED1, MITF, FGFR1, PCSK6, MMP2, GSN, NDN, PAPSS2, IL33, TGFB3, FBN1, AGTR1, PBRM1, POU3F1, NFIX, NRG1, ADIPOQ, BMPR2, COL1A2, CA3, YY1, RGS5, IGF1, TIMP1, C7, PDGFRA, MARCKS, AGT, DPP4, CTSK, AP1S2, ATRX, MFAP4, CYP1B1, KITLG, STRA6, COL1A1, NRTN, NTRK2, NT5E, CXCL12, ATP1A2, FCER1G, GAP43, PLAU, PSEN1
Hepatic System Disease	125ppm	TNFRSF11B
	500ppm	COL1A2, COL1A1, S1PR2, TIMP1, NT5E, IFNGR1, AGTR1, TIMP2, COL3A1
Tumor Morphology	2500ppm	NOV, SDC2, CXCR4, CTSS, MMP14, FGFR1, CXCL12, PCSK6, CAV1, SERPINF1, VIM, PLAU
	125ppm	DPP4, APOE, FN1, GAS6, RECK, PCSK6, GDF15, ADIPOQ, VIM, NOV, IGF1, CTSS, SDC2, TNFSF13, CXCL12, CAV1, TGFB3, ENPP2, PLAU, SFRP1, AKR1B1, TIMP2

	500ppm	FN1, MMP3, GAS6, RECK, MMP14, NRG1, ADIPOQ, SPDEF, IGF1, CTSS, SDC2, MCAM, CAV1, ENPP2, TIMP2, DPP4, FGFR1, PCSK6, VIM, MMP2, ID3, KITLG, NOV, TNFSF13, CXCL12, TGFB3, PLAU
Energy Production	2500ppm	ENTPD1, NT5E, ENTPD2
Nucleic Acid Metabolism	125ppm	GUCY1A3, AGTR1, AGT
	500ppm	WT1, AR, GHR, FST, FN1, TF, IGF1, AGT
	2500ppm	ENTPD1, NT5E, ENTPD2
Small Molecule Biochemistry	125ppm	PLA2G16, GUCY1A3, CXCL12, PPAP2B, CAV1, CYGB, PLTP, AGTR1, ACSL1, AGT
	500ppm	COL14A1, XDH, CP, TIPARP, MYLK, LPL, CAV1, GULP1, PTGIS, WT1, AQP7, FST, OAT, FXYD1, CIDEC, GSN, NDN, IL33, S100B, PLTP, AKR1B1, AGTR1, APOD, ARG1, APOE, FYN, LOX, FN1, SCARA5, ADIPOQ, CES1, AEBP1, AR, IGF1, PPAP2B, ANXA1, PDGFRA, C7, CAV2, PON3, AGT, APOBEC1, FCGR2A, CD36, VIM, GHR, TF, ACOT2, CXCL12, SLC16A1, EFEMP1, ACSL1
	2500ppm	AOC3, FYN, COL14A1, FN1, MMP3, XDH, NRG1, ADIPOQ, CES1, PLA1A, AEBP1, ANGPTL4, IGF1, TIMP1, ABCC1, LPL, CAV1, MARCKS, GULP1, AGT, AQP7, CYP1A1, APOBEC1, ENTPD1, FCGR2A, CIDEC, CD36, VIM, PCK1, GSN, CYP1B1, IL33, KITLG, GNAI3, NT5E, ENTPD2, SULT1A1, SLC16A1, CXCL12, IGFBP3, FCER1G, PLTP, ADIPOR2, AGTR1, ACSL1, APOD
Nervous System Development and Function	125ppm	NAB2, SLIT3, TTR, NFIX, CXCR4, FGFR1, LAMA2, VIM, VCAN, LAMC1, KLF9, PMP22, NTRK2, SDC2, CXCL12, CAV1, PLAU, AGT
	500ppm	FYN, APOE, NFIX, FN1, MAP1B, VCAN, AR, IGF1, FGF18, CAV1, AGT, WT1, VCAM1, CXCL9, GSTM3, LAMA2, VIM, SPOCK2, NDN, LAMB2, PMP22, NTRK2, CXCL12, S100B, PNOC, PLAU, GAP43, SYNGR1, MAOA, ARG1

	2500ppm	SLIT3, DPYSL2, SERPINI1, GDA, GAS6, NR2F2, MSX1, Dclk1, HES1, SPAG9, LATS2, LAMC1, EGR2, CAV1, NIPBL, CAST, CRIM1, TIMP2, IGFBP6, MED1, FGFR1, LAMA2, RDX, ZEB1, GSN, NDN, SPON2, RPS6KA6, NR1D1, S100B, TGFB3, MAP2, SPTBN1, POU3F1, FYN, LOX, FN1, NFIX, HTR4, NEFL, NRG1, EFHD1, LRP6, EXT1, VCAN, KLF9, IGF1, FGF18, PHYH, MARCKS, S1PR2, NBL1, ATRX, SERPINF1, ID3, SERPINE2, EBF1, PMP22, NRTN, NTRK2, CXCL12, S1PR1, EBF3, PLAU, GAP43, C5orf13, SEPT2, PSEN1
Organismal Functions	125ppm	PROS1, CXCL12, SERPINF1, CAV1, TFPI, THBD, AGT
	500ppm	APOE, GAS6, FCGR2A, PROS1, CXCL12, CAV1, SERPINF1, F13A1, AXL, THBD, F3
	2500ppm	ENTPD1, FCGR2A, GAS6, SERPINF1, F13A1, THBD, PAPSS2, SERPINE2, ENTPD2, CXCL12, PROS1, CAV1, FCER1G, P2RY12
Antigen Presentation	125ppm	CXCR4, CXCL12, FIGF, PLAU, AGT
	500ppm	MRC1/MRC1L1, APOE, FYN, SERPING1, RARRES2, FN1, PTGER3, HLA-DQA1, ADIPOQ, C1QA, GPC3, ANPEP, IGF1, PROS1, ANXA1, C7, CFB, FIGF, HLA-C, AGT, DPP4, VCAM1, FCGR2A, DCN, CD48, CD36, FMOD, AXL, F3, LTBP1, IL33, TNFSF13, CXCL12, LSP1, C4B (includes others), PLAU, CLEC10A
	2500ppm	FYN, SERPING1, RARRES2, FN1, PTGER3, MAF, ADIPOQ, C1QA, HLA-DMB, CD163, IGF1, PROS1, C7, CFB, FIGF, HLA-C, AGT, DPP4, FCGR2A, FMOD, SPON2, LTBP1, KITLG, IL33, CXCL12, TNFSF13, C4B (includes others), FCER1G, PLAU
Hepatic System Development and Function	125ppm	CXCR4, CXCL12, SLC9A4, AGTR1, AGT
	500ppm	FN1, TF, IGF1, CXCL12, XDH, ADIPOQ, PLAU, NDN, AGT
	2500ppm	SPTBN1, FN1, S1PR2, MED1, XDH, ADIPOQ, MMP13, GPC3, NDN, KITLG, IGF1, TIMP1, FGF18, CXCL12, PLAU, CFLAR, AGTR1, AGT

Renal and Urological System Development and Function	125ppm	CXCR4, FGFR1, MMP14, CXCL12, PTPN14, BRD4, FBN1, PLAU, TIPARP, AGTR1, AGT
	500ppm	APOE, CXCL9, FN1, IGF1, GAS6, SORBS1, SPARC, VIM, PLAU, GAP43, AXL, AGT
	2500ppm	CXCL9, IGF1, GAS6, FCER1G, SPARC, PLAU, AGT
Lipid Metabolism	125ppm	PLA2G16, CXCL12, PPAP2B, CAV1, PLTP, AGTR1, ACSL1, AGT
	500ppm	APOE, COL14A1, FN1, XDH, ADIPOQ, CES1, AEBP1, AR, IGF1, ANXA1, PPAP2B, LPL, CAV1, CAV2, PON3, GULP1, AGT, PTGIS, AQP7, APOBEC1, FCGR2A, CIDEC, CD36, VIM, GSN, IL33, GHR, ACOT2, SLC16A1, CXCL12, PLTP, AKR1B1, AGTR1, ACSL1, APOD
	2500ppm	FYN, COL14A1, FN1, MMP3, XDH, NRG1, ADIPOQ, CES1, PLA1A, AEBP1, ANGPTL4, IGF1, TIMP1, ABCC1, LPL, CAV1, MARCKS, GULP1, AGT, AQP7, CYP1A1, APOBEC1, FCGR2A, CD36, CIDEC, VIM, PCK1, GSN, CYP1B1, IL33, KITLG, GNAI3, SLC16A1, CXCL12, FCER1G, PLTP, ADIPOR2, AGTR1, ACSL1, APOD
Molecular Transport	125ppm	MRC1/MRC1L1, SFRP4, CXCR4, FGFR1, CXCL12, CAV1, PLTP, AGTR1, AGT, TNFRSF11B
	500ppm	APOE, COL14A1, FN1, XDH, ADIPOQ, CES1, AEBP1, AR, IGF1, ANXA1, PPAP2B, LPL, CAV1, CAV2, PON3, GULP1, AGT, PTGIS, AQP7, APOBEC1, FCGR2A, CIDEC, CD36, VIM, GSN, F3, IL33, GHR, ACOT2, SLC16A1, CXCL12, PLTP, AKR1B1, AGTR1, ACSL1, APOD
	2500ppm	DBN1, COL14A1, FN1, MMP3, XDH, NRG1, ADIPOQ, CES1, PLA1A, AEBP1, ANGPTL4, IGF1, TIMP1, ABCC1, LPL, CAV1, MARCKS, GULP1, AGT, AQP7, APOBEC1, FCGR2A, FGFR1, CD36, CIDEC, VIM, PCK1, GSN, IL33, KITLG, GNAI3, SLC16A1, CXCL12, FCER1G, PLTP, ADIPOR2, AGTR1, ACSL1, PSEN1, APOD
Cell Death	125ppm	TPM1, KLK1, EMILIN2, MSX1, SERPINA3, ANPEP, VCAN, SOD3, FSTL1, CTSS, SDC2, CAV1, AGT, TNFRSF11B, PLA2G16, SFRP4, TIMP3, TTR, DDIT4, CXCR4, FGFR1, LAMA2, CIDEC, SERPINF1, VIM, IGFBP5, THBD, ANGPTL1, CD3G, CIDEA, NTRK2, MYOC, CXCL12, LSP1, NGFRAP1, FBN1,

		PLAU, ADAMTSL4, AGTR1
	500ppm	GAS6, XDH, GSTA2, MSX1, C1QA, SERPINA3, MYLK, CTSS, MGP, CAV1, AIF1, TIMP2, PTGIS, SFRP4, WT1, DDIT4, DCN, CIDEC, THBD, FMOD, GPX7, NDN, SFRP1, ADAMTSL4, STEAP3, FYN, APOE, EMILIN2, FN1, GDF15, ADIPOQ, CES1, ANPEP, VCAN, SOD3, CA3, FSTL1, AR, IGF1, FGF18, PDGFRA, FAP, PLAC8, PLA2G16, EMP3, SERPINF1, VIM, AXL, F3, LTBP1, LAMB2, MYOC, TF, TNFSF13, ATP1A2, LSP1, IHH, PLAU, MAOA, FGL2, RTN1, MAP1B, GPC3, G0S2, ENTPD5, NUPR1, COQ6, CAST, TNFRSF11B, AQP7, IGFBP6, FST, LAMA2, RDX, GSN, ANGPTL1, NOL3, S100B, TGFB3, FBN1, AKR1B1, AGTR1, ARG1, TPM1, SRPX, PTGER3, NEFL, RECK, CLIC4, LOXL2, SDC2, ANXA1, C7, HSPB6, AGT, TIMP3, DPP4, RNASE3, CD48, CD36, F13A1, GRB10, PMP22, CIDEA, GHR, NTRK2, CXCL12, SPARC, CLEC10A, FAIM3
	2500ppm	GAS6, XDH, GSTA2, MAF, MSX1, C1QA, SERPINA3, HES1, SPDEF, EGR2, IKZF2, PTPRO, CTSS, ABCC1, CAV1, MGP, ANGPT4, AIF1, ALDH3A1, TIMP2, SFRP4, PRKCQ, DDIT4, MFAP5, MITF, MED1, DCN, CIDEC, MMP2, IGFBP5, ZEB1, FMOD, THBD, GPX7, NDN, NR1D1, JDP2, CFLAR, STEAP3, FYN, EMILIN2, FN1, LRP6, ADIPOQ, CES1, ANPEP, SOD3, VCAN, CA3, FSTL1, DUSP5, YY1, RIF1, IGF1, FGF18, MXD1, PDGFRA, PLAC8, FAP, EMP3, SERPINF1, VIM, ID3, CYP1B1, LTBP1, KITLG, TRIO, MYOC, TNFSF13, ATP1A2, LSP1, FCER1G, S1PR1, PLAU, RBBP6, HRASLS, PSEN1, CFD, SERPINI1, MMP3, RTN1, FGL2, MMP13, GPC3, LATS2, G0S2, CAST, KLF2, TNFRSF11B, ASGR2, IGFBP6, AQP7, CXCL9, FST, FGFR1, LAMA2, RDX, IFNGR1, GSN, ANGPTL1, IL33, CD3G, CBL, NOL3, CXCR7, S100B, TGFB3, IGFBP3, FBN1, AGTR1, BLNK, POU3F1, SRPX, NEFL, PTGER3, DNASE1L3, MMP14, RECK, NRG1, CLIC4, LOXL2, ANGPTL4, RGS5, TIMP1, SDC2, MCAM, C7, AGT, TIMP3, DPP4, RNASE3, S1PR2, ATRX, CD36, F13A1, SERPINE2, GRB10, PMP22, EBF1, NTRK2, NRTN, CXCL12, BIK, SPARC, CLEC10A, FAIM3
Hypersensitivity Response	125ppm	CXCL12, FIGF, PLAU
	500ppm	FYN, CXCL12, FIGF, PLAU

	2500ppm	KITLG, FYN, CXCL12, FIGF, PLAU
Cell Cycle	125ppm	FIGF, AGT
	500ppm	FYN, APOE, FN1, GAS6, AXL, NTRK2, AR, IGF1, TF, CXCL12, PDGFRA, TGFB3, SPARC, FIGF, AGT
	2500ppm	GAS6, C13orf15, HES1, LATS2, SPDEF, PTPRO, CAV1, FIGF, CAST, AIF1, KLF2, ALDH3A1, TIMP2, MITF, DCN, FGFR1, IGFBP5, ZEB1, CBL, JDP2, TGFB3, IGFBP3, BLNK, FYN, KDM5B, FN1, NEFL, TPR, NRG1, ADIPOQ, KLF9, YY1, IGF1, DDR2, PROS1, MXD1, PDGFRA, MARCKS, PLAC8, AGT, DPP4, FCGR2A, ID3, CYP1B1, GRB10, KITLG, GNAI3, COL1A1, NTRK2, CXCL12, BIK, S1PR1, SPARC, PLAU, AKAP9, PSEN1
Organismal Survival	500ppm	MRC1/MRC1L1, GAS6, GPC3, LPL, POSTN, ACTA1, TNFRSF11B, WT1, CXCL9, PCSK5, DCN, PCSK6, LAMA2, THBD, TGFB3, FBN1, AGTR1, COL3A1, ARG1, LOX, FYN, APOE, SERPING1, NFIX, NEFL, RECK, SOD3, KLF9, AEBP1, IGF1, ANXA1, PDGFRA, CFB, ENPP2, HSPB6, AGT, TIMP3, VCAM1, MYLPF, CD36, F13A1, F3, EGFL7, LAMB2, NTRK2, GHR, CLDN1, ANK2, CXCL12, C4B (includes others)
	2500ppm	MRC1/MRC1L1, GAS6, NR2F2, LATS2, GPC3, EGR2, LPL, POSTN, KLF2, TEK, TNFRSF11B, CXCL9, PCSK5, MED1, DCN, FERMT2, PCSK6, IGFBP5, IFNGR1, THBD, CBL, TGFB3, FBN1, CFLAR, WASF2, ELF5, AGTR1, FYN, POU3F1, LOX, SERPING1, NFIX, RECK, LRP6, SOD3, COL5A1, KLF9, AEBP1, IGF1, PDGFRA, CFB, LY6E, ENPP2, AGT, TIMP3, VCAM1, CYP1A1, S1PR2, EFEMP2, MYLPF, CD36, F13A1, NTRK2, CXCL12, C4B (includes others), FCER1G, S1PR1, PSEN1
Organ Morphology	125ppm	PVALB, TPM1, NTRK2, LAMA2, CAV1, BRD4, AGT
	500ppm	IL33, IGFBP6, AR, GHR, FST, IGF1, PTGER3, FGF18, TNFSF13, MAP1B, IHH, AGT
	2500ppm	SLIT3, FN1, LRP6, NRG1, MSX1, GPC3, COL5A1, COL1A2, YY1, IGF1, TIMP1, PDGFRA, NIPBL, WNT5B, COL5A2, HSD17B3, MED1, MITF, FGFR1, DCN, COL1A1, TGFB3, TMEM176B, PSEN1, RBP4

DNA Replication, Recombination, and Repair	500ppm	WT1, AR, GHR, FST, FN1, TF, IGF1, AGT
	2500ppm	COL14A1, FN1, MAF, NRG1, ADIPOQ, YY1, IGF1, PROS1, CAV1, PDGFRA, KLF2, ALDH3A1, TIMP2, AGT, IGFBP6, S1PR2, ENTPD1, GUCY1A3, FGFR1, IGFBP5, MMP2, KITLG, GNAI3, NOV, ENTPD2, CXCL12, IGFBP3, SPARC, AGTR1
Amino Acid Metabolism	500ppm	APOE, FYN, LOX, OAT, ADIPOQ, CP, TIPARP, MYLK, GHR, IGF1, PPAP2B, PDGFRA, EFEMP1, AGT, ARG1
	2500ppm	IGF1, IGFBP3, AGT
Cell-mediated Immune Response	125ppm	AOC3, CXCR4, CXCL12
	2500ppm	DPYSL2, AOC3, FYN, FN1, CXCL9, PRKCQ, FCGR2A, CD3G, COL1A1, GNAI3, CXCR7, ABCC1, CXCL12, S1PR1, PLAU, KLF2, AGT, TIMP2
Protein Synthesis	2500ppm	DPP4, TIMP3, CYP1A1, CTSK, FMO2, MMP3, MMP13, MMP2, ANPEP, TBL1X, CYP1B1, PCOLCE, SERPINE2, IGF1, CTSS, IGFBP3, LTBP4, PLAU, AGT, TIMP2
Endocrine System Development and Function	125ppm	AGTR1, AGT
	2500ppm	CYP1A1, CYP1B1
Gene Expression	125ppm	CAV1, MSX1
	2500ppm	KITLG, IGF1, NRG1, AGT
Infection Mechanism	125ppm	CXCR4, CXCL12, PLAU, THBD, TNFRSF11B
	500ppm	PLAU, THBD
	2500ppm	PLAU, THBD

Infectious Disease	125ppm	CXCR4, PROS1, THBD, IFITM3
	2500ppm	PRKCQ, RNASE3, TUBB2C, TUBB2A, IFNGR1, KLF2
Protein Degradation	125ppm	TIMP3, MMP14, CAV1
	500ppm	TIMP3, MMP16, CAV1
	2500ppm	TIMP3, DPP4, CTSK, MMP3, MMP14, MMP13, MMP2, ANPEP, TBL1X, PCOLCE, SERPINE2, IGF1, CTSS, CAV1, LTBP4, PLAU, TIMP2
Cell Signaling	125ppm	PVALB, ATP2B1, FGFR1, CAV1, CYGB, AGTR1, AGT
	2500ppm	BLNK, DBN1, GAS6, FGFR1, NRG1, BMPR2, ANGPTL1, KITLG, TRIO, NTRK2, NRTN, DDR2, CAV1, AGTR1, TEK, PSEN1, AGT
Humoral Immune Response	125ppm	CXCL12
	500ppm	C7, C4B (includes others), CFB, C1QA, FMOD
	2500ppm	C7, C4B (includes others), CFB, C1QA, FMOD
Vitamin and Mineral Metabolism	125ppm	PVALB, ATP2B1, FGFR1, CAV1, AGTR1, AGT
	2500ppm	KITLG, DBN1, FGFR1, CAV1, AGTR1, PSEN1, AGT
Antimicrobial Response	125ppm	CXCL12, CAV1, BST2
Carbohydrate Metabolism	125ppm	PLA2G16, PPAP2B, CAV1
	500ppm	APOE, SERPING1, FN1, IGF1, PPP1R1A, GAS6, TNFAIP6
Free Radical Scavenging	125ppm	AGTR1, AGT

	500ppm	XDH, CD36, F3, AGTR1, AGT
Cellular Compromise	125ppm	TPM1, NTRK2, MYOC, CXCR4, CXCL12, CAV1, SERPINF1, BST2, AGTR1
	500ppm	FN1, GHR, IGF1, CXCL12
Drug Metabolism	125ppm	PVALB
	500ppm	GSTA3, XDH, GSTM3, GSTA2
Protein Trafficking	125ppm	MRC1/MRC1L1, CAV1
Behavior	125ppm	KLF9, TTR, NTRK2, PLAU
	500ppm	APOE, FYN, NTRK2, IGF1, PLAU

*Classified from higher to lower statistical significance. Ingenuity Pathway Analysis-IPA.

CONCLUSION

In summary, the present study demonstrated that transcriptional profile analyses identified a dose-response both after 7 days and 20 weeks of continuous exposures of diuron. In the 7-day study, diuron affected several functions related with cell-to-cell interaction and tissue disorganization at transcriptional level. No corresponding morphological lesions were significantly registered. In the 20-week study, gene expressions clearly differ between higher (1250 and 2500 ppm) and lower (60 and 125 ppm) doses; gene expression profile was anchored by the morphological response and alterations induced in the urothelium by1250 and 2500 ppm do not differ, suggesting that 1250 ppm is also a carcinogenic level of exposure. The results suggest that 125 ppm of diuron in the feed is a no adverse effect level (NOAEL) for histologic alterations, and transcriptional changes are related to the preservation of urothelial homeostasis. Comparison of gene expressions observed at 7-day and 20-week time points indicates more differences than similarities. The present data suggest an initial adaptive response to protect the urothelium to the constant exposure to diuron. By the 20^{th} week, high dietary concentrations of diuron induces pathways related to oxidative stress, increased cellular metabolism, and cell death which is associated with sustained urothelial hyperplasia. This process can explain the development of urothelial bladder tumors at the end of a 2-year exposure to diuron.

Attachments

UNIVERSIDADE ESTADUAL PAULISTA
CAMPUS DE BOTUCATU
FACULDADE DE MEDICINA

unesp

FMB

CEEA

Comissão de Ética em Experimentação Animal

Criada através da Portaria DFM nº 30 de 25/04/08

Certificado

Certificamos que o Projeto de Pesquisa "Estudo da dose-resposta e perfil de expressão gênica do herbicida diuron (3-(3,4- dichlorophenyl)-1,1-dimethylurea) em bexiga urinária de ratos wistar macho", conduzido por Shadia Muhammad Ihlaseh, orientada pelo Prof. Titular João Lauro Viana de Camargo, com a colaboração de Maria Luíza Cotrim Sartor de Oliveira, Ana Paula Ferragut Cardoso e Mitscheli Sanches da Rocha está de acordo com os Princípios Éticos na Experimentação Animal adotado pelo Colégio Brasileiro de Experimentação Animal (COBEA). Os animais do estudo possuem Atestado de Sanidade fornecido pelo CEMIB da UNICAMP.

A Comissão de Ética em Experimentação animal esclarece que o projeto em epígrafe é parte integrante do Protocolo CEEA 686/2008, aprovado em 31/07/2008.

Projeto de Pesquisa aprovado em reunião da CEEA em **29/09/2011**.

Profª Drª Noeme Sousa Rocha
Vice- Presidente da CEEA

Alberto Santos Capelluppi
Secretário da CEEA

Distrito Rubião Junior, s/nº - Botucatu – S.P. CEP: 18.618-970 Fone/Fax: (0xx14) 3811-6143 e-mail secretaria: capellup@fmb.unesp.br

UNIVERSIDADE ESTADUAL DE CAMPINAS
Centro Multidisciplinar para Investigação Biológica na
Área da Ciência em Animais de Laboratório - CEMIB
INTERNATIONAL COUNCIL FOR LABORATORY ANIMAL SCIENCE
ICLAS MONITORING / REFERENCE CENTER
cemib@cemib.unicamp.br

Prof. Dr. João Lauro Viana de Camargo
TOXICAM
Faculdade de Medicina de Botucatu – UNESP
Botucatu-S.P.

Atestado de Saúde Animal

Atestamos que os ratos heterogênicos da linhagem **Wistar/Uni.** provenientes da Divisão de Produção de Animais S.P.F. (Specific Pathogen Free) deste Centro, pertencem à categoria sanitária S.P.F. e apresentam-se isentos dos agentes patogênicos pesquisados, relacionados abaixo. Informamos que os mesmos encontram-se livres de outros agentes infecciosos capazes de causarem riscos à saúde humana. A validade deste Atestado consta da data dos últimos testes do programa de monitorização sanitaria, rotineiramente realizados pelo Laboratório de Controle de Qualidade Animal - C.Q.S.(*).

O padrão sanitário dos animais será mantido quando acondicionados de maneira adequada, em microisoladores, que não devem ser abertos durante o transporte. Recomenda-se que a Instituição que receberá os animais mantenha-os em unidades isoladoras, racks ventiladas, câmaras ou salas dotadas de sistema de barreiras de proteção adequada para a manutenção de animais S.P.F.

(*) Data dos últimos testes de monitorização sanitária realizados: Abril 2008.

Campinas, 19 de junho de 2008

Dra. Delma Pegolo Alves
Diretora - Cemib/Unicamp
E-mail: diretoria@cemib.unicamp.br

Dr. Rovilson Gilioli
Controle de Qualidade Animal
E-mail: sanitario@cemib.unicamp.br